December 2021

Cooperative Perception for Social Driving in Connected Vehicle Traffic

Daniel Yoon
Clemson University, danielyoon.skr@gmail.com

Cooperative Perception for Social Driving in Connected Vehicle Traffic

---

A Dissertation
Presented to
the Graduate School of
Clemson University

In Partial Fulfillment
of the Requirements for the Degree
Doctor of Philosophy
Automotive Engineering

---

by
DoHyun Daniel Yoon
December 2021

Accepted by:
Dr. Beshah Ayalew, Committee Chair
Dr. Jim Martin
Dr. Yunyi Jia
Dr. Matthias Schmid

Abstract

The development of autonomous vehicle technology has moved to the center of automotive research in recent decades. In the foreseeable future, road vehicles at all levels of automation and connectivity will be required to operate safely in a hybrid traffic where human operated vehicles (HOVs) and fully and semi-autonomous vehicles (AVs) coexist. Having an accurate and reliable perception of the road is an important requirement for achieving this objective. This dissertation addresses some of the associated challenges via developing a human-like social driver model and devising a decentralized cooperative perception framework.

A human-like driver model can aid the development of AVs by building an understanding of interactions among human drivers and AVs in a hybrid traffic, therefore facilitating an efficient and safe integration. The presented social driver model categorizes and defines the driver's psychological decision factors in mathematical representations (target force, object force, and lane force). A model predictive control (MPC) is then employed for the motion planning by evaluating the prevailing social forces and considering the kinematics of the controlled vehicle as well as other operating constraints to ensure a safe maneuver in a way that mimics the predictive nature of the human driver's decision making process. A hierarchical model predictive control structure is also proposed, where an additional upper level controller aggregates the social forces over a longer prediction horizon upon the availability of an extended perception of the upcoming traffic via vehicular networking. Based on the prediction of the upper level controller, a sequence of reference lanes is passed to a lower level controller to track while avoiding local obstacles. This hierarchical scheme helps reduce unnecessary lane changes resulting in smoother maneuvers.

The dynamic vehicular communication environment requires a robust framework that must consistently evaluate and exploit the set of communicated information for the purpose of improving the perception of a participating vehicle beyond the limitations. This dissertation presents a de-

centralized cooperative perception framework that considers uncertainties in traffic measurements and allows scalability (for various settings of traffic density, participation rate, etc.). The framework utilizes a Bhattacharyya distance filter (BDF) for data association and a fast covariance intersection fusion scheme (FCI) for the data fusion processes. The conservatism of the covariance intersection fusion scheme is investigated in comparison to the traditional Kalman filter (KF), and two different fusion architectures: sensor-to-sensor and sensor-to-system track fusion are evaluated.

The performance of the overall proposed framework is demonstrated via Monte Carlo simulations with a set of empirical communications models and traffic microsimulations where each connected vehicle asynchronously broadcasts its local perception consisting of estimates of the motion states of self and neighboring vehicles along with the corresponding uncertainty measures of the estimates. The evaluated framework includes a vehicle-to-vehicle (V2V) communication model that considers intermittent communications as well as a model that takes into account dynamic changes in an individual vehicle's sensors' FoV in accordance with the prevailing traffic conditions. The results show the presence of optimality in participation rate, where increasing participation rate beyond a certain level adversely affects the delay in packet delivery and the computational complexity in data association and fusion processes increase without a significant improvement in the achieved accuracy via the cooperative perception.

In a highly dense traffic environment, the vehicular network can often be congested leading to limited bandwidth availability at high participation rates of the connected vehicles in the cooperative perception scheme. To alleviate the bandwidth utilization issues, an information-value discriminating networking scheme is proposed, where each sender broadcasts selectively chosen perception data based on the novelty-value of information. The potential benefits of these approaches include, but are not limited to, the reduction of bandwidth bottle-necking and the minimization of the computational cost of data association and fusion post processing of the shared perception data at receiving nodes. It is argued that the proposed information-value discriminating communication scheme can alleviate these adverse effects without sacrificing the fidelity of the perception.

Dedication

To my wife, Hannah, and to our little ones, Winslow and Isla, for their unconditional love and support, and to my mother, Ok-Kyung, for her lifelong sacrifices and wisdom.

Acknowledgments

I would like to express my sincere gratitude to my advisor, Professor Beshah Ayalew, who gave me the opportunity to pursue this journey and also patiently provided consistent guidance and invaluable advice throughout my study at CU-ICAR. My grateful thanks are also extended to my advisory committee members, Dr. Jim Martin, Dr. Yunyi Jia, and Dr. Matthias Schmid for their helpful suggestions.

I am greatly indebted to my life mentors, Dr. Charles Woody and Dr. Sandra Weber, for their wise counsel, loving inspiration, and enthusiastic encouragement, and to my true friends, Chris Woody and Macon McLean, for our special friendship that words cannot describe.

Lastly, I would like to give special thanks to my wife, Hannah, my father, Chan-Hong, my mother, Ok-Kyung, my brother, Sung-Hyun, my uncle, Inho, my aunt Sara, my parents-in-law, Chang and Hea, and my brother-in-law Paul for their care and support.

Table of Contents

List of Tables

List of Figures

Chapter 1

Introduction

The automotive industry has always been ever-changing with innovative technologies that improve the comfort, the safety, and/or the performance of automobiles. In the last decade, the field of automotive research has been revolutionized again with the introduction of vehicle autonomy and connectivity fueled by the development of advanced sensors and vehicular communication networks. Modern vehicles are being equipped with various types of on-board sensors including radar, LiDAR, camera, GPS, etc. as well as communication devices that allow vehicular connectivity via Dedicated Short Range Communication (DSRC) standard, cellular communication (3G, 4G LTE, or 5G C-V2X), or Wi-Fi, to aid the driver's perception of the road and traffic environment. Previewed horizon data (i.e. eHorizon data) such as predicted traffic motions, traffic signal timings, etc., are also available to provide additional information beyond one vehicle's restricted sensor Field-of-View (FoV) perception in real-time. All of this information can now be used to improve situational awareness and to compute energy-optimal motion/manuever plans for autonomous vehicles. Such technologies give significant advantages over traditional safety and control systems as it enables the ego-vehicle to know or accurately predict the motion of surrounding vehicles with improved traffic perception. As more vehicles adapt these technologies, the benefits will be amplified for vehicular traffics. With the on-going endeavor to create even safer yet more efficient transportation systems, these technologies are expected to be the crucial drivers for realizing the concept of connected traffic.

In the near future, road vehicles at all levels of automation and connectivity are expected to coexist. To allow these vehicles to operate safely in such an environment, understanding the inter-vehicular interactions and having a reliable situational awareness will be essential. First, un-

derstanding the interaction between human operated vehicles (HOVs) and autonomous vehicles (AVs) will be vitally important. Social driving models that capture the characteristics of HOVs can explain human-driving controls and its interactions with others. Second, vehicular network can be utilized to not only enhance the accuracy of the Field-of-View (FoV) perception but also to extend the perception boundary further. This enhancement and extension have a great potential in vehicular safety and motion planning applications. In the following section, these issues are discussed further along with reviews of existing literature.

1.1 Research Motivation

1.1.1 A Social Driver Model

The development of advanced driver models has been at the center of automotive research for several decades. From maneuver planning, lane change, to collision avoidance, numerous variants of driver models have been developed for traffic simulation studies as well as for refining advanced driver assistance systems (ADAS) [6, 30, 78]. One critical issue that many studies emphasize is the importance of developing human-like driver models. In an hybrid traffic environment where human operated vehicles (HOVs) and fully autonomous vehicles (AVs) coexist, the interaction between the two groups is inevitable and understanding the human-like psychological decision-making and planning processes becomes a crucial factor. While each system may utilize its own prediction or estimation model for tracking nearby object vehicles, rule-based or conventional vehicle control strategies are fundamentally different from the way human drivers behave. A human-like social driver model can not only benefit in the development of AVs but also help understanding of behaviors of human drivers and their interactions with AVs in traffics [19, 42, 144], thereby facilitating an efficient integration of hybrid traffic.

An early version of the social force model (SFM) was first proposed in 1998 by Helbing in [47] to model pedestrian movements. Social forces represent a measure for the internal motivations of the individuals to perform certain actions that determine their navigation behavior. While it is not a physical measure of any direct force, a social force can be interpreted as a psychological pressure that is indirectly exerted from the environment. The social force is divided into three different types for pedestrian applications: destination force, repulsive force, and attractive force. The destination force describes the willingness to reach the destination, which is the main drive

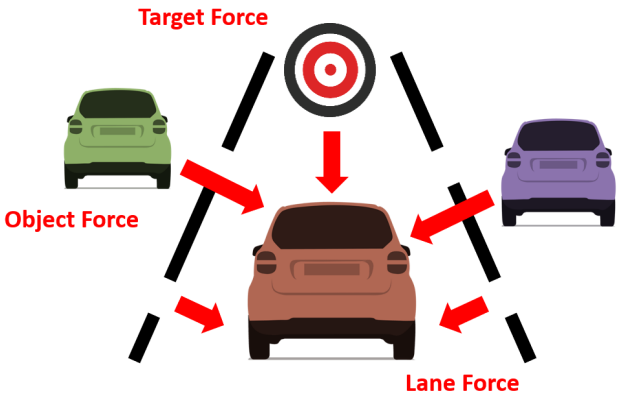

Figure 1.1: Vehicular Social Forces

force to move the subject forward. The repulsive force describes the subject's intention to avoid obstacles while the attractive force represents the opposite behavior. Similar social forces can be conceived to be at play when humans operate/drive vehicles in traffic. In particular, one can identify target force/attractor associated with reaching a destination, object forces/repulsors for collision-avoidance, and lane forces for road lane keeping. In the following chapter, we detail how these constituent forces may be modeled and used for vehicle control/driver modeling.

A number of researchers have already shown promising results of implementing the SFM for analyzing vehicular traffic. The collision risk of bicycle-car is analyzed in a shared space by using SFM to model the interactions among the subjects in the traffic in [71]. A mixed flow of electric bike-car is studied with a microscopic model that adopts SFM and simulates the flow in [98]. Using the same model, a lane-changing behavior of a vehicle in a car-only traffic is demonstrated in [45] but without considering vehicle dynamics. All of the studies mentioned above did not adopt any control strategy to optimize the input of the ego vehicle nor significantly modify the pedestrian SFM with a view to enhance its performance when used with vehicular traffic. A vehicle dynamics model is considered along with a PID controller that transforms the social forces into control inputs in [136]. Therein, the steering angle was computed by a simple PID controller and the longitudinal acceleration of the vehicle was managed by a rule-based control. Most of the studies mentioned above use SFM to model the equation of motion for multiple agents (pedestrians or vehicles) without any optimization of the total social force. In this dissertation, a vehicular SFM is proposed considering vehicle dynamics and both longitudinal and lateral actuation, and a nonlinear model predictive control (NMPC) framework is used as the predictive constrained optimization for an autonomous

vehicle control and prediction. The proposed scheme is presented in Chapter 2.

1.1.2 Cooperative Perception

Another primary requirement for operating in the hybrid traffic mentioned above is the ability to construct a reliable situational awareness for each automated vehicle. An accurate perception of other vehicles in traffic is a crucial element of emerging intelligent vehicle applications, such as advanced driver assistance system (ADAS), automated driving, platooning, etc. The perception constructed by one ego-vehicle is often limited to information that can be gathered by its own on-board sensors including GPS (Global Positioning System), radars, LIDARs, and cameras. The fidelity of the perception that can be achieved by these sensors is restricted by their technical limitations and is highly environment-dependent (e.g. lighting, obstacles, etc). Available GNSS (Global-navigation-satellite-system)-based GPS receivers suffer from positioning errors up to tens of meters [74, 16], and as such cannot be relied upon for accurate localization by themselves. Often a fusion of several on-board sensors is used to create a Field of View (FoV) for the ego vehicle, but the fused perception still inherits the limitations of the on-board sensors. Cooperative perception, where vehicles share their locally obtained information via a communication network, can help circumvent these limitations.

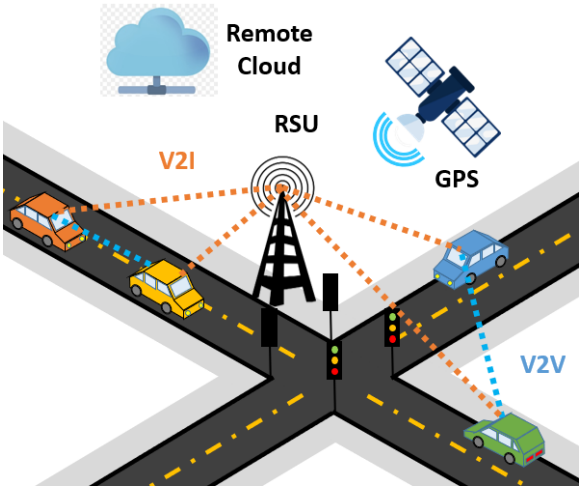

Figure 1.2: Vehicular Communication Network

The simplest form of a cooperative perception strategy involves Basic Safety Messages (BSM) which is standardized by the Society of Automotive Engineering (SAE). Each BSM only

includes the sender's ego-vehicle information such as location, velocity, driving direction, etc, and this type of messages is also referred as Cooperative Awareness Messages (CAM). The simple architecture and its relatively low payloads, 49 Bytes in average [75], make it attractive especially for emergency and safety applications [130]. However, due to the limited information given in each message, a high participation rate is often essential to fully capture the traffic environment especially in a highly dense vehicular traffic. European Telecommunications Standards Institute (ETSI) is continuing to develop and standardize cooperative messages that contain information about the surrounding traffic (object vehicles within sensor FoV) in addition to those of the ego-vehicle [113, 126]. Such messages are widely known as Cooperative/Collective Perception Messages (CPM) or Environmental Perception Messages (EPM). Since each message consists of information on multiple vehicles, the average packet size is much greater than the BSM.

The exchange of CPM can be readily supported by V2V standards such as DSRC, which can support data rates of 4.5 to 27 Mbps, as demonstrated by several studies [86, 4]. The experimental analysis of communication parameters based on IEEE 802.11p in [100] demonstrated the applicability of DSRC for V2X-based cooperative perception. Closely related to the concept of cooperative perception strategies, Simultaneous Localization and Mapping (SLAM) as well as see-through perception technologies have also been introduced to achieve more detailed visual perception of the environment [137, 86, 62]

In the literature, a common cooperative perception or localization strategy uses an ad hoc trilateration technique to fuse the received position information from Received Signal Strength Indicators (RSSIs) of received BSM / CAM (Cooperative Awareness Message) of neighbor vehicles with on-board GNSS-based position estimates [61, 53, 54, 52]. The absolute and relative position estimates through Vehicle to Vehicle (V2V) or Vehicle to Infrastructure (V2I) (or generically (V2X)) communication are analyzed in a distributed manner in [70]. By sharing positions, pseudo-range estimated errors and DR (Dead Reckoning) in the distributed environment, the position estimate is enhanced by applying set-inversion and constraint-propagation techniques. A number of works have demonstrated potential benefits of the extended view of a V2X-enabled vehicle using cooperative perceptions from gathered sensory data in vehicle maneuver planning and control as well as energy management [141, 114, 117, 63, 64]. A likelihood-based weighted average method is proposed in [35] to discover non-DSRC equipped vehicles and estimate the position of equipped vehicles through wirelessly exchanging sensor information. A Kalman Filter (KF) or an Extended Kalman Filter

(EKF) is the most commonly used method to fuse multiple groups of information ranging from on-board ranging sensors, DSRC transceivers and GPS receivers for improving the perception of nearby vehicles [109, 96, 145, 103, 106, 77, 87]. A number of studies adopt Particle Filters (PF) for more accurate and robust simultaneous localization and mapping (SLAM) [56, 128, 84, 20] with increased computational complexity as a tradeoff.

1.1.3 Data Processing Architectures for Cooperation

Vehicular data sharing and management is a broad-ranging field of research. At one level, there are many studies on medium access channel assignment mechanisms [37, 69, 82] as well as data forwarding and routing mechanisms [138, 150, 146, 147, 4] intended to improve the reliability and performance of vehicular networks. In this dissertation, we focus on the lower level algorithms and evaluations of cooperative perception schemes given a V2V broadcast network of participating vehicles in traffic.

Two commonly proposed architectures for cooperative perception can be identified in the literature. The first is a sensor-level distributed fusion framework in which each participating vehicle shares minimally pre-processed on-board sensor data. Such a framework is commonly adopted in cooperative Simultaneous Localization and Mapping (SLAM) where participating agents contribute to the construction of a detailed map of the surroundings [137, 62]. This deals with large packets of data (sensor point clouds, or compressed images/videos) and is, therefore, severely constrained by the bandwidth limitation of vehicular networks [86]. Furthermore, as the number of participating connected vehicles increases, the computational demands increase significantly as each fusion node/vehicle must manipulate large data sets [41, 64]. To address these limitations, the use of infrastructure-based Roadside Units (RSUs) is proposed to perform the data processing and to relay processed information to vehicles thereby reducing the computational, if not the communication, burdens for each vehicle [148, 15]. To reduce the complexity at the fusing node without the use of such road-side infrastructures, other studies have proposed effective mapping techniques to achieve a global map with lower computational complexity [64, 22, 84]. Still another major difficulty that limits the applicability of sensor-level fusion is the lack of general data modularity at the sensor level [101]. As each raw sensor data will have a specific format and defined characteristics, performing a consistent data association and fusion process can be difficult without knowing the specifications of the sensors at the fusing nodes.

The second is a vehicle-level cooperative perception architecture in which each participating vehicle communicates only processed track data. A modern ego-vehicle has its own integrated data processing unit to process local sensor FoV information and to generate tracks of objects in the traffic around the ego-vehicle. Communicating such track data (composed of state estimates often with corresponding covariances) [44, 119, 35] significantly reduces the bandwidth requirements while providing high data modularity to work with heterogenous capabilities of the participating vehicles. These track data can be efficiently handled via track-to-track fusion schemes [101]. The most studied and minimalist version of these vehicle-level cooperative perception architectures involve exchanging of BMS or CPM [81, 86, 4]. A communication network solution for sharing CAM or CPM is demonstrated based on IEEE 802.11p in [100].

It is this second architecture that is adopted in this dissertation. Here, some of other related works that exploited this second architecture are highlighted. A high-level data processing architecture of CAM and CPM in V2X-based cooperative perception systems was demonstrated in [101, 102] focusing on the spatial and temporal alignments of the communicated data [101] and the data association process using Auction-ICP (Implicit Cooperative Positioning) algorithm [102]. In [119, 18], another set of ICP data association methods were proposed where connected vehicles share additional CPMs of passive features in the driving environment in order to enhance the association process of the shared localization data. The results demonstrated that the proposed method outperformed the conventional Global Navigation Satellite Systems (GNSS). A robust cubature Kalman filter (CKF) was proposed in [73] to enhance the utilization of GNSS data with a DSRC network under uncertain sensor observation environments. The performance of various data fusion methods for CPMs were compared for a real time cooperative localization in [17]. A decentralized Bayesian-based approach was proposed in [104] to improve GPS vehicle position estimates using vehicular ad hoc network (VANET)-based inter-vehicle distance measurements. A Sequential Monte-Carlo Probability Hypothesis Density (SMC-PHD) filter for GPS data association and fusion is proposed in [41] and showed a three fold increase in localization accuracy. The central limit theorem for classification of estimates is presented in [35] and claimed an 85% improvement compared to GPS-only estimates at a signalized intersection. The details of the adopted architecture and its associated methods are discussed further Chapter 3 and 4.

1.1.4 Vehicular Data Association and Fusion

Since the cooperative perception schemes we focuse on operate based on broadcast data without commonly interpretable object tags, participating vehicles have to deal with data association to sort/cluster received data before proceeding to fusion computations [102]. A Mahalanobis Distance (MD)-based Chi-square test is a widely adopted statistical method to evaluate the compatibility of data and associate the estimates from different sources [55, 109, 129, 90, 96]. The fundamental assumption for computing MD is that the distributions of two estimates are assumed identical. Since FoV perception estimates are obtained by vehicles of varying capabilities, and are likely to have distinct distributions, MD is unsuitable for vehicle-level data association. Bhattacharyya Distance (BD) gives a statistical measure of similarity between two distinct distributions, often over large distances in pattern space [3]. In this dissertation, we adopt the BD-based gating test to associate received track data.

There are also several choices of methods for the fusion computations. A Bayesian-based approach is perhaps the most popular formulation for a sensor-level data fusion [55, 103, 38, 124] as well as for a higher-level fusion dealing with heterogenous information ranging from on-board ranging sensors, DSRC transceivers and GPS receivers [109, 106, 77, 7]. Typically, these are reduced to multi-level Kalman Filters (KFs, regular, extended or unscented). A number of studies adopted Particle Filters (PF) for robust localization and mapping [56, 84, 20] with increased computational complexity as a tradeoff. A significant challenge in the fusion computations is in what to do with data correlation, i.e, double counting of information which leads to overconfidence in the fused estimates. This, for example, is a significant drawback of most Bayesian-based (and so, KF-based) approaches, which often ignore or assume no correlation in the received data in order to facilitate factorizing of the relevant distributions. In contrast, Covariance Intersection (CI) has been known for its ability to yield consistent fused estimates given an unknown degree of inter-estimate correlation [58, 25, 72]. In [17], CI-fused estimates showed higher accuracy compared to extended KF-based ones and the variance in estimated moving direction of vehicles is significantly reduced. In [113], various CI methods are evaluated for active road safety applications (e.g. BSM, CAM networks), and the suitability of the Improved Fast Covariance Intersection (I-FCI or FCI) is demonstrated. In [46], Split Covariance Intersection Filter (SCIF) is proposed for localization of a single chain of road vehicles and achieved more accurate cooperative multi-vehicle localization than an extended

KF. The superior performance of Fast CI in comparisons to KF in road vehicle data fusion is also noted in Chapter 3 along with the adopted fusion approach.

1.1.5 Effects of Participation Variations in the Connected Traffic

An important line of inquiry in studies on cooperative perception has been the question of the effect of the rates of participation of the connected vehicles(equipped vehicles) in the cooperative perception scheme. The participation rate is often interpreted as the level of penetration of technologically equipped vehicles in the prevailing traffic. Most evaluations of the perception schemes with regard to participation/penetration rates seem to have been done in closed-loop. That is, the participating vehicles (their human/automated drivers) were made to respond to and/or act on the collaboratively computed perception. In [83, 43], it was shown that a higher number of connected vehicles reduced the impact of aggressive behaviors in traffic as cooperation increased the stability domains and homogenized the traffic. In [119], an improvement in the Root Mean Square Error (RMSE) of the position estimates was noted with increasing number of connected vehicles when an implicit cooperative positioning (ICP) algorithm was used. In [91], an extended multi-class gas-kinetic theory was used to model the dynamics of cooperative traffic where connected vehicles share a warning message about downstream congestion. A critical participation rate that avoids traffic flow instabilities and eliminated shock waves was found to be around 50% under their assumed model. In [35], the recognition ratio, defined as the average ratio of the vehicles whose positions are estimated uniquely within a set Euclidean threshold distance to all vehicles within the evaluation region, was shown to gradually increase with increasing participation rate. It was also noted that the recognition ratio plateaus near 80% participation rate with slightly above 80% recognition ratio. [44] defined an awareness ratio as the ratio of the number of unique vehicles known to the ego-vehicle to those within the communication range. They used this metric to evaluate the collective perception with varying communication message types and participation rates. They showed a superior performance for the cooperative perception over radar-only perception, with full participation (100%) achieving a perfect awareness ratio. On the other end of the spectrum, in [9], the importance of performance at low participation rates was highlighted for the near future scenario when only a small fraction of the vehicles in traffic will be utilizing the vehicular connectivity for cooperative perception. In Chapter 2 and refchapter3, we introduce a modification of the Optimal Sub-pattern Assignment (OSPA) metric [112] and illustrate its use to evaluate the achieved "accuracy" of cooperative perception in

dynamic traffic (Section 4.3.7). This modified metric allows us to naturally take into account effects, not only of the estimation uncertainty, but also of the dynamic and random changes in sensor FoV (obstructions) and communication losses (path losses, drops and fades) towards the computed state estimates and cardinality errors.

1.1.6 Limitations of Vehicular Networks

In spite of the potential advantages of V2V cooperative perception, a number of critical requirements and limitations still exist. A cooperative perception strategy generally requires a high level of participation rate to ensure robust performance [91, 35]. In [35, 83, 44, 43], the performance of cooperative perception (as measured by some metrics involving average position estimation or object recognition errors) is shown to monotonically improve with increase in participation rates. One significant drawback of high participating rates is that the grow in data traffic loads can be exponential. The generation and the dissemination of messages is a critical parts of a CPM management. Many of existing standardized strategies follow a set of rule-based methods to generate CPMs where the system parameters are determined experimentally. Such frameworks seem easy to implement for a wide range of applications as they do not require sophisticated tuning algorithms. The ETSI standards, for example, state three main CPM generation conditions that consider the changes in absolute position ($> 4m$), speed ($> 0.5m/s$), and communication interval ($> 1sec$) [32], and all detected object vehicles that satisfy at least one of the conditions are to be included in the CPM to be broadcasted. In a dynamic environment (e.g. high density highway traffic), such a method can be inefficient as it would frequently generate a new set of CPM on a limited number of vehicles. This is undesirable as each CPM requires a header which accounts for a significant portion of the packet size regardless of the number of object vehicle information included. In [126], the conditions are modified by predicting the states of object vehicles and their qualification of the CPM generation conditions for the next planned communication and transmitting them in the current CPM. The proposed method resulted in a better utilization of the communication channel by reducing the CPM generation rate. While such a strategy may have potential benefits managing the communication of CPMs in a predictable environment, a simple rule-based periodic broadcasting strategy can be ineffective due to the dynamic nature of vehicular traffic especially in a congested and unpredictable road traffic situations [79].

To achieve more robust and effective performance, one can rely on distributed or decen-

tralized schemes which allow each participant to evaluate and make decisions on the contents of its CPM considering their potential impact on the cooperative perception. To this end, each participant should evaluate not only the quality of the information (e.g. position errors), but also some notion of the value of information. For detailed definitions and discussions of these notions, we refer the reader to [13, 50, 40]. In the present context, the focus is on the value of information included in CPM. One attribute of value is the degree to which redundancy is avoided, or equivalently, to which the novelty of information in emphasized. For example, in [127], the ETSI standards are further improved where the CPM generation frequency is adjusted based on the presence of corresponding object vehicle information in the recently received CPM from other connected vehicles to reduce the redundancy of information in the pool of communicated CPM. In [40], an adaptive generation rule that conditionally removes Sensor Information Container (SIC) from CPM based on a set threshold of Access Layer (AL)-specific Maximum Transmission Unit (MTU) is proposed for ETSI standards to reduce the packet size. The result showed a similar service quality as the standard static rule while significantly reducing the overall channel load. In [50], a value-anticipating scheme is proposed where each participating vehicle evaluates the value of its perception information from the perspective of receivers by leveraging anticipated CPM history as well as inferences about the communication network status. In this strategy, each piece of information in a CPM is selected based on its relative entropy with respect to the recorded CPM histories of remote vehicles and their expected prior knowledge about the specific information. The feasibility of the strategy is demonstrated where increased packet reception ratio and reduced object tracking errors are reported. In [79], a dynamic dissemination method is proposed where the expected position error of each perception measurement is evaluated based on a set threshold to dynamically adjust the communication interval. In an urban traffic simulation, the proposed method achieved 20% improved perception accuracy. In this dissertation, we present a V2V cooperative framework that evaluates the novelty of information by comparing the new perception information to be communicated with historical communication data. In this framework, each participating vehicle is able to evaluate the value of the message contents in the current communication network without any anticipation or assumption on other vehicles' perspective. The details of the proposed framework will be discussed in Chapter 4.

1.2 Contributions

The main contributions of the dissertation can be summarized as follows:

- A social driver model is developed to provide a human-like driver model. By representing internal motivations of human drivers and their decision processes, the completed model is expected to be feasible as an autonomous vehicle control model and also as a motion prediction model for other human operated vehicles in traffic.
  - *D. D. Yoon and B. Ayalew, "Social Force Control for Human-Like Autonomous Driving", Proceedings of the ASME 2018 International Design Engineering Technical Conferences & Computers and Information in Engineering Conference (IDETC 2018), August 2.*
- A social driver model controller that leverages vehicular connectivity is developed by adopting a hierarchical (two-level) predictive architecture to utilize communication information among vehicles in traffic. The extended perception provided by the vehicular connectivity allows more efficient plan and control of the vehicle (e.g. optimal lane change).
  - *D. D. Yoon and B. Ayalew, "Social Force Aggregation Control for Autonomous Driving with Connected Preview," 2019 American Control Conference (ACC), 2019, pp. 1388-1393, doi: 10.23919/ACC.2019.8814725.*
- A decentralized cooperative perception framework that allows scalability, with variable participation in the communication scheme (changing traffic density, non-connected vehicles, road topology, etc.), is developed. By evaluating the performance of the framework via a Monte Carlo approach, valuable insights will be provided for devising an effective implementation of the framework with an intent of optimizing resource utilization (communication network bandwidth and computational complexity).
  - *D. D. Yoon, G. G. M. N. Ali and B. Ayalew, "Data Association and Fusion Framework for Decentralized Multi-Vehicle Cooperative Perception", Proceedings of the ASME 2019 International Design Engineering Technical Conferences and Computers and Information in Engineering Conference IDETC/CIE2019, August 18-21, 2019.*
  - *D. D. Yoon, G. G. M. N. Ali and B. Ayalew, "Cooperative Perception in Connected Vehicle Traffic under Field-of-View and Participation Variations," 2019 IEEE 2nd Connected and Automated Vehicles Symposium (CAVS), 2019, pp. 1-6, doi: 10.1109/CAVS.2019.8887832.*

  - *D. D. Yoon, B. Ayalew and G. G. M. N. Ali, "Performance of Decentralized Cooperative Perception in V2V Connected Traffic," in IEEE Transactions on Intelligent Transportation Systems, doi: 10.1109/TITS.2021.3063107.*

- A novelty-value discriminating method is developed that works in a decentralized manner and allows each participating vehicle to filter communicable Field-of-View (FoV) perception data based on the novelty-value of information prior to broadcasting it in the vehicle-to-vehicle (V2V) communication network. The framework will improve bandwidth utilization and latency without significant compromises on the average cooperative perception metric for participants.
  - *D. D. Yoon and B. Ayalew, "A Novelty Discrimination Method for V2V Decentralized Cooperative Perception," in IEEE Transactions on Vehicular Technology, 2021 (In Review)*

The following list of work has also been completed during the dissertation. The details of these studies are not included, although some of the tools are related, the specific topics are deemed out of scope of the dissertation.

- *D. D. Yoon, B. Ayalew, A. Ivanco, and K. Loiselle, "Predictive Kinetic Energy Management for an Add-on Driver Assistance Eco-driving of Heavy Vehicles," in IET Intelligent Transport Systems, 2020, 14(13), pp.1824-1834.*
- *D. D. Yoon, B. Ayalew, A. Ivanco and Y. Chen, "Predictive Kinetic Energy Management for Large Electric Vehicles using Radar Information," 2020 IEEE Conference on Control Technology and Applications (CCTA), 2020, pp. 82-87, doi: 10.1109/CCTA41146.2020.9206307.*
- *L. Kerbel, D. D. Yoon, K. Loiselle, B. Ayalew, and A. Ivanco, "Assessment of Driver Assistance Controls for Efficient Driving in Randomized Traffic," in IET Intelligent Transport Systems, 2021 (In Review)*
- *H. Zomorodi, D. Yoon and B. Ayalew, "Use of Predictive Information for Battery pack Thermal Management," 2017 American Control Conference (ACC), 2017, pp. 5020-5025, doi: 10.23919/ACC.2017.7963733.*

1.3 Dissertation Organization

The dissertation is organized as follows. In Chapter 2, a social driver model is presented with a nonlinear model predictive controller (NMPC) to mimic the predictive planning behavior of social human drivers. A hierarchical control scheme is also presented to exploit vehicular connectivity and integrate extended perception information into more efficient maneuver planning. In Chapter 3, a unified cooperative perception framework that employs vehicle-to-vehicle (V2V) connectivity is presented along with a decentralized data association and fusion process that is scalable with respect to participation variances. In Chapter 4, a novelty discrimination method for decentralized cooperative perception is presented for the reduction of bandwidth bottle-necking and the minimization of the computational cost of data association and fusion post processing of the shared perception data at receiving nodes. Then Chapter 5 summarizes the main conclusions and points out directions for further research.

Chapter 2

Social Force Model Control for Human-like Autonomous Driving[1]

2.1 Abstract

An autonomous driving control system that incorporates notions from human-like social driving could facilitate an efficient integration of hybrid traffic where fully autonomous vehicles (AVs) and human operated vehicles (HOVs) are expected to coexist. This chapter aims to develop such an autonomous vehicle control model using the social-force concepts, which was originally formulated for modeling the motion of pedestrians in crowds. Nonlinear model predictive control (NMPC) scheme is formulated to mimic the predictive planning behavior of social human drivers where they are considered to optimize the total social force they perceive. In addition, an extended preview afforded by vehicular connectivity can be exploited to bring additional information about downstream traffic to be incorporated in the planning and guidance computations for an autonomous vehicle. For this purpose, a hierarchical vehicular social force control scheme that integrates both ideas is also presented. At the upper level, social force aggregation is applied to predictively select the

[1]The contents of this chapter have appeared in conference publications:

- *D. D. Yoon and B. Ayalew, "Social Force Control for Human-Like Autonomous Driving", Proceedings of the ASME 2018 International Design Engineering Technical Conferences & Computers and Information in Engineering Conference (IDETC 2018), August 2.*
- *D. D. Yoon and B. Ayalew, "Social Force Aggregation Control for Autonomous Driving with Connected Preview," 2019 American Control Conference (ACC), 2019, pp. 1388-1393, doi: 10.23919/ACC.2019.8814725.*

most efficient lane over a long horizon covered by connectivity. This is then passed down to a lower level controller that enforces lane tracking while considering higher fidelity social force resolution and lane-changing dynamics within the shorter horizon captured by the ego vehicle's sensor field of view. The workings and performance of the proposed framework are illustrated via simulations of the connected autonomous vehicle in multi-lane highway scenarios.

2.2 Introduction

The social force model (SFM) was first introduced by Helbing [47] in 1995 to model pedestrian movements. Social forces can be thought of as Newtonian interpretations of the psychological pressure exerted on a human subject from the surroundings. They are quantitative representations of the internal motivations for the maneuvering actions (heading and speed selections) of humans walking in crowds/traffic. Considering the significant similarity between a pedestrian and a human driver in their maneuver planning, a few recent works have considered the use of the notion of the SFM to model social behaviors of human drivers (or human-driven vehicles) in traffic [71, 98, 45, 136]. However, the demonstrations were mostly limited in sophistication to simple PID-like feedback controllers that regulate the total social force to its minimum.

A human-like autonomous driver model using SFM is presented in a nonlinear model predictive control (NMPC) framework. The NMPC framework is a natural choice as the predictive constrained optimization seems to parallel or at least model the navigation decisions made by human drivers. Based on the data received through sensory perception, human drivers endeavor to predict and analyze the behavior of other vehicles before executing the next move. The generic framework of NMPC bears a resemblance to such a process very well. This has been explored in a number of studies, [28, 107, 94].

In mathematical terms, this SFM formulation differs from other NMPC formulations proposed for autonomous vehicle guidance [134], where cost functions involved path and speed tracking errors while obstacles and lanes are expressed as constraints, including in probabilistic terms [132]. Therein, finite state machines (FSMs) or rules are often listed to dictate lane change and other pre-defined discrete driving states [134, 67]. These are executed outside optimization or result in mixed integer programs (as in choosing between lanes), which in turn require a relaxation that increases the dimensionality of the optimization problem to be solved at every update [133] (e.g. by

a number of lane selection variables). The formulation presented here, however, does not require such rule-based assigners for treatment of lanes or objects. The overall concept of the presented approach rather resembles potential field methods (PFM) [66, 118]. By minimizing the social force potentials along the path of travel, it provides an alternative method for formulating autonomous driving without additional rules or such accommodations [67]. In the following section, we detail the NMPC formulation where we consider the driver to optimize the total social force experienced in the presence of obstacles, lanes and a description of a target.

The potential of vehicular connectivity towards enabling more efficient and safer traffic has been widely explored [151, 117]. Vehicular communication allows participating vehicles to engage in cooperative perception, where connected vehicles collect and share information about their observations (and intentions) of the surroundings thereby enhancing participants' awareness of the neighboring or upcoming traffic [63, 100]. Having such communicated information enables more efficient maneuvering that may reduce unnecessary lane changes or speed selections by incorporating what is beyond the limited field of view (FOV) of the ego vehicle's on-board sensors. In the presented scheme, the SFM NMPC formulation is refined by integrating hierarchy in the social force aggregation which makes it even more attractive for socially-inspired guidance of an automated ego vehicle in a connected traffic. To do so, an upper traffic-level social force controller is introduced which generates a reference trajectory based on such communicated data with long spatial preview and passes it for a lower level social force controller to follow. As we shall detail in this chapter, the two controllers would use different evolution models and compute their respective optimal solutions by evaluating different cost functions. While they also execute at different sampling rates, the overall control scheme achieves a coherent guidance of the ego vehicle.

The hierarchical approach is indeed a commonly used approach to manage the complexity of motion planning from guidance of autonomous ground robots [85, 97] to aerial flight control [31, 10]. For road vehicles, hierarchical formulations abound, including those mentioned above that use finite state machine assigners as upper level generating references for lower level NMPC trackers [132, 133, 67, 111]. There are also proposals to use hierarchical two-level MPC that delegate the path planning and path tracking objectives to the two levels [33]. A key observation of the hierarchical approaches is that pre-computing feasible references for the lower-level control using upper level schemes helps reduce the computational cost of the lower level controller and leads to a more robust performance for the overall guidance scheme. In this chapter, we exploit these observations in the

specifics of our proposed hierarchical social-force control scheme.

2.3 System Framework and Modeling Details

The schematic of the proposed framework is shown in Figure 2.1. Object vehicle locations and speeds are detected through the environmental perception module (on-board sensors and processing) and transmitted to the lower level MPC. Therein, the SFM and a suitable vehicle dynamics model are used to compute the optimal set of inputs (steering angle and accelerations) for the ego vehicle. If we consider communicated information acquired via vehicular connectivity (V2V, V2I) on vehicles in traffic that include those beyond the FOV of the on-board sensors, the upper level control must be used. The communicated information is considered to be used mainly in the upper level controller although for those vehicles within the FOV, the communicated information can be fused with the FOV to enhance the lower level control.

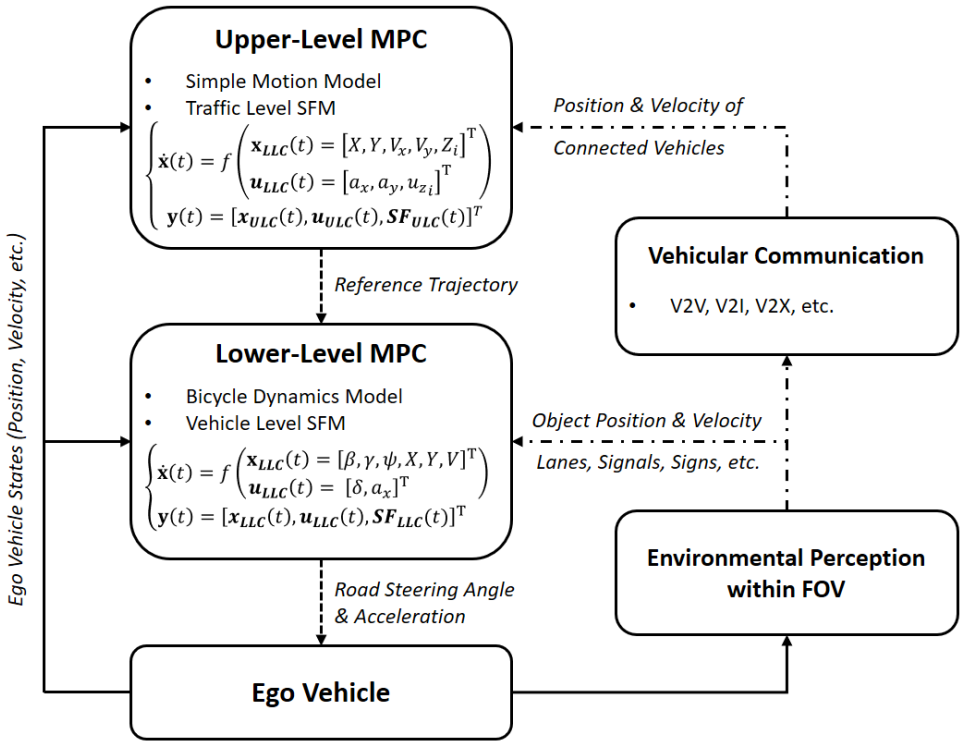

Figure 2.1: Overview of the Social Force Model Framework

While the SFM will be used in both levels of the hierarchy, we adopt different social force aggregations in the two levels. The upper level aggregates object social forces for each lane in the

communication range along with a simpler motion model therefore optimizing newly introduced lane selection variables. The lower level maintains a detail accounting of all vehicular social forces in the field of view irrespective of the lane position. In cases where the vehicular network is unavailable or the SFM is being purposed as a simple controller or as a prediction model for human operative vehicles, simply only the lower level controller scheme can be utilized. This has been also demonstrated in 2.4.2. It is important to note that the two controllers deal with different dynamics and different preview and prediction horizons. At the upper level, which typically has the longer preview than the on-board sensor FOV, coarse sampling and MPC update rates can be adopted, while at the lower level where higher resolution plans are needed for immediate use the prediction horizon and the sampling rates will be shorter and faster, respectively.

2.3.1 Social Force Model

The social force model (SFM) includes the following four components.

2.3.1.1 Target Social Force

The purpose of the target force is to encourage the vehicle to reach the target as soon as possible. It is formulated as:

$$SF_T = |V_{ego} - V_{max}| \tag{2.1}$$

where V_{ego} is the current ego vehicle speed and V_{max} is the maximum allowable speed on the road. Minimizing the energy associated with this force, $SF_T^2 = (V_{ego} - V_{max})^2$, encourages the vehicle to continuously attempt to maintain the maximum velocity thereby ensuring the vehicle to travel as fast as possible. V_{ego} will also be constrained not to exceed V_{max}.

2.3.1.2 Object Social Force

Object force is the most important social force that models collision-avoidance behavior. This social force is represented as a repulsive force acting on the vehicle and modeled with the monotonically decreasing function:

$$SF_O = K_1 \left(\frac{1}{S_j - D_{BD}} - \frac{1}{D_{LAH} - D_{BD}} \right) \tag{2.2}$$

where D_{LAH} ($\approx 200m$) is the look-ahead visual distance of the vehicle, D_{BD} ($\approx V_{ego} \bullet t_b$) is the safety braking distance corresponding to a braking time t_b ($= 2 \sim 3s$), K_1 is a scaling factor, and S_j is the major axis of the hyper elliptical region:

$$S_j = \sqrt[n]{\frac{1}{K_2^n}(X_j - X)^n + (Y_j - Y)^n} \tag{2.3}$$

where (X, Y) is the position coordinate of the ego vehicle, (X_j, Y_j) is the position coordinate of object j , n is the order of the hyper ellipse, and K_2 is the ratio of the major to the minor axis of the hyper ellipse. The above formulation allows the object force to rise to infinity as the distance between the vehicle and an object nears the braking distance, $lim_{S_j \to D_{BD}} SF_O = \infty$, which ensures that no other social force components (target, lane, etc) can dominate in the total social force.

2.3.1.3 Lane Social Force

The lane force consists of two different parts. Assuming that the lane center reference is available, the first part of the lane force can be formulated as:

$$SF_{cen} = \left| Y - L_{cen} \left(\sum_{i}^{N_{lane}} Sig_i\,(Y) \right) \right| \tag{2.4}$$

where Y is the lateral position of the ego vehicle, and L_{cen} is computed from a look up function for the identified lane. Lane identification is done by using a set of sigmoid functions defined by upper and lower bounds:

$$Sig_i\,(Y) = \frac{1}{1+e^{-k\left(Y - L_{lower_i}\right)}} - \frac{1}{1+e^{-k\left(Y - L_{upper_i}\right)}} \tag{2.5}$$

where L_{upper_i} and L_{lower_i} are the bounds of each lane i $(1 \ldots N_{lane})$, and k is a constant that governs the smoothness of the sigmoid function. The second part of the lane force is to track the yaw angle error in reference to the curvature of the road. This is defined as:

$$SF_{agl} = |\psi - \theta_l| \tag{2.6}$$

where ψ is the yaw angle of the ego vehicle and θ_l is the angle representing the curvature of the road. This will ensure that vehicle heading angle is aligned with the curvature of the road. This portion of the lane force is important especially for stabilizing the lateral motion of the vehicle during lane

change.

$$SF_L = \begin{bmatrix} SF_{cen\,LLC} & SF_{agl\,LLC} \end{bmatrix}^T \tag{2.7}$$

The total energy associated with the lane social force is defined by simply taking the weighted sum of the squares of the two forces SF_{cen} and SF_{agl} with weights W_{cen} and W_{agl} applied to each part, respectively.

2.3.1.4 Tracking Social Force

In addition to the three main forces described above, another social force is defined the hierarchical controller scheme is being utilized with the upper level controller. This force takes the form:

$$SF_R = |Y - Y_{ref}(X)| \tag{2.8}$$

where Y_{ref} will be interpolated from the upper level planned trajectory at the current ego vehicle X-coordinate, X.

2.3.2 Lower Level NMPC Formulation

2.3.2.1 Motion Models for Lower Level NMPC

For the ego vehicle, we adopt the bicycle (single-track) vehicle dynamics model [29] considering the body slip angle, the yaw rate, the yaw angle, the X and Y coordinates, and the vehicle speed as the states of the system; the road steering angle and the vehicle longitudinal acceleration as the inputs. Then we consider object motions to follow simplified constant velocity models for the purposes of computing the social forces in the short prediction horizon of the lower level MPC which updates fast enough to make this assumption reasonable.

$$\begin{bmatrix} \dot{\beta} \\ \dot{\gamma} \\ \dot{\psi} \\ \dot{X} \\ \dot{Y} \\ \dot{V} \end{bmatrix} = \begin{bmatrix} -(\frac{C_1+C_2}{mV} + \frac{a_x}{V})\beta - \left(1+\frac{1}{mV^2}\left(aC_1-bC_2\right)\right)\gamma + \frac{C_1}{mV}\delta \\ -\frac{(aC_1-bC_2)}{I_z}\beta - \frac{1}{I_z V}\left(a^2C_1+b^2C_2\right)\gamma + \frac{aC_1}{I_z}\delta \\ \gamma \\ V(cos\beta cos\psi - sin\beta sin\psi) \\ V(cos\beta sin\psi - sin\beta cos\psi) \\ a_x \end{bmatrix} \tag{2.9}$$

The evolution model of the whole local traffic system can be written compactly as:

$$\begin{aligned} \dot{\mathbf{x}}_{\mathbf{LLC}}(t) &= f\left(\mathbf{x}_{\mathbf{LLC}}(t), \mathbf{u}_{\mathbf{LLC}}(t)\right) \\ \mathbf{y}_{\mathbf{LLC}}(t) &= \left[\mathbf{x}_{\mathbf{LLC}}(t), \mathbf{u}_{\mathbf{LLC}}(t), \ \mathbf{SF}_{\mathbf{LLC}}(t)\right]^{\mathrm{T}} \end{aligned} \tag{2.10}$$

where the states denoted with $\mathbf{x_{LLC}}$ are the ego vehicle and object motion states, the inputs are $\mathbf{u_{LLC}}$=$[\delta, a_x]^{\mathrm{T}}$, the steering and longitudinal acceleration, and f is vector function composed of the right hand side of 2.9 and of the constant velocity models for the traffic objects in the FOV. The social force vector aggregated for the lower level controller (LLC) is denoted as: $\mathbf{SF_{LLC}} = [SF_{TLLC} \ \ SF_{OLLC} \ \ SF_{LLLC} \ \ SF_{RLLC}]^T$. Note that the total object force SF_{OLLC} will be a force field peaking near all detected objects in the FOV. Note also that due to the state-dependent ego vehicle dynamics and the nonlinear object forces, the overall system is nonlinear.

2.3.2.2 Cost Function and Constraints for Lower Level NMPC

The objective of the lower level NMPC is optimizing the total social force, which is a measure of internal motivation or psychological pressure that drivers and autonomous vehicles that mimic human drivers, wish to minimize while allowing the vehicle to maneuver safely and travel as fast as possible. Each social force component described above needs to be weighted appropriately to achieve the desired behavior. For example, the weights on the object forces must be carefully adjusted to ensure comfortable and safe collision-avoidance behavior. However, only minimizing the social force does not guarantee feasible vehicle control without taking the control inputs into consideration. Therefore, the cost function is formulated as follows:

$$J_{LLC} = \sum_{k=0}^{N_{pLLC}} \left\|\mathbf{SF_{LLC_k}}\right\|_{Q_L}^2 + \sum_{k=0}^{N_{cLLC}-1} \left\|\mathbf{u_{LLC_k}}\right\|_{R_L}^2 \tag{2.11}$$

where $k \in \{0,\ N_{pLLC}\}$ the prediction step index, N_{pLLC} is the prediction horizon length, N_{cLLC} is the control horizon length. We set $N_{pLLC} = N_{cLLC}$. Q_L and R_L are the weighting matrices for the social forces and the inputs, respectively. The optimization problem at each NMPC update is formulated as:

$$\min_{\mathbf{u}_{LLC_0}\ \ldots\mathbf{u}_{LLC_{N_{pLLC}-1}}} J_{LLC} \tag{2.12}$$

subjected to the time-discretization of the evolution model 2.10 and the following additional constraints applied at each prediction step:

$$\begin{cases} \alpha_{x,min} \leq \alpha_x \leq \alpha_{x,max} \\ \alpha_{y,min} \leq \alpha_y \leq \alpha_{y,max} \\ 0 \leq V \leq V_{max} \\ 0 \leq Z_i \leq \end{cases} \tag{2.13}$$

where, a_{max} and a_{min} are the maximum and the minimum allowable acceleration of the vehicle, δ_{max} and δ_{min} are the maximum and the minimum allowable road wheel steering angles of the vehicle. The Y coordinate of the vehicle is constrained so that the vehicle does not cross the edges of the road. L_{max} and L_{min} are the left and the right edges of the road (not individual lanes). The vehicle velocity is upper bounded by the road speed limit V_{max}, and reverse motion is not allowed.

2.3.3 Upper Level NMPC Formulation

2.3.3.1 Motion Models for Upper Level NMPC

The main task of the upper level NMPC is to compute a reference trajectory with an optimal lane selection based on the downstream traffic information assumed to be available from V2V and V2I connectivity. For this purpose, we use a reduced acceleration-controlled motion model for the ego vehicle as opposed to the more detailed one considered above for the lower level control:

$$\begin{bmatrix} \dot{X} \\ \dot{Y} \\ \dot{V}_x \\ \dot{V}_y \end{bmatrix} = \begin{bmatrix} 0 & 0 & 1 & 0 \\ 0 & 0 & 0 & 1 \\ 0 & 0 & 0 & 0 \\ 0 & 0 & 0 & 0 \end{bmatrix} \begin{bmatrix} X \\ Y \\ V_x \\ V_y \end{bmatrix} + \begin{bmatrix} 0 & 0 \\ 0 & 0 \\ 1 & 0 \\ 0 & 1 \end{bmatrix} \begin{bmatrix} a_x \\ a_y \end{bmatrix} \tag{2.14}$$

where the longitudinal and the lateral positions, X and Y, as well as velocities, V_x and V_Y, are the states, and the accelerations, a_x and a_Y, are the inputs.

For the upper-level MPC, the object forces are to be aggregated for each lane. To facilitate lane selection with consideration of this aggregation, we introduce lane selection variables, Z_i, with $i = 1 \dots N_{lanes}$. In order to encourage only one of the lanes to be chosen at a time, we impose the integrality constraint [14], [16]:

$$\sum_{i=1}^{N_{lanes}} Z_i = 1, \;\; Z_i \in [0, 1] \tag{2.15}$$

We model the lane selection variables as additional states in the upper-level MPC with the auxiliary dynamics:

$$\begin{cases} \dot{Z}_i = u_{zi} & i \neq N_{lanes} \\ \dot{Z}_i = -\sum_{i=1}^{N_{lanes}-1} u_{zi} & i = N_{lanes} \end{cases} \tag{2.16}$$

where u_{zi} is an auxiliary input used to manipulate Z_i. The lane selection variables are applied as additional weights on the object and lane forces on each lane (see use in cost function below). This formulation encourages the controller to identify the lane with the object forces that minimizes the overall cost function. The model of the system including the lane selection variables can be written compactly as:

$$\begin{aligned} \dot{\mathbf{x}}_{\mathbf{ULC}}(t) &= g\left(\mathbf{x}_{\mathbf{ULC}}(t), \mathbf{u}_{\mathbf{ULC}}(t)\right) \\ \mathbf{y}_{\mathbf{ULC}}(t) &= \left[\mathbf{x}_{\mathbf{ULC}}(t), \mathbf{u}_{\mathbf{ULC}}(t), \; \mathbf{SF}_{\mathbf{ULC}}(t)\right]^T \end{aligned} \tag{2.17}$$

where the states in $\mathbf{x}_{\mathbf{ULC}}$ are of motion states of the ego vehicle and other traffic objects (vehicles) in the connectivity range and the lane selection variables, and the inputs in $\mathbf{u}_{\mathbf{ULC_k}} = [a_x, \; a_y, \; u_{zi}]^{\mathrm{T}}$ are the longitudinal and lateral accelerations for the ego vehicle and the auxiliary inputs for manipulating the lane selection variables. Function g includes the motion model for the ego vehicle 2.14 and

assumed constant velocity models for the detected objects in the connectivity range.

2.3.3.2 Cost Function and Constraints for the Upper Level NMPC

As stated above, by aggregating the object and lane forces in the connectivity range for each lane, the cost function of the upper-level NMPC becomes:

$$J_{ULC} = \begin{array}{l} \sum_{k=0}^{N_{pULC}-1} \|u_{ULC_k}\|^2_{R_U} + \sum_{k=0}^{N_{pULC}} \left(\left\| SF_{T_{ULC_k}} \right\|^2_{Q_{U_T}} \right) \\ + \sum_{k=0}^{N_{pULC}} \sum_{i=1}^{N_{lanes}} Z_i \left(\left\| SF_{O_{ULC_k}} \right\|^2_{Q_{U_O}} + \left\| SF_{L_{ULC_k}} \right\|^2_{Q_{U_L}} \right) \end{array} \tag{2.18}$$

where, $k \in \{0,\ N_{pULC}\}$ is the prediction step index, N_{pULC} is the prediction horizon length $\left(N_{pULC} \gg N_{pLLC}\right)$, Q_{U_T} and Q_{U_O} , and Q_{U_L} are the weight matrices for the target, the object , and the lane social forces, respectively, and, R_U is the weighting matrix for the inputs. The optimization problem to be solved at each upper level NMPC update is then:

$$\min_{\mathbf{u}_{ULC_0} \ \cdots \ \mathbf{u}_{ULC_{N_{pULC}-1}}} J_{ULC} \tag{2.19}$$

subjected to the time-discretization of the evolution model 2.17 and the following additional constraints applied at each prediction step:

$$\begin{cases} \alpha_{x,min} \leq \alpha_x \leq \alpha_{x,max} \\ \alpha_{y,min} \leq \alpha_y \leq \alpha_{y,max} \\ 0 \leq V \leq V_{max} \\ 0 \leq Z_i \leq 1 \end{cases} \tag{2.20}$$

Given the solution of this optimization problem at each update of the upper level control, the coordinates of the upper level motion model, are passed down to the lower level control as reference trajectory $[X_{ref},\ Y_{ref}]$.

2.4 Results and Discussion

2.4.1 Simulation Settings

The NMPC formulations posed above were solved by utilizing a sequential quadratic programming (SQP) solver implemented in the ACADO Toolkit in MATLAB R2017b interface [30]. A multi-shooting method was used for the discretization of the NMPC problems posed above for both levels. For the lower level NMPC, a discretization time step of 0.05 seconds was selected; while for the upper level NMPC, a time step of 0.25 seconds was used. Prediction horizon lengths of 5 sec (100 steps) and 20 sec (80 steps) are used for the lower and the upper level, respectively. For integration of the motion models, a 4^{th} order Runge-Kutta explicit integration method was used.

To illustrate the performance of the proposed social driver model, a several simple scenarios are presented first. For the purposes of the illustrations, the positions and velocities of the object vehicles are assumed available by measurement, and measurement uncertainties are not considered. Simulations are done for single-lane and multi-lane roads with different initial conditions. The lane identification is numbered from the right to the left as [Lane 1, Lane 2, . . . , Lane 4] for 4-lane roads. For each scenario, weighted social forces, lateral trajectory, velocity, acceleration, yaw rate, and road steering wheel angle history are plotted along with a few snapshots of the traffic on the road. To illustrate the performance of the proposed hierarchical framework, two additional scenarios are presented which will highlight the benefits of the proposed framework.

Table 2.1: Single-level Social Driver Model: Initial Condition for Scenario 1

Vehicle	X (m)	Lane Number	V (m/s)
Ego	0	1	17.89
OV 1	150	1	3.58

2.4.2 Single-level Social Driver Model

The first scenario represents a case when there is a slow vehicle in a single-lane road. The initial conditions are shown in Table 2.1. A few snapshots along with the vehicle dynamics plots are presented in Figure 2.2. The lateral trajectory, yaw rate, and steering input plots are omitted since there were no dynamics observed. The initial velocities are set as 17.9 m/s (40 mph) and 3.58 m/s (8 mph) for the ego and the object vehicle, respectively. As the NMPC attempts to minimize the cost function 2.11 by optimizing the inputs, the ego vehicle accelerates to reach the

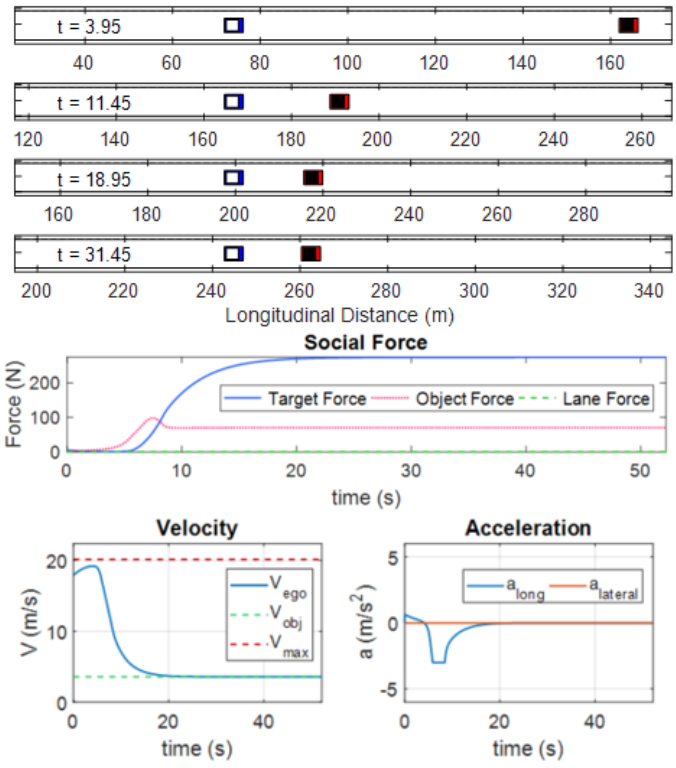

Figure 2.2: Single-level Social Driver Model: Results of Scenario 1

speed limit of the road (20.1 m/s or 45 mph) since the target force is the dominant force due to the initial conditions. The object force starts to increase as the ego vehicle approaches the object vehicle. As the inter-vehicle distance nears the braking distance defined by the object force in 2.2, the object force becomes the dominant cost in 2.11. In spite of the increase in the target force, the ego vehicle decelerates significantly to prevent the object force increasing toward infinity. After t $\approx$ 20s, the velocity of ego vehicle matches the velocity of the object vehicle and maintains a safe braking distance between them. This scenario demonstrates an adaptive cruise control (ACC) function in the social-force based autonomous driving scheme. The flexibility of the proposed model excludes the need of specific rules defined for each traffic scenario.

The second scenario represents a 4-lane road where there is a slow vehicle in front (Figure 2.3). The major difference from the first scenario is the existence of empty lanes allowing the ego vehicle to change its lane. The initial conditions are shown in Table 2.2. As in the first scenario, the ego vehicle accelerates due to the initial target force then decelerate to compensate the increase in the object force as the ego vehicle approaches the object. In this case, the ego vehicle is affected

Table 2.2: Single-level Social Driver Model: Initial Condition for Scenario 2

Vehicle	X (m)	Lane Number	V (m/s)
Ego	0	3	17.89
OV 1	150	4	3.58
OV 2	200	3	4.47
OV 3	170	1	4.47
OV 4	350	4	3.58
OV 5	380	2	4.02
OV 6	370	1	3.58

by the object forces from the two vehicles in lane 3 and 4. As the NMPC tries to minimize the cost function in 2.11, the ego-vehicle is encouraged to perform a lane change from lane 3 to lane 2. A peak of lane force appears as the vehicle from the center of lane 3 to that of lane 2 in 2.4 and adjusts its heading angle in 2.6. An increase in target force is also observed as the vehicle slows down and steer away from lane 3. The combined amount of increase in the target and lane forces is still minimal compared to the potential increase in the object force when the lane-changing behavior is delayed or not executed. This is the benefit of the use of the NMPC formulation, which evaluates the cost for the given prediction horizon.

Table 2.3: Single-level Social Driver Model: Initial Condition for Scenario 3

Vehicle	X (m)	Lane Number	V (m/s)
Ego	0	3	17.89
OV 1	150	4	3.58
OV 2	200	3	4.47
OV 3	170	1	4.47
OV 4	350	4	3.58
OV 5	380	2	4.02
OV 6	370	1	3.58

The third scenario illustrates a case with the presence of additional object vehicles (Figure 2.4). The ego vehicle encounters a group of three object vehicles twice during the given similar amount of time as the second scenario. The initial condition of the third scenario is listed in TABLE 3. FIGURE 6 shows the ego vehicle changing its lane from lane 3 to lane 2 at t $\approx$ 8.85s as it sees a group of vehicles and especially an object vehicle (Object 2) traveling at 4.47 m/s in the lane 3. At t $\approx$ 21.10s, the ego vehicle changes its lane once again due to the slow vehicle (Object 5 in lane 2) in front. Object 5 is even slower (v = 4.02 m/s) than Object 2 (v = 4.47 m/s), and the ego vehicle is still experiencing the object forces from the first group of vehicles as they are still traveling toward the same direction. Therefore, the second lane-change is more delayed and more aggressive

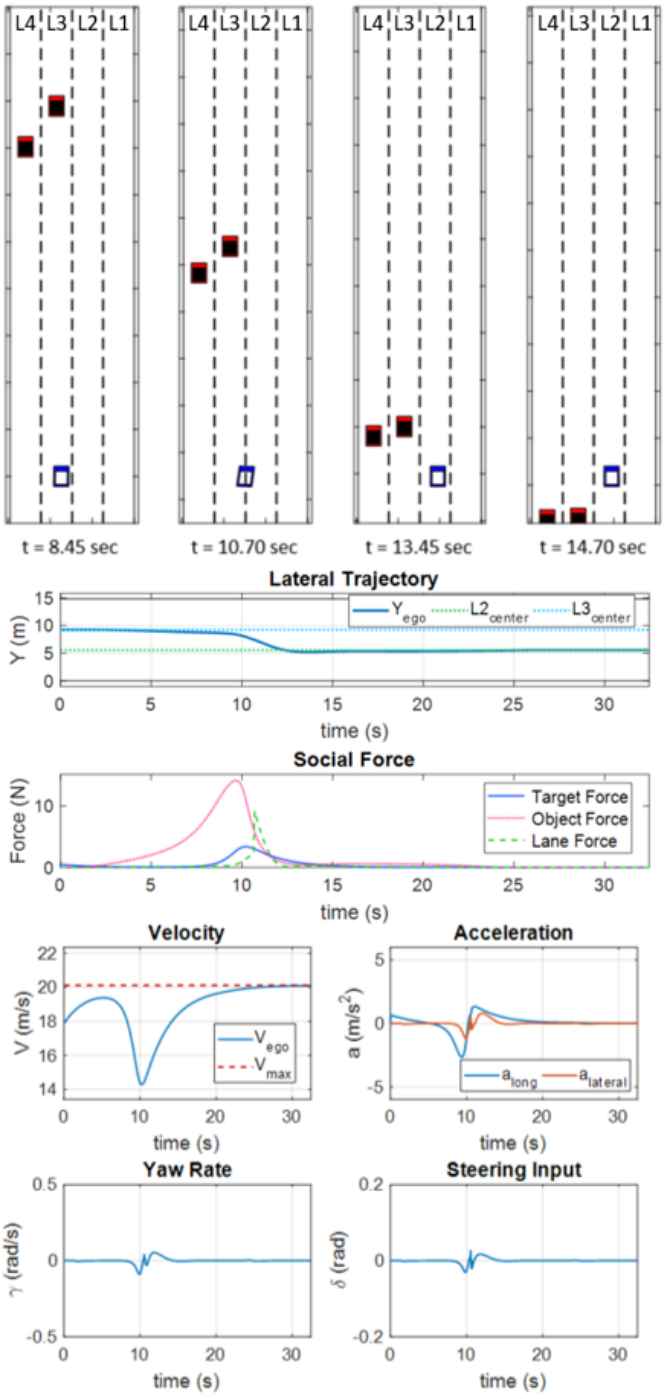

Figure 2.3: Single-level Social Driver Model: Results of Scenario 2

compared to the first lane-changing behavior.

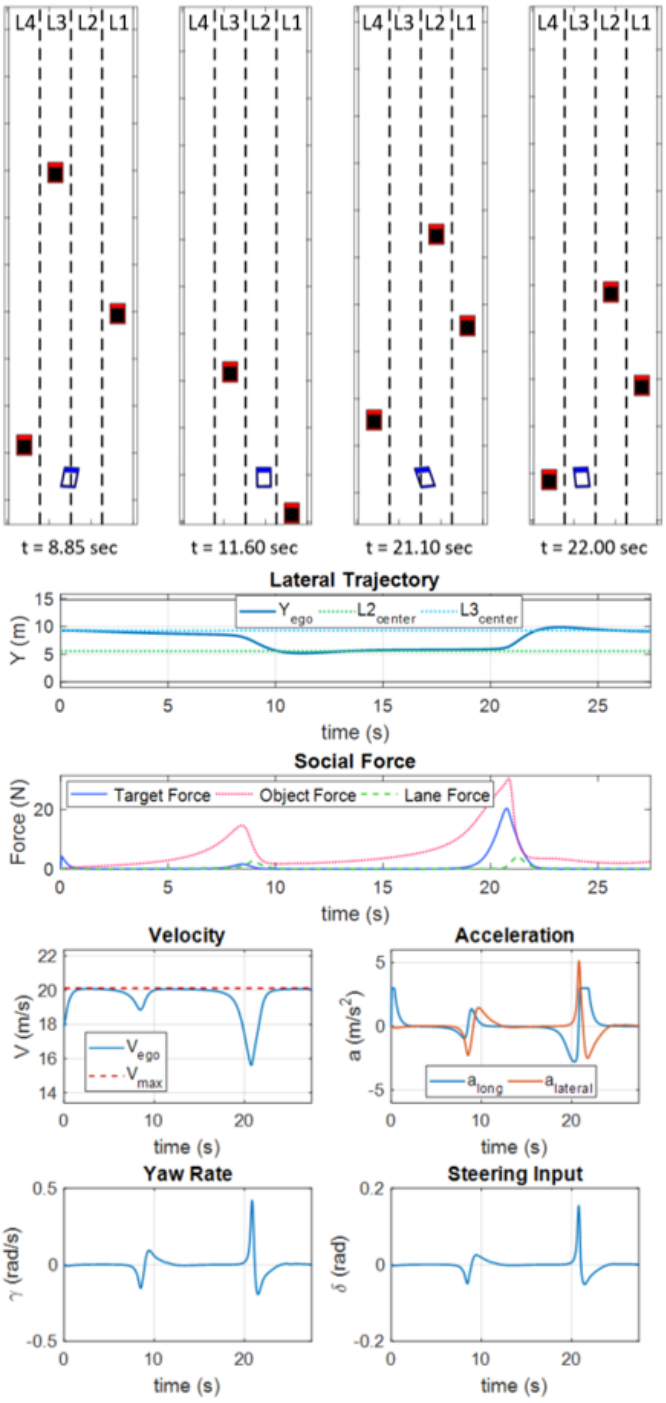

Figure 2.4: Single-level Social Driver Model: Results of Scenario 3

2.4.3 Hierarchical Social Driver Model

The first result demonstrates the ability of hierarchical social-force MPC to achieve long horizon maneuver planning using downstream information in a typical highway traffic. The scenario is depicted in Figure 2.5, where the blue vehicle is the ego vehicle, the yellow vehicles represent the object vehicles within FOV of the ego vehicle, and the green vehicles represent connected vehicles that are downstream of the ego vehicle and beyond its sensor FOV. The yellow-shaded area is the sensor FOV, and the green-shaded area, which covers all vehicles in the figure, represents the communication range, noted as COM.

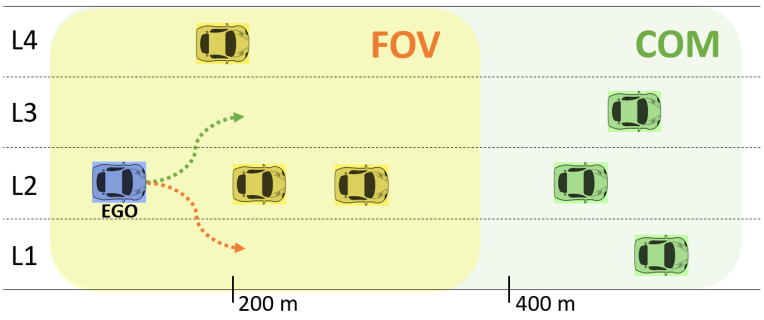

Figure 2.5: Hierarchical Social Driver Model: Overview of Scenario 1

In this particular scenario, the motion of the other vehicles (all slower than the ego vehicle) is such that the lane-change decision near the 200m mark significantly affects the subsequent motion of the ego vehicle. Changing its lane to Lane 1 will results in it having to perform a series of lane-changes from Lane 1 to Lane 4 in order to pass another slow traffic. The optimal lane-change decision is to move from Lane 2 to Lane 3 (near 200 m) and then Lane 3 to Lane 4 (near 400 m). An SFM control that evaluates the total social force/energy only within the FOV without downstream information and lane-based aggregation, would not be able to capture this desirable decision. In such a control, changing its lane to Lane 3 near the 200m mark leads to an increase in total social force perceived compared to changing to Lane 1 due to the ego vehicle's proximity to the vehicle in Lane 4. This would force the ego vehicle to change its lane to Lane 1, which would soon lead to it being stuck behind slow downstream traffic or make more aggressive (potentially unsafe) lane changes.

By contrast, the proposed hierarchical social force controller, which uses downstream information and lane-based social force aggregation, manages to find the optimal maneuver as shown in

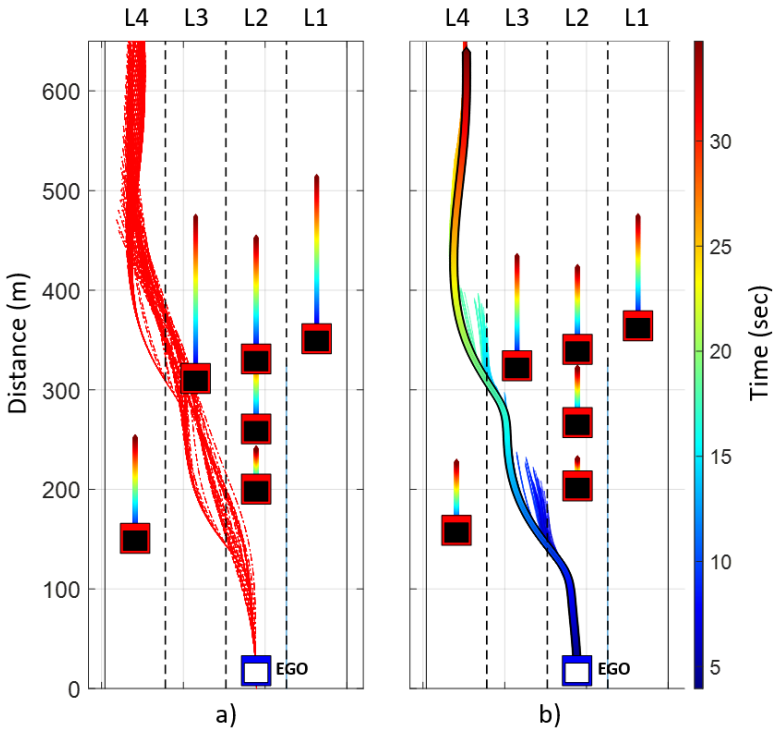

Figure 2.6: Hierarchical Social Driver Model: Predicted Maneuvers for Scenario 1 a) by Upper Level b) by Lower Level

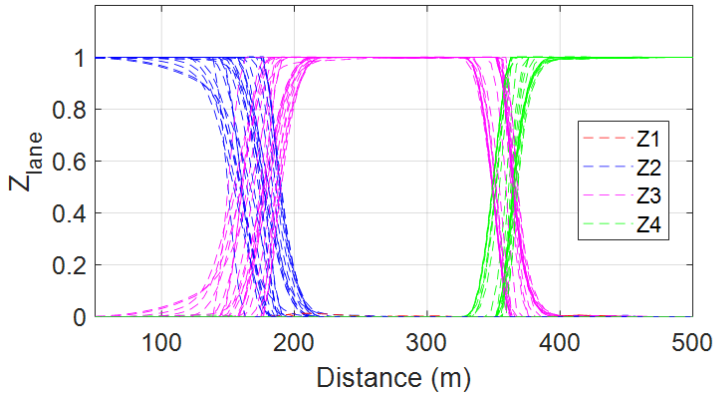

Figure 2.7: Hierarchical Social Driver Model: Lane Selection Variable History for Scenario 1

Figure 2.6, where the dotted thin lines show the predicted trajectories at different MPC updates in a) and the overlay of final trajectory of the ego vehicle is shown with the thick line in b). Since the upper level controller plans the optimal maneuver for a longer horizon, it minimizes the number of lane changes required to achieve a low total social force/energy state for the ego vehicle. Figure 2.7 shows the optimal sequence of the lane selection variables corresponding to the upper level predicted

trajectories shown in part a) of Figure 2.6. The lower level controller successfully tracks the reference trajectory. The ego vehicle makes optimal lane changes that allows it to travel at the top speed possible for each phase of the scenario.

The second scenario has a merging lane that can only be seen though the extended preview. Without the proposed framework, the ego vehicle will be unable to see the merging/ending lane. This merging lane can also be considered as an obstacle or a stopped vehicle. In a similar context to the first scenario, the presence of the object vehicles in Lane 3 encourages the ego vehicle to change its lane to Lane 1. By the time, the ego vehicle encounters a blockage, the vehicles in Lane 2 prevents the ego vehicle from changing its lane (Figure 2.8).

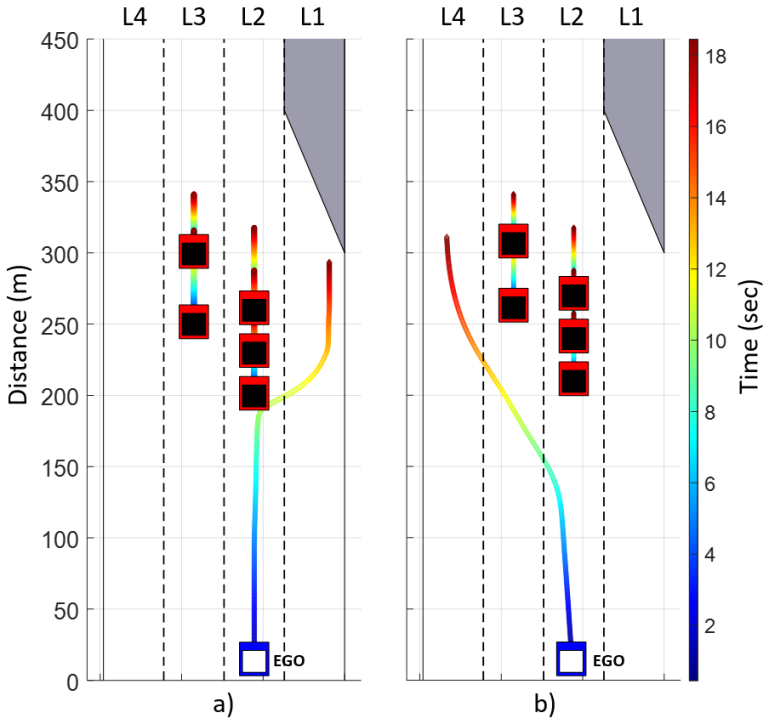

Figure 2.8: Hierarchical Social Driver Model: Final Trajectory of the Ego Vehicle for Scenario 2 a) without ULC b) with ULC

Comparing the resulting ego vehicle dynamics shown in Figure 2.9 clearly shows the advantage of the proposed framework. With the proposed upper level controller, the ego vehicle is capable of more efficient motion without much deceleration (saves energy and travel time). By tracking the optimal reference trajectory computed by the upper level, the lower level controller manages to stay near the speed limit with minimal longitudinal and lateral acceleration efforts.

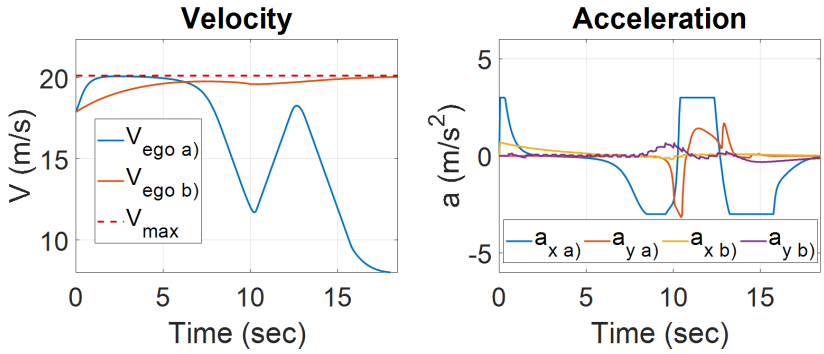

Figure 2.9: Hierarchical Social Driver Model: Vehicle Dynamics Comparison for Scenario 2 a) without ULC b) with ULC

2.5 Conclusion

In this chapter, a human-like autonomous driver model is presented. The social aspect of human driving behavior is captured using a modified social force model (SFM) which is then implemented for predictive guidance and control via a nonlinear model predictive control (NMPC) framework. The proposed driver model showed good performance and proper behavior in various simulated scenarios which include single-lane, as well as multi-lane traffic situations. The ego vehicle was able to prevent collision when there was a slow-traveling vehicle in front and perform adaptive cruise control (ACC) adjusting its speed to that of the slow vehicle, and it was also able to change its lane when there was an available option. Most importantly, the ego vehicle was able to perform such tasks while maintaining reasonable vehicle dynamic response.

In addition to the modeling and control of the social driver model, a hierarchical vehicular social force control scheme is presented to utilize lane-based social force aggregation utilizing downstream traffic information via V2V or V2I connectivity. This hierarchy includes a coarsely-sampled long horizon upper level NMPC and a more detailed short horizon lower level NMPC which does local motion planning and guidance with its limited sensor FOV information. The upper level NMPC with a long preview performs optimal lane selection computations. The planned lanes are then passed as the reference trajectories for the lower-level NMPC which enforces lane tracking along with other social forces while maintaining proper vehicle dynamics. The presented results showed clear performance benefits in terms of more efficient guidance of the ego vehicle.

It is important to note that a simple constant velocity and constant acceleration models are used for estimation and prediction of the states of object vehicles. While these were sufficient for the

presented scenarios and the NMPC settings used (justified by considering relatively fast update time steps of 0.05 seconds for the lower level NMPC and 0.25 seconds for the upper level NMPC), it may require other sophisticated prediction models to accurately track object vehicles in more dynamic traffic environments.

Chapter 3

Performance of Decentralized Cooperative Perception in V2V Connected Traffic[1]

3.1 Abstract

This chapter presents and evaluates a unified cooperative perception framework that employs vehicle-to-vehicle (V2V) connectivity. At the core of the framework is a decentralized data association and fusion process that is scalable with respect to participation variances. The evaluation considers the effects of the communication losses in the ad-hoc V2V network and the random vehicle motions in traffic by adopting existing models along with a simplified algorithm for individual vehicle's on-board sensor field of view. Furthermore, a multi-target perception metric is adopted

[1]The contents of this chapter have appeared in conference and journal publications:

- *D. D. Yoon, G. G. M. N. Ali and B. Ayalew, "Data Association and Fusion Framework for Decentralized Multi-Vehicle Cooperative Perception", Proceedings of the ASME 2019 International Design Engineering Technical Conferences and Computers and Information in Engineering Conference IDETC/CIE2019, August 18-21, 2019.*
- *D. D. Yoon, G. G. M. N. Ali and B. Ayalew, "Cooperative Perception in Connected Vehicle Traffic under Field-of-View and Participation Variations," 2019 IEEE 2nd Connected and Automated Vehicles Symposium (CAVS), 2019, pp. 1-6, doi: 10.1109/CAVS.2019.8887832.*
- *D. D. Yoon, B. Ayalew and G. G. M. N. Ali, "Performance of Decentralized Cooperative Perception in V2V Connected Traffic," in IEEE Transactions on Intelligent Transportation Systems, doi: 10.1109/TITS.2021.3063107.*

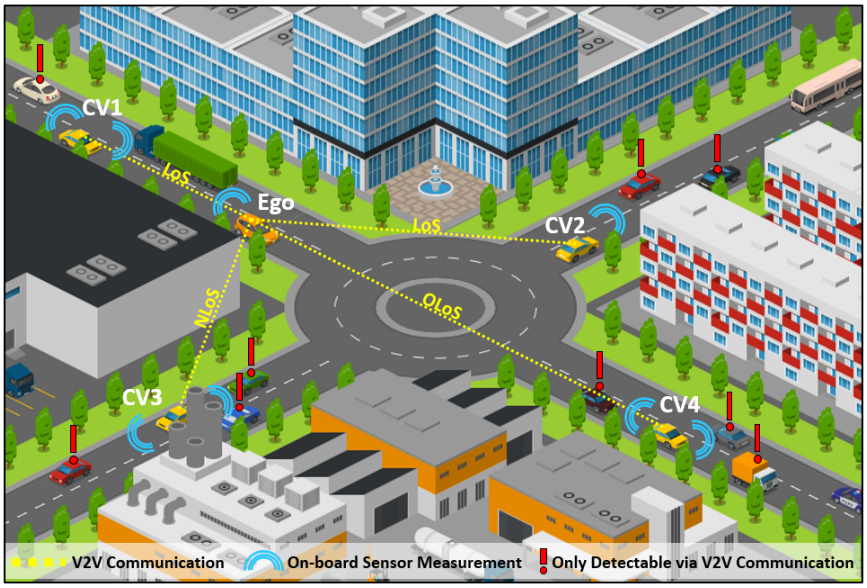

Figure 3.1: Cooperative Perception in an Urban Roundabout Obstructed with Building. OLoS: Obstructed Line of Sight (LoS), NLoS (Non-LoS), CV: Connected Vehicle, Ego: Ego-Vehicle

to evaluate both the errors in the estimation of the motion states of vehicles in the surrounding traffic and the cardinality of the fused estimates at each participating node/vehicle. The extensive analysis results demonstrate that the proposed approach minimizes the perception metric for a much larger percentage of the participating vehicles than a baseline approach, even at modest participation rates, and that there are diminishing returns in these benefits. The computational and data traffic trade-offs are also analyzed.

3.2 Introduction

The reliability of state-of-the-art vehicular safety features such as Advanced Driver Assistance Systems (ADAS) heavily depends on perception information, i.e., state estimates of position, velocity, etc., about surrounding vehicles. In autonomous vehicle applications, having a reliable and accurate perception is critical to ensure safety and also for secondary benefits such as traffic harmonization and reduced collective energy utilization [141, 10, 29].

Advanced on-board sensing technologies, such as Radar, LiDAR, GPS etc., [149, 68, 55] still suffer from reliability issues due to the inherent limitations of the sensors (e.g., range vs. resolution trade-offs) and their high environment dependencies, e.g., direct Line-of-Sight (LoS) or lighting

requirements. While one can utilize a set of these on-board sensor technologies to enhance an ego-vehicle's perception via sensor-level fusion, the fused perception is likely to inherit the drawbacks of each sensor [23, 2]. Moreover, one or more sensors can be frequently obstructed especially in dense traffic. To address these limitations and improve on the achievable coverage and accuracy of the perception for an ego-vehicle, there has been several recent proposals to leverage vehicular connectivity technologies, be it the Dedicated Short Range Communication (DSRC) standard, cellular communication (3G, 4G LTE, or 5G C-V2X), or Wi-Fi [139, 39, 44]. These proposals, broadly called Cooperative Perception frameworks, enable participating vehicles to broadcast their perception of self and/or surrounding vehicles, thereby ultimately allowing multiple participating vehicles to extend and enhance both the range and the fidelity of their perception of the traffic [104, 41, 44]. See illustration in Fig. 3.1 for a roundabout intersection.

In this chapter, we detail a generalized framework for decentralized multi-vehicle cooperative perception and provide a systematic analysis of the framework to expose the inherent limitations and opportunities. Our main consideration is that the framework must take into account the ad-hoc and random nature of traffic and connectivity, thereby offering scalability and robustness to work at different traffic densities and scenarios.

Specifically, we seek to allow and evaluate the effects of variable participation rates in the cooperative scheme and consider the effects of bulk sensor resolution grades for all participants. We introduce a summarizing error metric to assess the average "accuracy" of the cooperative perception and to analyze its variations under different scenarios. This metric takes into account the uncertainties in the state and cardinality estimates from the point of view of each participating vehicle. For the evalution, the basic functionality of the framework will be first demonstrated under restrictive assumptions (no participation rate variances, without communication loss models, etc.). It is observed that the overall cooperative perception framework does indeed reduce the perception error metric compared to traditional Bayesian-based fusion schemes; or compared to a perception scheme based on on-board sensors only. In addition, we give a more complete description of the cooperative perception framework, with updated models of the main components, and also conduct a systematic evaluation of the scalability and robustness of the scheme in both urban and highway scenarios to understand its fundamental limitations in heterogeneous traffic involving connected and unconnected vehicles. The main contributions of this chapter can be summarized as follows:

- We present the details of a robust and decentralized data association and fusion framework for cooperative perception that considers uncertainties associated with the sensor FoV (Field of View) changes, stochastic communication losses, random vehicular motions in multi-lane traffic, and participation rate variances. These are often disparately treated in the literature.
- We evaluate the cooperative scheme in both highway and urban scenarios utilizing a comprehensive cooperative perception metric that considers traffic-relevant kinematic states and their associated uncertainties, where the latter requires additional details in the communication loss modeling and thereby the characterization of the results.
- We discover some fundamental properties of the cooperative perception scheme by evaluating the proposed framework via Monte Carlo simulations of random heterogeneous traffic. The results show that beyond some moderate levels of participation, the perception metric does not improve further for most participants while the network and the computational costs continue to increase substantially. We also conduct comparative analysis of the proposed approach with a standard baseline approach.

The consideration of communication uncertainties (due to path loss, fading and shadowing, packet collision, etc.) is important for a realistic evaluation of the performance of any cooperative scheme. The distance between transmitting and receiving vehicles can vary, and a signal may be blocked or reflected by obstacles, such as buildings, trees, long and tall vehicles (e.g., commercial trucks) [21, 120, 5, 131]. In [1], the path loss for LOS (Line-of-Sight) / OLOS (Obstructed LOS) pathways for highway scenario was studied; however, it neglected the impact of shadowing by buildings. [120] proposed an empirically approximated method validated by the experimental results to capture the effect of obstacle shadowing in vehicular networks. [21] indicated the high comparative performance difference between the obstacle fading and the stochastic fading communication models. Recently, further experimental and simulation evaluations of the communication aspects of vehicular networks have been done in [89]. In this chapter, we adopt a combination of these models to explicitly include communication uncertainties in the evaluation of our decentralized cooperative perception scheme. The specific models are describe in Section 3.3.3 below.

We briefly mention one other important consideration. Communication bandwidth management (minimizing network congestion) is often needed to minimize packet drops in dense traffic. Communication congestion detection can be done via advanced prediction of traffic density using

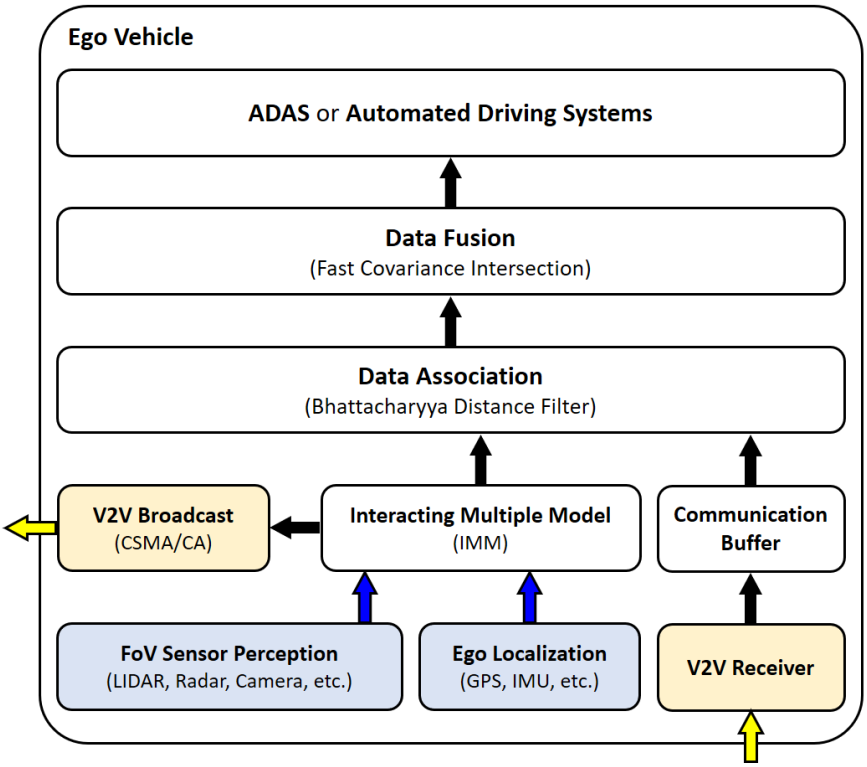

Figure 3.2: Overview of the Proposed Perception Computations at Each Participating Ego-Vehicle

communicated beacons [36, 8, 59]. Congestion control algorithms aim to manage the channel load by dynamically adapting the packet transmission power and frequency thereby providing harmonized access to the wireless medium [115, 80]. Given the extensive work on the topic of network congestion management, we do not delve further into it in this chapter. Instead, we evaluate our cooperative perception scheme at varying participation rates and traffic density by adopting the Carrier Sense Multiple Access with Collision Avoidance (CSMA/CA) protocol for sharing the wireless medium.

The remainder of this chapter is organized as follows. Section 4.3 gives an overview of the system architecture as well as the details of each subsystem. Section 4.4 provides the results and discussions starting with definitions of the evaluation settings and culminating in discussions of the observed increases in the costs of the cooperative perception at high perception rates. Section 3.5 summarizes the main conclusions of this chapter.

3.3 System Framework and Modeling Details

3.3.1 Overall System Framework

A schematic overview of the proposed framework is shown in Fig. 4.1. For local FoV perception, each participating vehicle is equipped with a set of on-board sensors (LIDAR, Radar, Camera, etc.) for object vehicle estimation (within the combined FoV of its sensors) and execute ego localization schemes for self state estimation (using GPS, IMU, odometry system, etc.). Both sets of estimates (ego and other object tracks) are managed by an Interacting Multiple Model (IMM) filter (Section 4.3.3). The state estimates and corresponding covariance data, transformed to global (road-fixed) coordinates, are shared with other connected vehicles via V2V communication. At each participating vehicle, received data are processed through a communication buffer (Section 3.3.4) which accounts for the lossy or intermittent nature of the communication.

When object estimates are communicated among participating vehicles, a data association process (Section 4.3.4) is needed at the receiver since the measurements (the shared state estimates) and the identification/tagging information used are ego-centric to each sender. The goal of the data association step is to cluster information about potentially the same object(s). Then, each set of associated data needs to be processed to yield a single fused state estimate for each object. This is done via a track-to-track data fusion algorithm to be described later (Section 3.3.6). The final fused estimates will likely include estimates of several objects beyond the ego-vehicle's FoV, which extends the perception horizon.

We make several simplifying assumptions in our modeling, some of which are listed below and others will be made in the relevant sections to follow:

- We consider vehicles in traffic to be the only relevant objects for discussing the cooperative perception scheme in this chapter. However, not all vehicles in the traffic need to participate in the cooperative scheme (they may not be so equipped or choose not to participate).
- Each vehicle in traffic is represented as a point mass; vehicle size and geometry variations are not considered in this study.
- Each vehicle can detect and estimate its own kinematic state, as well as of all other vehicles located within the set sensor range of 150 m, provided conditions for the combined FoV of its sensors are met (See Appendix for the simplified FOV model adopted which accounts for

occlusions in traffic). Hereafter, we simply say ego-vehicle's FoV to refer to the combined FoV of its sensors.

- Each participating vehicle computes sensor-level data association and fusion to generate state (2D position and velocity) estimates of all detected vehicles in its FoV. We reduce this process to IMM filters that generate object kinematic data prior to communication. In these filters, sensor noise is modeled as additive Gaussian noise on each vehicle's FoV measurement data.
- Each connected vehicle shares its FoV generated IMM filter outputs by broadcasting to surrounding vehicles (single-hop V2V) utilizing CSMA/CA (Carrier Sense Multiple Access with Collision Avoidance) protocol with a maximum communication range of 300 m (subject to losses).

3.3.2 Vehicle State Estimation and Tracking

We apply an interactive multiple model (IMM) filter for the estimation and tracking of self as well as of nearby object vehicles, connected or not connected, within the ego-vehicle's FoV. Utilizing constant velocity (CV) and constant acceleration (CA) based Kalman filters, the IMM filter can be compactly written as

$$\begin{aligned} X^m_{t+1|t} &= A^m X^m_{t|t} + B^m w^m_{t|t} \\ Z_{t|t} &= C^m X^m_{t|t} + v^m_{t|t} \end{aligned} \tag{3.1}$$

where m indicates the mode (1 for CV and 2 for CA) with process noise $w^m_{t|t} \approx N(0, Q^m)$ and the measurement noise $v^m_{t|t} \approx N(0, R^m)$ for each model respectively. t is the time-index. In this chapter, the motion states of interest X are the 2D position and velocity in both the longitudinal and the lateral directions (expressed in a global frame after necessary transformations are applied at each ego-vehicle). A^m and C^m are the mode-parameterized state transition and measurement matrices, and B^m is the disturbance input matrix for the respective mode m. Z are on-board (FoV) sensor measurements. By blending hypothesis of each mode, the IMM filter can obtain more consistent estimates of the motion state of vehicles than what can be obtained by assuming any one of the modes alone. For details on this, we refer the readers to, for example, [105].

Denoting the set of indices for the vehicles in the shared traffic T (set of vehicles) at time t by $\zeta_{T,t}$, the detected subset $\zeta_{FoV_i,t}$ in the FoV of vehicle i at time t is defined as:

$$\zeta_{FoV_i,t} = \{j \in \zeta_{T,t} | d_{(i,j),t} < R_i \wedge j \in LoS_{i,t}\} \tag{3.2}$$

where $d_{(i,j),t}$ is the Euclidean distance between vehicles i and j, at time t. Eq. (4.4) defines the FoV neighborhood such that each vehicle i has a FoV measurement Z on vehicle j, if and only if vehicle i and j are within a set on-board sensor detection range, R_i, and the line-of-sight (LoS) between the two vehicles is unobstructed ($j \in LoS_{i,t} \Leftrightarrow i \in LoS_{j,t}$). More discussion about the LoS computations is given in the Appendix.

To prevent broadcasting track data comprised of estimates with premature convergence (or of large uncertainties), we set an allowable maximum threshold for the determinant of covariance matrix accompanying each track. This identifies a communicable set of FoV generated track data $\Phi_{c_i,t}$ as:

$$\Phi_{c_i,t} = \{[X_{j,t}, P_{j,t}] | det(P_{j,t}) \leq \phi_{IMM_i} \wedge j \in \zeta_{FoV_i,t}\} \tag{3.3}$$

which is about vehicles j ($j \in \zeta_{FoV_i,t}$) that are detected and estimated by vehicle i, $P_{j,t}$ is the covariance matrix accompanying IMM estimates of the states $X_{j,t}$, and t is the time index for the send time. ϕ_{IMM_i} is an allowable threshold on the convergence of the IMM filter for each track. This issue becomes more important in rapidly changing traffic where track birth and death effects are frequent [142].

3.3.3 Communication Loss Model

The following is a generic statement of communication losses between a sender/transmitter and a reciever [24]:

$$P_{RX}(d) = P_{TX} + G - \sum PL(d) \tag{3.4}$$

where P_{RX} is the received power, P_{TX} is the transmitted power, G is the antenna gain, $PL(d)$ is the path loss component due to various fading effects. We consider empirical shadow fading models suitable for VANETs, which take a dual-slope form as discussed in [1, 93]. For line of sight (LoS) / Obstructed LoS (OLoS) cases, the path loss model for LoS/OLoS is shown in Eq. (3.6), where d is the distance between the transmitter and the receiver, PL_0 is the path loss at a reference distance

$$PL_{LoS/OLoS}(d) = \begin{cases} PL_0 + 10n_1 log_{10}(\frac{d}{d_0}) + X_\sigma & \text{if } d_0 \leq d \leq d_b \\ PL_0 + 10n_1 log_{10}(\frac{d_b}{d_0}) + 10n_2 log_{10}(\frac{d}{d_b}) + X_\sigma & \text{if } d_b \leq d \end{cases} \tag{3.6}$$

$$PL_{NLoS}(d_t, d_r) = \begin{cases} PL_{0_{NLoS}} + 10n_3 log_{10}(\frac{d_t^{0.957}}{(d_w w_r)^{0.81}} \frac{4\pi d_r}{\lambda})) + X_\sigma & \text{if } d_r \leq d_b \\ PL_{0_{NLoS}} + 10n_3 log_{10}(\frac{d_t^{0.957}}{(d_w w_r)^{0.81}} \frac{4\pi d_r^2}{\lambda d_b})) + X_\sigma & \text{if } d_b < d_r \end{cases} \tag{3.7}$$

d_0, d_b is the breakpoint distance, n_1 and n_2 are the path loss exponents estimated by regression, and X_σ is a zero-mean Gaussian distributed random variable with a standard deviation of σ. For non-line of sight (NLoS) scenarios, where the pathway between a transmitter and a receiver is blocked by obstacles such as structures, buildings, etc., as happens in urban roundabouts/intersections, the adopted path loss model is shown in Eq. (3.7). d_t is the distance of a transmitter to the center of the intersection, d_r is the distance of a receiver to the center of the intersection, w_r is the width of the street, d_w is the distance between a transmitter and a wall, and λ is the wavelength. The values of aforementioned model parameters can be found in [1] for both urban and highway conditions.

An additional stochastic fading model is applied using the Nakagami-m model to account for the path loss due to small scale fading of transmitted rays between a transmitter and a receiver [89]. The probability density function is defined as:

$$PL_s(d) = \frac{2\nu^\nu}{\Gamma(\nu)\Omega^\nu} d^{2\nu-1} e^{(\frac{-\nu d^2}{\Omega})}, \forall d \geq 0. \tag{3.5}$$

where d is the distance, ν is the Nakagami parameter $\nu \geq 0.5$, $\Gamma(\nu)$ is the gamma function, Ω is the average power of multipath scatter field and controls the spread/variance of the distribution.

3.3.4 Communication Buffer

To compensate for intermittent communications resulting from packet drops and time synchronization issues, receivers are required to maintain a data buffer of received information. Any missing information due to an unsuccessful communication can be estimated based on recent successfully communicated prior data. While the buffer time window is preset, the oldest data set are continuously replaced with newly received data upon availability. Such a communication buffer was investigated for the estimation of static objects in [108, 125]. Considering the dynamic nature of vehicular traffic for the current application, the following formulation uses the latest set of stored

data to estimate and fill in for recently missed information assuming a constant velocity motion model to predict the states of those object vehicles in the buffer to the current time index. Let $\mathbf{X}_{i,j} = \{X_{t_c-N_{bf}}, \ldots, X_{t_c-1}, X_{t_c}\}$ be the series of estimates that have been communicated between vehicles $i \rightarrow j$, where t_c is the most current time index, and N_{bf} is the length for the communication buffer/window. Each communication may be either successful $\xi_{i,j,t} = 1$ or unsuccessful $\xi_{i,j,t} = 0$. Then, the buffered estimate at the most current step, X_{i,j,t_c} can be computed from:

$$\begin{aligned} X_{i,j,t_c} &= \xi_{i,j,t_c} X_{i,j,t_c} + \ldots \\ &+ \sum_{l=1}^{N_{bf}} \{ (\prod_{q=1}^{l} (1 - \xi_{i,j,t_c-q+1})) \xi_{i,j,t_c-l} O(\Delta t) X_{i,j,t_c-l} \} \end{aligned} \tag{3.8}$$

where $O(\Delta t)$ is a state transition matrix of the constant velocity model with time step $\Delta t = t_{t_c} - t_{t_c-l}$. If no data is received about an object for longer than the set buffer window, no information will be retained about that object until the next successful communication.

3.3.5 Data Association

At any one receiver, there are likely multiple track data sets that are about the same object(s) being tracked by multiple participating vehicles' FoV. Dropping the time index for clarity, let $\mathbf{\Phi}_f$ be the set of FoV data (state estimates and corresponding covariances) and $\mathbf{\Phi}_c$ be the set of buffered communicated data. The combined set of estimates is:

$$\mathbf{\Psi}_r = \mathbf{\Phi_f} \cup \mathbf{\Phi_c} \tag{3.9}$$

where the cardinality of the union set is $|\mathbf{\Psi}_r| = N_r$. For each indexed pair $i, j = 1, \ldots, N_r$, the Bhattacharyya distance is computed as [11]:

$$\begin{aligned} BD_{(i,j)} = &\frac{1}{8}(X_i - X_j)^T (\frac{P_i + P_j}{2})^{-1} (X_i - X_j) \\ &+ \frac{1}{2} \ln(\frac{det(\frac{P_i + P_j}{2})}{\sqrt{det(P_i) det(P_j)}}) \end{aligned} \tag{3.10}$$

where $BD_{(i,j)} = 0$ for $i = j$. We define a set threshold, ϕ_{BD}, to identify a group of pairs of estimates

that are reachable (directly or via neighboring estimates) from one another whenever ($BD_{(i,j)} \leq \phi_{BD}$). Such a group/cluster of associated estimates are considered to potentially represent the same object or vehicle. We denote all such groups of associated estimates by:

$$\mathbf{S}_{asso} = \{\mathbf{\Psi}_{a_1}, \mathbf{\Psi}_{a_2}, \ldots, \mathbf{\Psi}_{a_{N_v}}\} \tag{3.11}$$

where $\mathbf{\Psi}_{a_1} \cup \mathbf{\Psi}_{a_2} \cup \mathbf{\Psi}_{a_3} \cdots \cup \mathbf{\Psi}_{a_{N_v}} \subseteq \mathbf{\Psi}_r$, each $\mathbf{\Psi}_{a_n} = [\mathbf{X}_{a_n}, \mathbf{P}_{a_n}]$ is a cluster set of associated estimates ($n = 1, \ldots, N_v$), with $\mathbf{X}_{a_n} = \{X_{a_{n_1}}, \ldots, X_{a_{n_{N_{est,n}}}}\}$ and $\mathbf{P}_{a_n} = \{P_{a_{n_1}}, \ldots, P_{a_{n_{N_{est,n}}}}\}$, and $|\mathbf{\Psi}_{a_n}| = N_{est,n}$ is the cardinality of the corresponding cluster $\mathbf{\Psi}_{a_n}$. N_v is the number of clusters.

3.3.6 Data Fusion

Since there is an unknowable correlation between the received and associated data, we adopt the Covariance intersection (CI) fusion algorithm which can manage an unknown degree of inter-estimate correlation and compute a consistent, albeit conservative, fused estimate [58, 25, 72]. Furthermore, since the original covariance intersection formulation involves computationally expensive optimizations for the fusion weights, we use the aforementioned FCI algorithm for which analytical approximations have been offered [34, 92]. The consistency of the fused estimate remains guaranteed with the FCI algorithm. For details on this, we refer the readers to [34]. Using FCI, we fuse the group of estimates in each associated cluster $\mathbf{\Psi}_{a_n}$ into the single estimate $\Psi_{f_n} = [X_{f_n}, P_{f_n}]$ where:

$$\begin{aligned} P_{f_n}^{-1} &= \sum_{k=1}^{N_{est,n}} \omega_{a_{n_k}} P_{a_{n_k}}^{-1} \\ X_{f_n} &= P_{f_n} \sum_{k=1}^{N_{est,n}} \omega_{a_{n_k}} P_{a_{n_k}}^{-1} X_{a_{n_k}} \end{aligned} \tag{3.12}$$

where the non-negative fusion weights satisfy $\sum_{k=1}^{N_{est,n}} \omega_{a_{n_k}} = 1$. Dropping the subscript a_n for brevity, each ω_k is calculated as:

$$\omega_k = \frac{\eta + det(P_k^{-1}) - det(\eta - P_k^{-1})}{\eta N_{est,n} + \sum_{m=1}^{N_{est,n}} \{det(P_m^{-1}) - det(\eta - P_m^{-1})\}} \tag{3.13}$$

where $\eta = det(\sum_{k=1}^{N_{est,n}} P_k^{-1})$. Repeating this for all associated clusters, ($\mathbf{\Psi}_{a_n} = [\mathbf{X}_{a_n}, \mathbf{P}_{a_n}] \rightarrow \Psi_{f_n} = [X_{f_n}, P_{f_n}]$ for all $n = 1, \ldots, N_v$), we arrive at the final set of fused estimates with the final fused

cardinality of N_v:

$$\mathbf{\Psi}_f = \{\Psi_{f_1}, \Psi_{f_2}, \ldots, \Psi_{f_{N_v}}\} \tag{3.14}$$

3.3.7 Performance Metric

We set to evaluate the performance of the cooperative perception scheme at scale, on numerous traffic scenarios and at various participation rates. To this end, we need a compact metric that takes into account the multi-target estimation error from the perspective of any one participating vehicle. The optimal subpattern assignment metric (OSPA) [112] is one such metric that weighs all possible pair-wise (estimate to true target) assignments and corresponding errors along with the possible differences in cardinality between the associated and fused outputs and the ground truth. The original OSPA metric, however, does not consider the uncertainty information associated with the estimates, considering only on the localization error measured via the Euclidean distance. In [88], a modified OSPA metric was proposed involving the Hellinger distance (related to the Bhattacharya distance) that accounts for uncertainty; however, it needs covariance information about the ground truth data which is generally absent in our setting. In this chapter, we modify the metric by using Mahalanobis distance (MD) to incorporate the covariances obtained with the state estimates. We also use the metric to compactly quantify both the localization and 2D velocity state estimation errors. Our final modified OSPA metric is given by Eq. (4.13) (See top of this page), where $MD^{(c)}(\cdot)^p$ is given by:

$$MD^{(c)}(\cdot)^p = (\min(c, MD(\cdot)))^p \tag{3.15}$$

where the exponent p is within $1 \leq p \leq \infty$, c is the cut-off distance ($c > 0$) for un-assignable estimates[112], and $MD(\cdot)$ is:

$$\begin{aligned} &MD(X_{g_i}, \Psi_{f_{\pi(i)}}) \\ &\qquad = \sqrt{(X_{g_i} - X_{f_{\pi(i)}}) P^{-1}_{f_{\pi(i)}} (X_{g_i} - X_{f_{\pi(i)}})} \end{aligned} \tag{3.16}$$

where $\mathbf{X}_g = X_1, \ldots, X_r$ is a set of ground truth states with r being the number of vehicles in the evaluation range (in the ground truth), and Π_{N_v} is a set of permutations $\pi \in \Pi_{N_v}$ that assign each of the estimates to the true target states in the ground truth.

$$d^{(c)}_{OSPA_{MD}}(\mathbf{X}_g, \mathbf{\Psi}_f) = \left(\frac{1}{N_v} \left(\min_{\pi \in \Pi_{N_v}} \sum_{i=1}^{m} MD^{(c)}(X_{g_i}, \Psi_{f_{\pi(i)}})^p + c^p(|\mathbf{\Psi}_f| - |\mathbf{X}_g|) \right) \right)^{\frac{1}{p}} \tag{3.17}$$

In addition to the modified OSPA metric, in our evaluation of the cooperative perception, we will also use the (unscaled) cardinality error metric defined as $|\mathbf{\Psi}_f| - |\mathbf{X}_g|$ (the number of fused estimates - the number of vehicles in the ground truth within the evaluation region). This metric primarily measures detection errors and is only indirectly related to state estimation at the data association/fusion steps.

3.4 Results and Discussions

3.4.1 Simulation Settings

A number of traffic environments are created using the traffic microsimulation software PTV VISSIM [95]: a unidirectional 4-lane highway and a roundabout (rotary) intersection with 4-lane bidirectional (2-lane each) roads. We applied a Monte Carlo approach for evaluating the cooperative perception scheme in order to account for the stochastic nature of the simulated traffic, the communication network, as well as the sensor FoV and IMM filtering processes at each vehicle. A set of 30 samples were taken for each case of 5 different traffic flow rates (3500, 5500, 7500, 9500, and 11500 veh/hr) with 5 different prescribed average traffic speeds (60, 70, 80, 90, and 100 kph) for the highway, and 3 different traffic flow rates (1500, 2500, and 3000 veh/hr) with 3 different average traffic speeds (60, 70, 80 kph) for the roundabout scenario. In summary, a total of 750 and 270 samples were generated, respectively, for the highway and roundabout environments using randomized driver and vehicle models in VISSIM to represent realistic traffic. For space and clarify of exposition, in the discussions below, we present detailed results for only three representative traffic density settings for each environment: 35, 94, and 192 veh/km for the highway and 19, 36, 50 veh/km for the roundabout scenario. However, the observations are also corroborated with the remainder of the data generated. As a baseline for comparison, we also considered a modification of the BSM-based cooperative scheme standardized by SAE [81], where the received BSMs are associated and fused with local FOV data at each participating ego-vehicle to enhance its perception. In the following discussions and the figures, we will use the shorthand DCP (Decentralized Cooperative

Perception) to refer to our proposed approach, and the shorthand BSM for the baseline approach. The performance of both schemes is evaluated by computing the modified OSPA metric from the perspective of each participating vehicle for a region of 150-m radius centered on that vehicle at the various geographic locations in the traffic environment under consideration (excluding the boundary entry/exit regions). The modified OSPA metric is denoted as $OSPA_{MD}$. In all evaluations, we vary the participation rate from 0 (no cooperation) to 100% (fully cooperative).

Each vehicle is given a uniformly distributed random value between 0 to 50 ms as its initial clock setting and set to broadcast its FoV track information at a rate of 20 Hz [93]. Each participating vehicle is assumed to perform the data association and fusion process at a rate of 10 Hz. The communication buffer window is taken to be 150 ms (a width of 3 nominal broadcast intervals). To consider the Medium Access Control (MAC) layer issues with the ad-hoc vehicular communication network, the Carrier-Sense Multiple Access with Collision Avoidance (CSMA/CA) protocol is adopted from [12, 51]. Even with the CSMA/CA protocol, packet collisions is still possible due to hidden nodes. While more advanced solutions exist to alleviate such issues including handshaking protocols, increasing transmitting power, etc., these are beyond the scope of the current study.

As mentioned previously, the effect of FoV is crucial for evaluating the effectiveness of cooperative perception in realistic traffic. To model the effect of the dynamic traffic on the FoV of each vehicle (obstructing each other), we use the simple exclusion algorithm given in the Appendix. We then vary the FOV sensor angular resolution of the exclusion algorithm in three settings: Fine (5^o), Medium (10^o), Coarse (30^o); each setting being applied for all participating vehicles. The angular sensor resolution represents the smallest sector angle from the ego-vehicle in which nearby object vehicles can be detected as distinct (not overlapping). If there are two or more object vehicles where the sensor detection rays (LoS) from the ego-vehicle to each nearby vehicle form an angle smaller than the set angular sensor resolution, only the closest object vehicle is considered detectable to the ego-vehicle, see Fig. 1. In this way, we seek to evaluate the effect of the trade-offs in investments in sensing capability (finer resolution settings corresponding to more capable on-board sensing with, say, more cameras and/or radar/LiDAR units around each vehicle) vs. participation in the cooperative perception.

3.4.2 Ego Vehicle Evaluation Scenario

First, the effectiveness of the framework is evaluated on one vehicle which is randomly chosen as the ego vehicle from whose perspective we evaluate the cooperative perception. The first scenario is a low-density highway traffic scenario where the traffic flow is defined as 10 vehicles per minute with an average speed of 120 km/hr. In Figure 3, the % error for two cases are shown. The first case is single-vehicle perception (SP) with information acquired only through the on-board sensors (FoV) of the ego vehicle, without vehicular communication. The second case is the proposed data association and fusion architecture, BDF and CIF. The effect of cooperative perception is trivial for the first 10 sec of time as the ego vehicle can accurately estimate all nearby vehicles via on-board sensors without any obstruction in its FoV. As the ego vehicle or other nearby vehicle changes its lane and adjusts speed however, a couple of vehicles become no longer detectable within the FoV of the ego vehicle without communication (Figure 3.4). For example, as the ego vehicle changes its lane ($\sim$ 10 sec), from lane 3 to lane 2 (numbered left to right as lane 1 to 4), the rearmost vehicle becomes undetectable by the on-board sensors due to another vehicle in between but still remains perceptible via vehicular communication. The corresponding change in the overall cardinality is clearly noted in Figure 3.3.

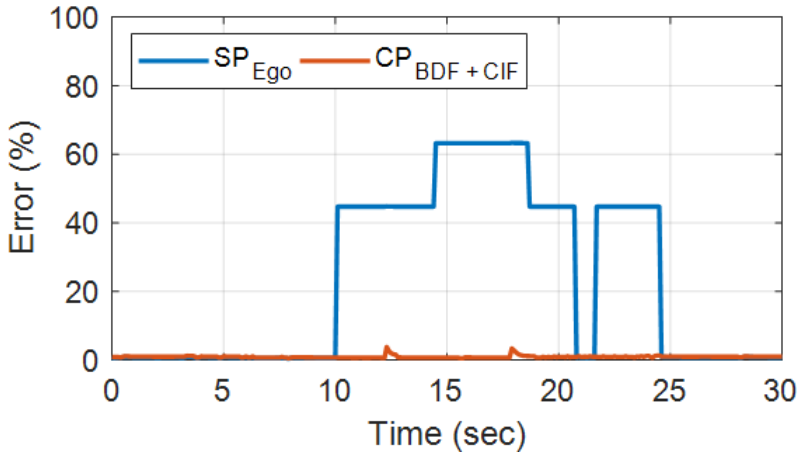

Figure 3.3: Scaled OSPA metric (0 to 100%) Comparison For Low Density Highway Traffic – Scenario 1

The second scenario (Figure 3.6) is a high-density highway traffic where the traffic flow is defined as 100 vehicles per minute with an average speed of 90 km/hr. In such a traffic, the benefit of vehicular communication is apparent. In addition to the two cases observed in the first scenario,

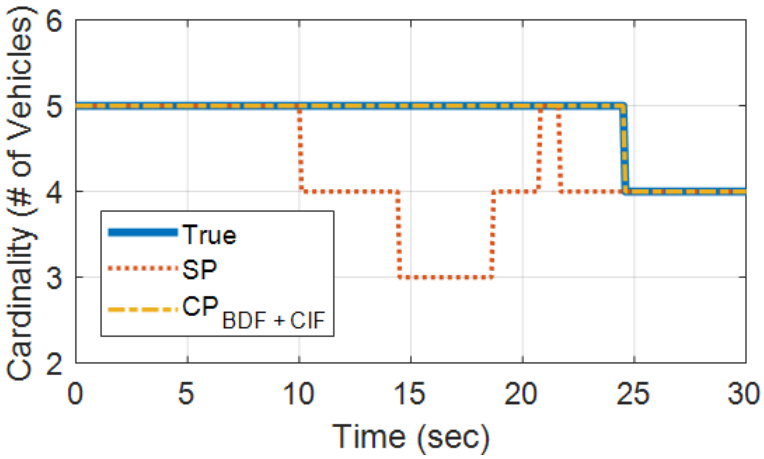

Figure 3.4: Cardinality History For Low Density Highway Traffic – Scenario 1

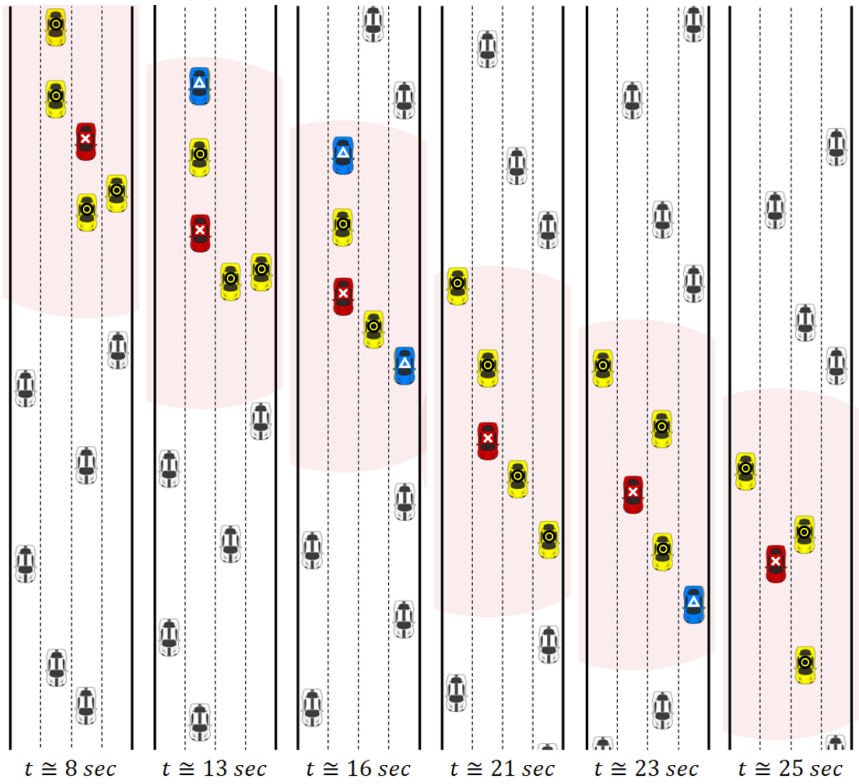

Figure 3.5: Snapshots of Low Density Highway Traffic Scenario: Red: ego vehicle, Yellow: detectable via on-board sensors & communication, Blue: detectable only via communication, White: out of evaluation range.

a cooperative perception (CP) with BDF and traditional Kalman Filter Fusion (KFF) is added for comparison. To do so, a parallel KF [39] is used to fuse the associated estimates along with the

proposed BDF association process. As shown in Figure 3.6a, the proposed framework achieved the lowest % error while SP had the highest. The high % error (∼70 %) of SP is mainly caused by the high-density traffic which blocked the ego vehicle's FoV. The difference in cardinality is shown in Figure 3.6. It is important to note the same number of spikes are shown in Figure 3.6a for both of the cooperative perception (CP) cases. These are due to sharing initial poor quality (yet to converge) estimates (from IMM) of newly detected vehicles.

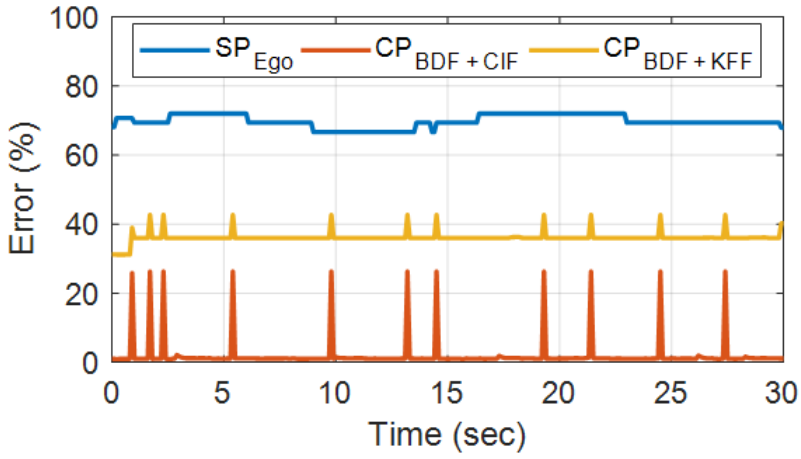

(a)

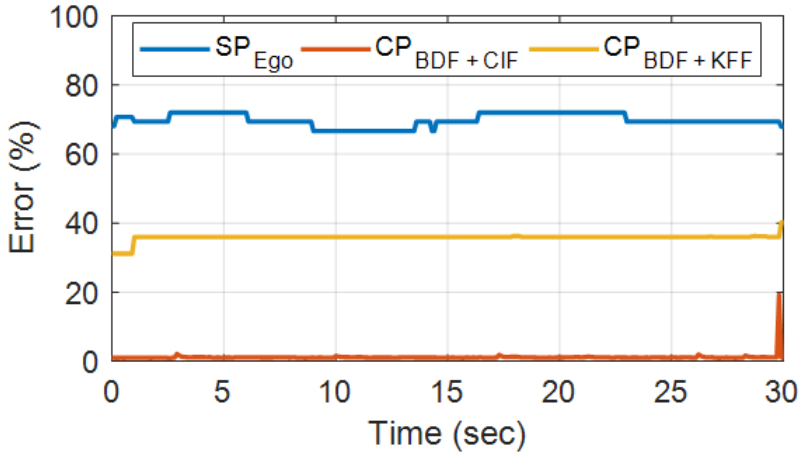

(b)

Figure 3.6: Scaled OSPA metric (0 to 100%) Comparison For High Density Highway Traffic – Scenario 2

As some vehicles enter and exit the evaluated region or as vehicles adjust their speeds and perform lane changes within the high-density traffic, the FoV of some CP-participating vehicles change.

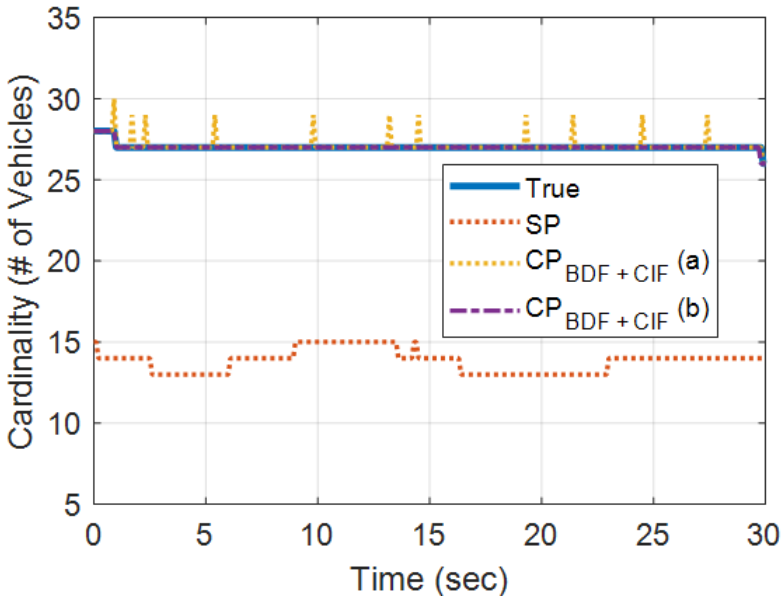

Figure 3.7: Cardinality History For High Density Highway Traffic – Scenario 2

Once new vehicles are detected within the FoV, observing vehicles initiate the tracking (e.g. using IMM), improving their estimates iteratively with new measurements. Communicating these early estimates, which are most likely deviating from the true states, results in creating outliers as they are not associated with other estimates, thereby artificially increasing the cardinality of the fused estimates (Figure 3.7). This why 4.5 is used to observe the determinant of the covariance matrix within the IMM filter and limit the object state estimates to be broadcast to only those that have converged below a set threshold. The results are shown in Figure 3.6b.

3.4.3 Cooperative Perception in a Highway Scenario

Fig. 3.8 and 3.9 show results for the traffic evaluation of the 4-lane highway scenario. Comparisons with modified BSM-based baseline scheme are included in Fig. 3.9. The plots in Fig. 3.8 report the average $OSPA_{MD}$ and cardinality error with varying participation rates. These are computed by averaging the results from Monte Carlo simulations for all participating connected vehicles at selected traffic densities (35, 94, and 192 veh/km) and the three representative angular sensor resolution settings. The negative average cardinality errors in Fig. 3.8 show the average number of undetected vehicles at each setting.

We make the following observations from the results in Fig. 3.8. First, there is a con-

tinuous improvement in the average $OSPA_{MD}$ and the cardinality error as the participation rate increases from 0 to 100% for all traffic density settings. Second, the lowest participation rate for the minimum average $OSPA_{MD}$ and cardinality error have some dependence on the sensor resolution settings. Whereas, for coarse sensor resolution, the minima are achieved at full participation, at finer sensor resolutions, there is only a marginal improvement in the perception metrics beyond a 70-80% participation rate. In particular, the cardinality error doesn't improve beyond 50% participation at finer sensor resolutions. Third, the trend for the average $OSPA_{MD}$ seems independent of traffic density, although the (unscaled) cardinality error metric clearly shows that more vehicles become undetectable at the higher traffic density and low participation rates due to the higher LoS restrictions of the on-board sensors.

In order to provide a comparison to the baseline modified BSM-based approach, and to take a closer look at the trends of the distributions of the lower values of $OSPA_{MD}$ among the participants, in Fig. 3.9, we plotted the percentage of participating vehicles that achieve a value of $OSPA_{MD}$ below a given threshold across their time in the evaluation region for both the proposed DCP and the BSM-based framework. The threshold is taken as 10 based on the numerical results in Fig. 3.8 for all three sensor settings. Recall that the states and the associated uncertainties being evaluated include not only the localization errors but also the 2D velocity state estimation errors; as such the threshold should be interpreted in relative terms considering the definition of the OSPA metric in Eq. 4.13. We observe in Fig. 3.9 that: 1) At participation rates lower than 30% for DCP (at much higher 85% for BSM), only a small number of participants benefit from the cooperative scheme with $OSPA_{MD}$ <10, specially if the sensor resolutions are coarse. 2) The percentage of the vehicles that benefit from the DCP scheme plateaus at moderate participation rates, specially at finer sensor resolutions. 3) In all settings, it was not possible for all participants (100%) to achieve $OSPA_{MD}$ <10 ; that is, not all participants are able to minimize their perception error. We attribute part of this to the cost of participation and this will be discussed more in Section 3.4.5. For the case of BSM which is outperformed by the proposed DCP in all cases, the maximum share of benefiting vehicles is noted as 40% at a full participation rate, and as should be expected there is minimal effect from sensor resolution. 4) With respect to traffic density, at lower participation rates and higher traffic density, fewer participants benefit from the cooperative scheme due to the high likelihood of restricted FOVs by neighboring vehicles. This latter aspect is also partly an artifact of boundary region effects on the evaluation, especially in low density settings. As the participation

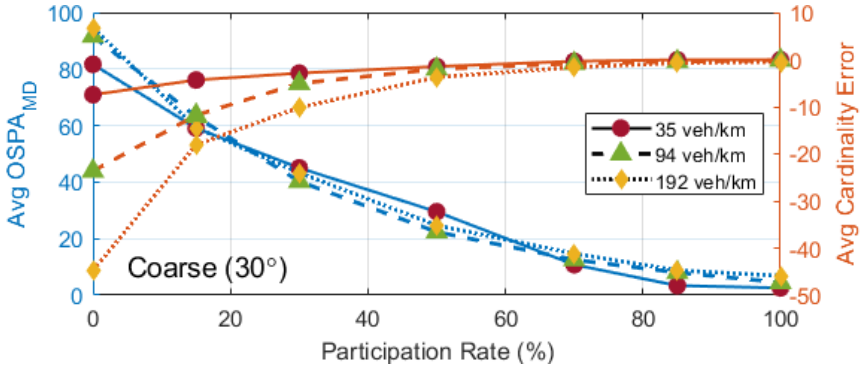

(a)

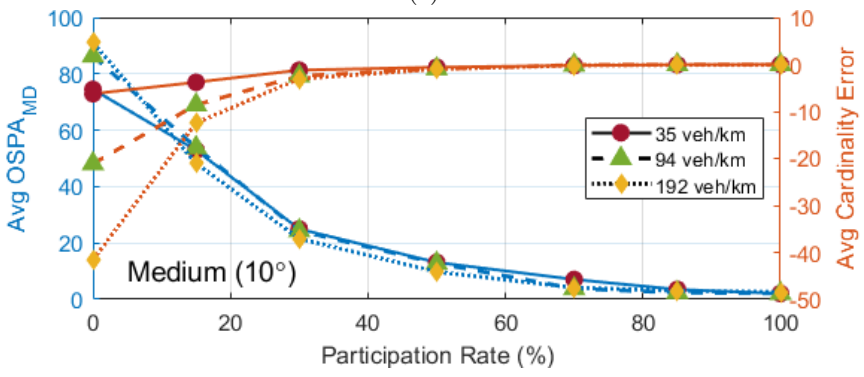

(b)

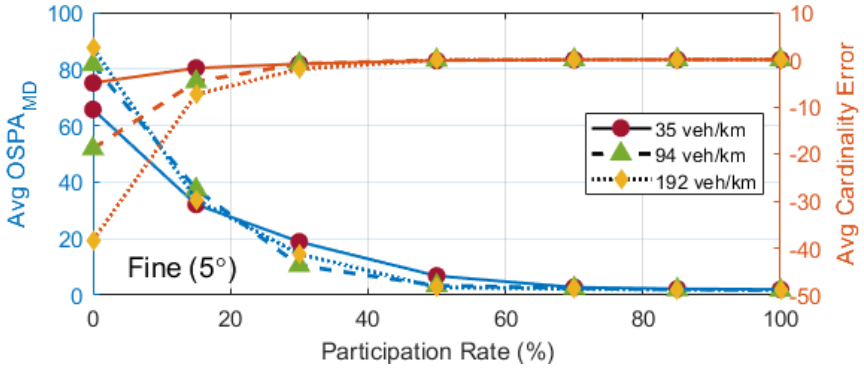

(c)

Figure 3.8: Average $OSPA_{MD}$ and Cardinality Error (#Estimates - #True) for an Ego-Vehicle in Highway Scenario with Varying Angular Sensor Resolution: (a) Coarse (30^o), (b) Medium (10^o), and (c) Fine (5^o).

rate increases, however, more vehicles in the higher traffic density benefit compared to those in the lower density settings.

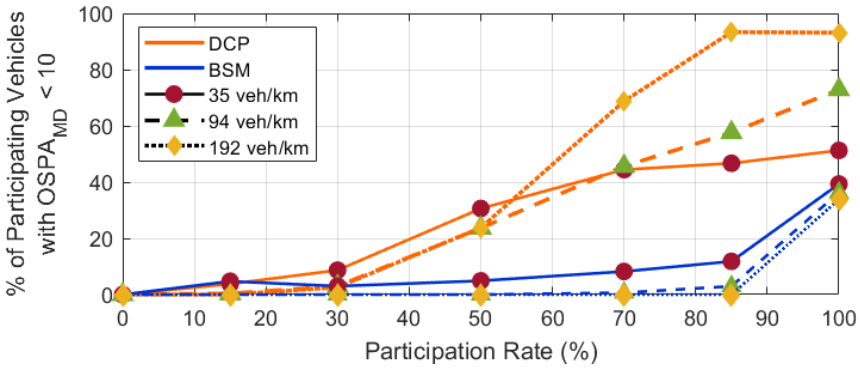

(a)

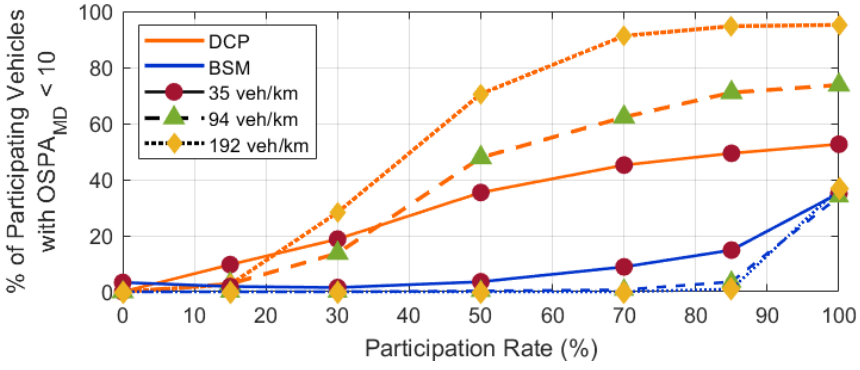

(b)

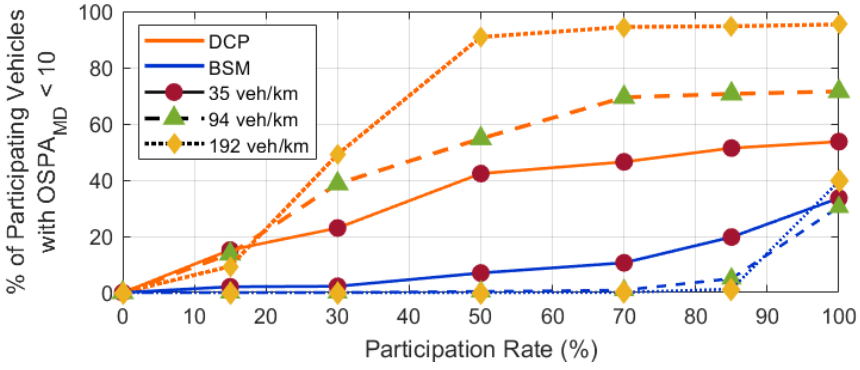

(c)

Figure 3.9: Percentage of Participating Vehicles with $OSPA_{MD}$ less than 10 for the Highway Scenario with Varying Angular Sensor Resolution: (a) Coarse (30^o), (b) Medium (10^o), and (c) Fine (5^o).

3.4.4 Cooperative Perception in a Roundabout Scenario

Fig. 3.10 and Fig. 3.11 show results for the roundabout scenario, all with the fine (5^o) angular sensor resolution setting. In this scenario, vehicular communications and FoV perception are drastically restricted due to the presence of buildings and other structures near the roads (see

the environment illustrated in Fig. 3.1). The overall observations from these results are consistent with that of the highway scenario. However, due to the more complex environment and associated costs to be discussed in the Section 3.4.5, here the minimum $OSPA_{MD}$ is generally higher than in the highway scenario in all tested traffic density settings. In addition, the results suggest that there is marginal improvement in the minimum average $OSPA_{MD}$ beyond moderate participation rates. As the vehicles near the entry or the exit of the roundabout, the evaluation range includes a portion of the roundabout while their FOV as well as communications are hindered by the presence of buildings. As a result, $OSPA_{MD}$ is shown to be highest in those areas ($50 \leq |D| \leq 100$ m, where D is the distance to the center of the intersection). When the vehicle enters the roundabout ($|D| \leq 50$ m), the effect of the participation rate on the perception metric changes remarkably. There, a participating vehicle is able to form a LoS on-board perception as well as LoS/OLoS communication with other vehicles at all four segments of straight roads connecting to the roundabout. Similar to the results of the highway scenario, the highest percentage of participating vehicles with $OSPA_{MD}$

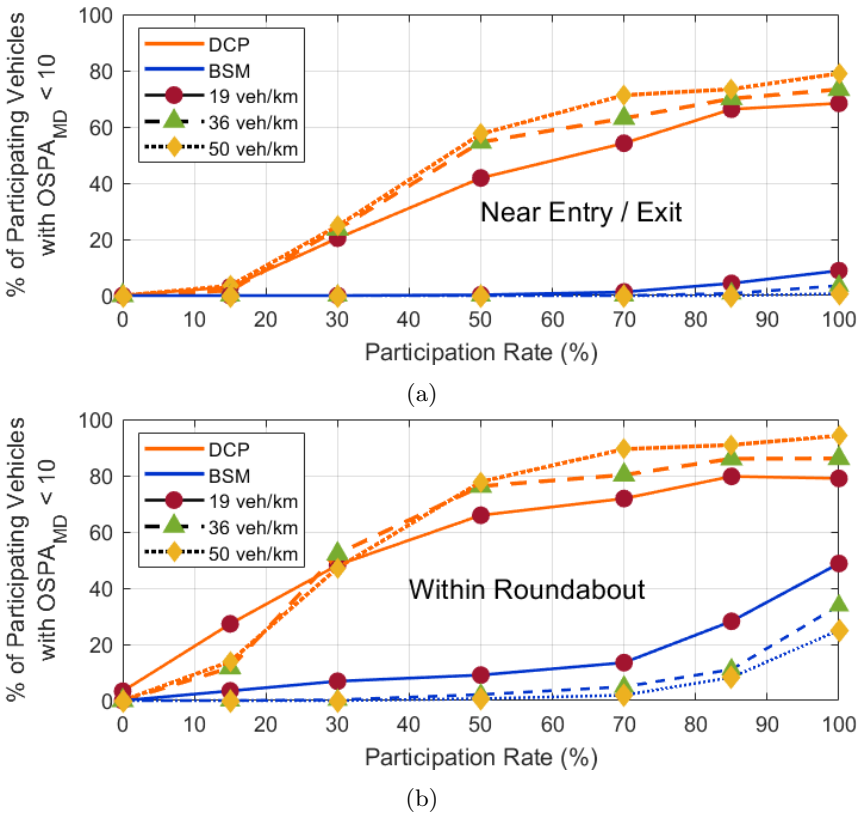

Figure 3.10: Percentage of Participating Vehicles with $OSPA_{MD}$ less than 10 for Roundabout Scenario: (a) near the Entry or the Exit (b) within the Roundabout

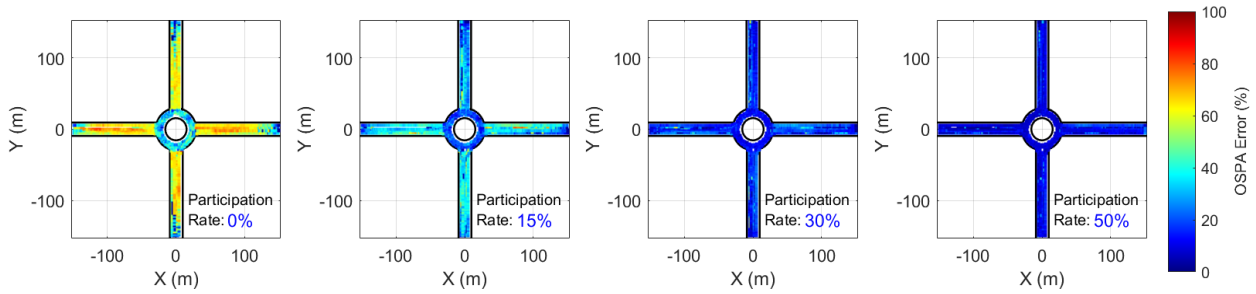

Figure 3.11: $OSPA_{MD}$ for Roundabout Scenario with Traffic Density of 36 veh/km (2500 veh/hr with 70 kph average speed) with Varying Cooperative Perception Participation Rate.

<10 is measured to be around 50% at the center of the roundabout with the lowest density setting. It is shown that the performance of the BSM-based scheme is significantly exacerbated when the vehicles are located further away from the center (near entry / exit) and as the traffic density is increased even with higher participation rates.

Fig. 3.11 shows a heat map of the $OSPA_{MD}$ for a closer look at the spatial distribution of the metric in the roundabout scenario. It shows that significant improvement is achieved at the center starting at 15% participation. Increasing the participation rate further improves the perception on the straight road segments. Beyond the participation rate of 50%, the overall perception does not improve significantly.

3.4.5 Costs of Increasing Participation Rates

We estimate the communication costs of the cooperative perception scheme by computing the packet delivery ratio (PDR). For our purposes, it is defined as:

$$PDR = \frac{\#\ of\ successfully\ received\ packets}{\#\ of\ expected\ received\ packets} \tag{3.18}$$

Fig. 3.12a and 3.12b show plots of the PDR for the indicated settings. Increasing the participation rate results in a lower PDR, more in the roundabout intersection scenario than in the highway scenario, although the traffic densities considered are lower at the intersection. Note that the significant drops in the PDR at high participation rates and high traffic density settings do not totally negate the benefits of the cooperative perception; they serve to level-off its benefits to the participants. That there is some tolerance of the deterioration of the PDR at high participation rates is an inherent application-level reliability of the cooperative framework[89]. Not all of the broadcast

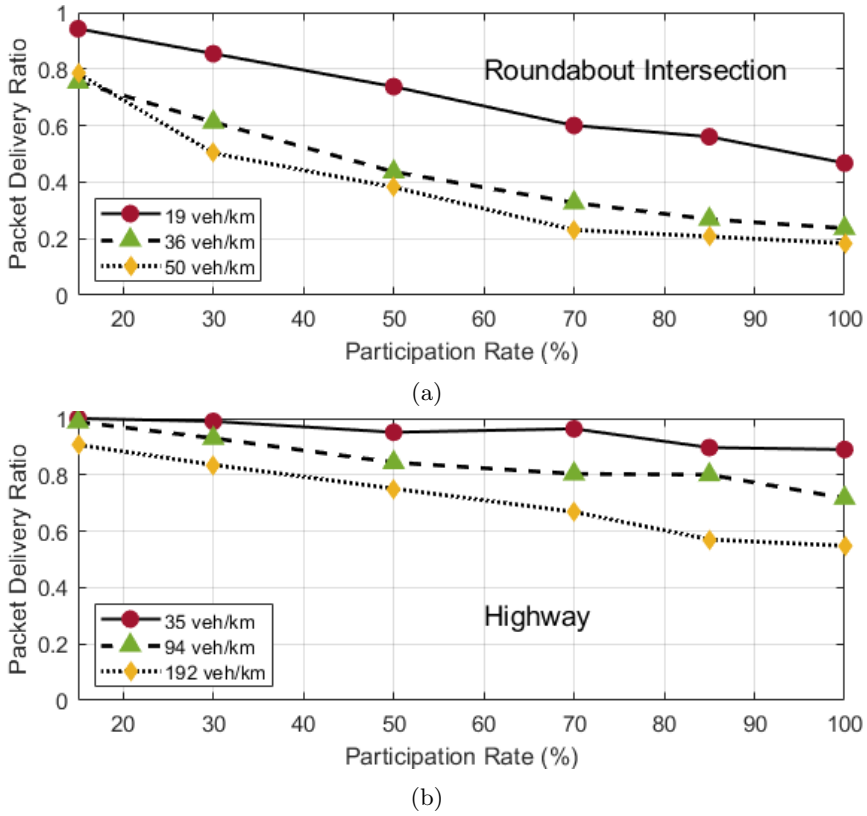

Figure 3.12: Average Packet Delivery Ratio (PDR) for (a) Roundabout and (b) Highway Scenarios.

information at 20 Hz may be needed to compute the perception metric at 10 Hz. Furthermore, we had included a communication buffer to offset some of this effects. Still, the lower PDR noted at high participation rates, is one of the limiting costs for the plateauing of the benefits of the cooperative scheme as shown in Fig. 3.9 and 3.10. In more heavily congested traffic, a severe communication network congestion may not permit high participation rates due to bandwidth bottlenecking. This could result in a further decrease in the overall PDR thereby necessitating advanced network congestion control schemes [121]. For the presented scenarios, however, the average packet delay (Fig. 3.13) is shown to be around 22 ms for the highest density test setting. With a slower data rate of 4.5 Mbps, the average delay with the maximum participation rate could be as high as 200 ms which is still manageable with the presented framework. These results match that of previous vehicular network studies [93, 60, 4].

Next we consider the computational costs. Compared to the BSM scheme, the additional computational costs of the proposed framework mainly arise from the data processing, especially

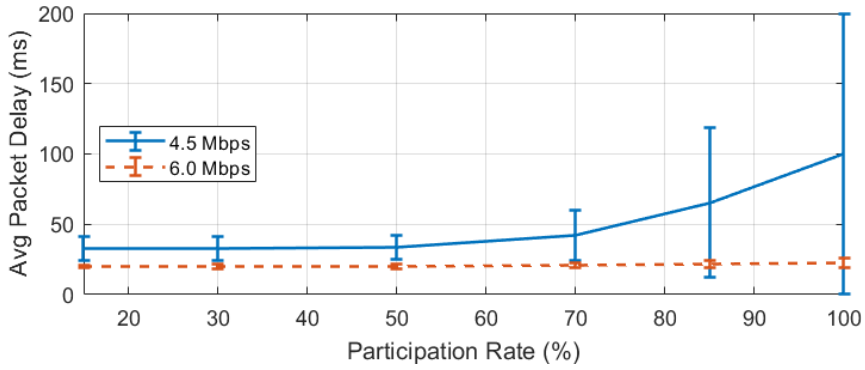

Figure 3.13: Average Packet Delay for the High Traffic Density (192 veh/km)

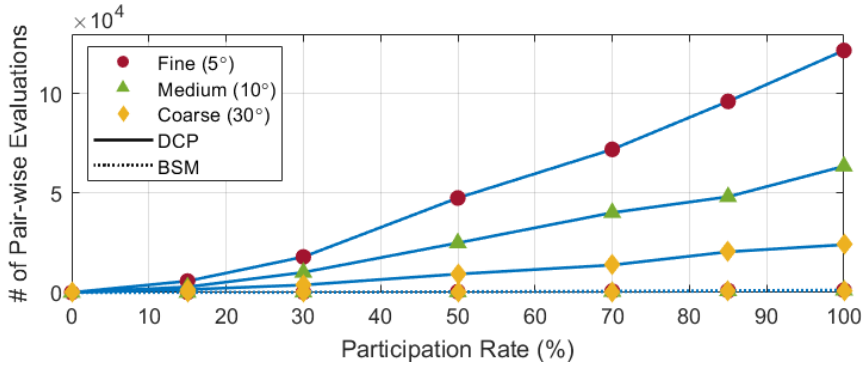

(a)

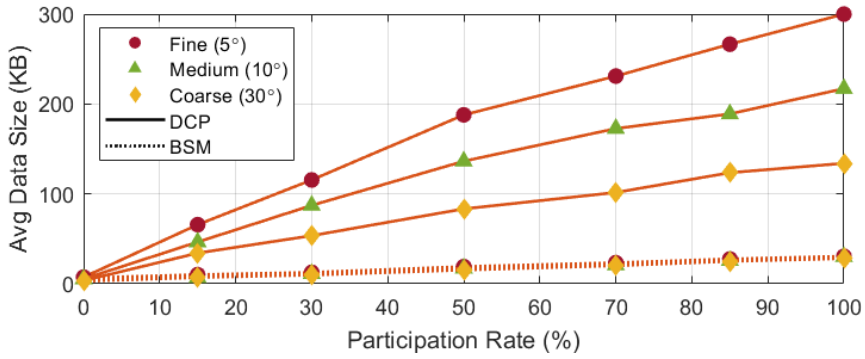

(b)

Figure 3.14: (a) Average Number of Pair-wise Evaluations Required for Data Association (b) Average Processed Data Size per Second for the High Traffic Density (192 veh/km)

the data association step. This is due to the increased cardinality of the data set $|\mathbf{\Psi}_r| = N_r$ (Eq. 4.6) which includes both FOV sensor generated and received data. For the proposed framework, the cardinality is approximately equal to $N_{r,DCP} \approx \Phi_{c,cav}(\theta) \cdot (N_{cav} + 1)$, where $\Phi_{c,cav}(\theta)$ is the average number of communicable FoV data per vehicle (Eq. 4.5) which monotonically increases with a finer

sensor resolution, θ, and N_{cav} is the total number of vehicles successfully communicating with the ego-vehicle. For the BSM scheme, the cardinality simply becomes $N_{r,BSM} = \Phi_{c,ego}(\theta) + N_{cav}$. It can be easily seen that the cardinality difference between the two schemes will increase significantly as the traffic density increases and/or the average sensor resolution becomes finer for a given participation rate. The latter will further amplify the computational effort and data size for the DCP approach compared to the BSM. The results for the high traffic scenario in Fig. 3.14 shows the number of required pairwise evaluations for the data association process (Fig. 3.14a) and the average data size, assuming 39B for the headers and 60B for each object vehicle information, which need to be processed by each participating vehicle per second (Fig. 3.14b). For details of packet size estimation, we refer the readers to [135, 122]. The computational effort for the association process is $O(C(N_r, 2))$ as it requires $C(N_r, 2) = \frac{(N_r)!}{2(N_r-2)!}$ pair-wise evaluations (See Fig. 3.14a). Each iteration involves matrix inversion computations of the covariance matrix for the uncertainty of the shared estimate which as complexity $O(n^3)$, where n is the size of the matrices inverted. Here, $n = 4$ for covariance matrices associated with the 2D position and velocity estimates. [99]. Considering the fusion computations in Eq. 4.9 as well, we observe that the needs for these computations grows only linearly with participation and traffic density. Therefore, we conclude that, although the proposed DCP approach involves more computations and data sizes than the baseline BSM approach, the needs may not be prohibitively expensive for modern and future on board computing devices. The benefits depicted in Fig. 3.9 and 3.10 may outweigh the added costs from these drawbacks.

However, since we observed diminishing returns of the benefits of the DCP at high participation rates (especially at high sensor resolutions, where the computations and data size are highest), there is an imperative to reduce the amount of data communicated, not only to reduce computational cost, but also to alleviate potential bandwidth bottle-necking. In this regard, one attractive approach is to develop algorithms where senders filter the information they broadcast based on some value criteria [123, 50].

3.5 Conclusion

In this chapter, we have provided a generalized cooperative perception framework based on decentralized V2V vehicular communication. We presented evaluations of the framework based on randomized traffic simulations for multi-lane highway and roundabout intersection scenarios,

considering both communication losses and sensor FOV resolution issues.

The summarizing observation is that there are levels of optimal participation rates for cooperative perception beyond which the overall perception does not improve significantly while the cost of communication losses and computation increases dramatically. The optimal participation rates are a function of the traffic scenario and assumptions about the individual vehicle's FoV sensor resolution. In particular, investments on more sensors (in number and capability) alleviate the need for very high participation rates for the most number of participants to benefit from engaging in the cooperative scheme. Comparisons with a BSM-based baseline cooperative perception scheme shows that the proposed approach benefits a much larger percentage of participating vehicles with lower perception errors, even at modest participation rates, in both highway and urban roundabout scenarios.

We also observed that these benefits come with higher data traffic and computational costs than the baseline, specially at high participation rates, although the computational needs remain within the realm of modern on-board devices. One solution to reduce the data traffic in the communication medium and the associated computational needs at each receiver is to allow senders reduce the cardinality of the data they broadcast using one or more value criteria [50, 110, 57].

Chapter 4

A Novelty Discrimination Method for V2V Decentralized Cooperative Perception in V2V Connected Traffic[1]

4.1 Abstract

In this chapter, we propose a novelty discrimination method for decentralized cooperative perception and evaluate its performance in high density vehicular traffic scenarios. The presented scheme aims to filter communicable Field-of-View (FoV) perception data based on the novelty-value of information prior to broadcasting it in the vehicle-to-vehicle (V2V) communication network. The potential benefits of these approaches include, but are not limited to, the reduction of bandwidth bottle-necking and the minimization of the computational cost of data association and fusion post processing of the shared perception data at receiving nodes. We provide the details of the proposed method along with its evaluation in stochastic traffic settings at various rates of participation of

[1]The contents of this chapter have appeared in a journal publication:

- *D. D. Yoon and B. Ayalew, "A Novelty Discrimination Method for V2V Decentralized Cooperative Perception," in IEEE Transactions on Vehicular Technology, 2021 (In Review)*

individual vehicles in the cooperative perception framework. The proposed method does indeed improve bandwidth utilization and latency without significant compromises on the average cooperative perception metric for participants.

4.2 Introduction

The potential benefits of vehicular communication technologies such as Dedicated Short Range Communication (DSRC), cellular communication (4G LTE or 5G), or Wi-Fi [139, 39] have received significant attention in recent decades. These technologies enable an Internet of Vehicles (IoV) where connected vehicles can utilize the communication medium to exchange various types of information. For example, vehicles may share their Field-of-View (FoV) sensing information with others via inter-vehicular networks, allowing them to leverage each other's raw sensor measurements or even processed perception information. This allows participating vehicles to expanding their situational awareness (SA) by overcoming technical limitations (e.g., Line-of-Sight (LoS), detection range, resolution) of their on-board sensors (e.g. radar, LiDAR, and camera) and improving the robustness and the reliability of their local composite FoV perception [149, 68, 55]. Such use of vehicular network technologies has come to be known as cooperative perception, although it is also often called collaborative perception when the perception information is shared for the purpose of achieving a common goal in a centralized scheme. The cooperative/collaborative perception scheme is vital for advancement of intelligent transportation systems such as intelligent traffic management systems, Advanced Driver Assistance Systems (ADAS), and autonomous driving systems [48, 23, 2].

A number of studies have introduced network-level strategies devised to relieve vehicular network congestion, such as packet-dropping [116], adaptive packet transmission [115, 80], optimized channel modeling [76], and prioritized packet assignments [140]. While these methods can potentially alleviate the network congestion by delaying or even rejecting communications, they may still lead to significant computational demands or delays of essential contents of information being shared.

To minimize the chances of information of negligible novelty-value being disseminated in the network, the issue can be addressed by careful design of data discrimination or filtering methods at all sender vehicles (of the information). [123, 50]. By doing so, each participating vehicle can actively reduce the size of the packet it communicated by retaining only valuable information and thereby minimize the overall load on the communication medium.

Despite the positive results of existing studies [127, 40, 50, 79], the limitations for real traffic applications still exist in their underlying assumptions. For example, it is not possible to know the absolute error of its perception information since the ground truth of an object vehicle cannot be known. Evaluation of other vehicles' communication environment is also extremely difficult even with the utilization of RSUs, and maintaining V2V communication history with respect to all participating vehicles will significantly increase the computational complexity and data intensity especially in a congested environment. In this chapter, we propose a V2V cooperative framework that evaluates the novelty of information by comparing the new perception information to be communicated with previously communicated data that are either transmitted by ego-vehicle or received from other participating vehicles within a set time window. Without any anticipation or assumption on other vehicles' perspective, ego-vehicle attempts to evaluate the value of the contents of its CPM in the current communication network.

In this chapter, we investigate the potential of a novelty-based discrimination method for selective dissemination of vehicular information in a vehicle-to-vehicle (V2V) decentralized cooperative perception framework. The proposed method constantly evaluates the novelty of newly acquired FoV perception data prior to the broadcast and selectively communicates information of novelty-value above a certain threshold. Novelty of new information can be assessed based on the relative entropy of the newly acquired FOV perception data with respect to the previously communicated information from other vehicles' as well as the ego-vehicle's own prior broadcast data. Since there will be multiple estimates being shared, especially in high vehicular traffic density, some discrimination or filtering can be made based on the statistics of the relative entropy values. The relative entropy has also been used in [50] as a way to assess the anticipated value of information before broadcasting. Although the approach in [50] is similar to ours, their method required a participating ego vehicle to make inferences about communications among other vehicles that the ego-vehicle may not necessarily be communicating with. While probabilistic models can be constructed to attempt to predict the traces of all nearby communications, the application is unlikely to robust and it significantly increases the computational loads for participants. By contrast, our approach relies on information already available at each participating ego-vehicle thereby avoiding a need for making inferences about communications among other vehicles.

The main contributions of this chapter can be summarized as follows:

- We present the details of a vehicular perception data discrimination method that statistically

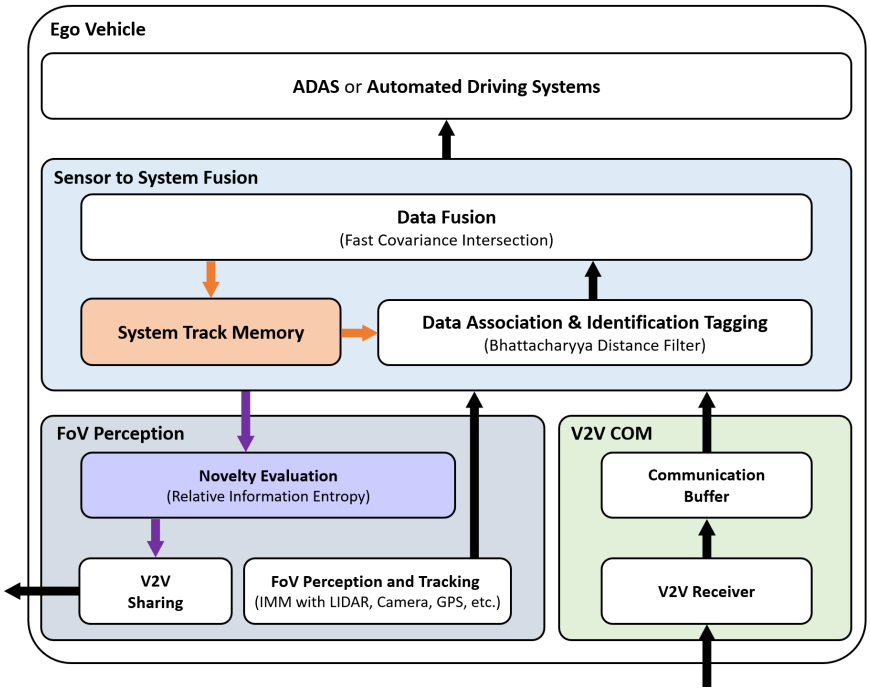

Figure 4.1: Overview of the Proposed Novelty Discrimination Computations at Each Participating Ego-Vehicle

evaluates the novelty of the new perception information to be broadcasted for decentralized cooperative perception frameworks in V2V networks.

- We evaluate the presented method in highway scenarios at different vehicular traffic density settings utilizing a comprehensive cooperative perception metric that considers traffic-relevant kinematic states and their associated uncertainties.
- We discover that there are promising benefits for the novelty discrimination method with respect to improving bandwidth utilization at moderate participation rates and minimizing communication delay with insignificant compromises on the perception accuracy.

The rest of the chapter is organized as follows. Section 4.3 gives the system framework and modeling details. Section 4.4 gives the results and discussion from the evaluation of the proposed framework. Section 4.5 summarizes the main conclusions and directions for further investigation.

4.3 System Framework and Modeling Details

4.3.1 Data Processing Framework

A schematic overview of the proposed framework is shown in Fig. 4.1. The framework consists of three main parts, which are the FoV perception management, the V2V communication data collection and synchronization, and the sensor to system fusion processes. For the FoV perception, each vehicle employs a set of on-board sensors (radar, LIDAR, camera, etc.) for object vehicle estimation and another set of sensors (GPS, IMU, etc.) for ego localization. These measurements are processed by an Interacting Multiple Model (IMM) filter to form sensor tracks for the ego vehicle as well as each vehicle in its sensor's composite FoV. In the following, we refer to the output of this process as *sensor track* data. At the same time, all participating vehicles receive a set of sensor tracks from others via the V2V network which are processed through a communication buffer for time synchronization. The combined set of sensor tracks are then associated and fused with the *system tracks* (tracks held in system track memory at the ego-vehicle) via a data association and fusion process. Therein, the data association step clusters the collected information into newly identified or pre-existing tracks, and each set of associated data are processed to yield a single fused system track for each object. Following this step, the ego sensor tracks are evaluated for their relative novelty against other sensor tracks and if deemed valuable, they are shared with other connected vehicles via V2V broadcast.

We keep several simplifying assumptions from [143] as listed below:

- Each vehicle in traffic is represented as a point mass; vehicle size and geometry variations are not considered in this study.
- Each vehicle can detect and estimate its own kinematic state, as well as of all other vehicles located within the set sensor range of 150 m. We adopt the sensor FoV angular obstruction filtering model from [143]. See Section. 4.3.3 later.
- Each participating vehicle computes sensor-level data association and fusion to generate state (2D position and velocity) estimates of all detected vehicles in its FoV. We reduce this process to IMM filters in which sensor noise is modeled as additive Gaussian noise on each vehicle's FoV measurement data.
- Each connected vehicle shares its FoV generated IMM filter outputs by broadcasting to surrounding vehicles (single-hop V2V) utilizing CSMA/CA (Carrier Sense Multiple Access with

Collision Avoidance) protocol.

4.3.2 Novelty-aware CPM Selection

4.3.2.1 Design Overview

The objective of novelty-aware evaluation is to exclude redundant sensor tracks (low novelty-value) in CPMs and broadcast only the sensor tracks with high novelty-value. The evaluation must be performed by each participating vehicle by computing the novelty-value of the new FoV data with respect to its previously broadcasted CPMs as well as other vehicles' communicated CPMs on the corresponding vehicle. In order to do so, the ego-vehicle must store and maintain the following information in memory over the past buffer window (BW), $t_{N_{bf}}$, or the communication time interval (CTI) ,t_{n_c},:

- Measured FoV history (BW): Records of FoV sensor tracks that the ego-vehicle has maintained over the past buffer time window.
- Ego-broadcasted CPM history (BW): Records of CPMs that the ego-vehicle has successfully broadcasted over the past buffer time window.
- Newly received CPMs (CTI): A set of new CPMs that the ego-vehicle has received since its last communication interval.
- Connected vehicle list (CTI): A list of connected vehicles $S_{v,t}$ that the ego-vehicle updated based on CPMs that the ego-vehicle successfully received over the past communication interval.

An example scenario is illustrated in Fig. 4.2. To focus on the workings of the novelty-aware evaluation, we will only consider communicating sensor tracks on object vehicles which are non-connected vehicles labeled as $OV1, OV2$, and $OV3$. Connected vehicles are labeled as $CV1, CV2, ..., CV4$. In the scenario shown, the ego-vehicle can only perceive $OV2$ and $OV3$ directly. During the communication interval, the ego-vehicle has received sensor tracks of all three object vehicles from different sets of connected vehicles as shown on the table: CPM_{CV1} containing $OV1_{CV1}$ and $OV2_{CV1}$, CPM_{CV2} containing $OV2_{CV2}$ and $OV3_{CV2}$, CPM_{CV3} containing $OV3_{CV3}$, and CPM_{CV4} also containing $OV3_{CV4}$. Prior to broadcasting, the ego-vehicle evaluates each of its FoV sensor tracks ($OV2_{Ego}$ and $OV3_{Ego}$) to corresponding sensor tracks received from other vehicles. Since the ego-vehicle does not have any perception information on $OV1$, it does not attempt any evaluation on the received $OV1$ sensor track. The details of the novelty-value computations are

given in the next subsection below. For now, the results of the novelty evaluation given in the table insert in Fig. 4.2 show that the $OV2_{Ego}$ sensor track of the ego-vehicle has a high novelty-value compared to he CPM broadcast by $CV1$ and $CV2$, which contain $OV2_{CV1}$ and $OV2_{CV2}$, respectively. Based on this result, the ego-vehicle decides to share only its $OV2_{Ego}$ sensor track during the following transmission. While this scenario provides a basic understanding of the framework, a number of exceptions must also be defined. In the following conditions, the ego-vehicle must share its sensor track with others:

- A new connected vehicle is detected since the last ego CPM transmission.
- A new object vehicle is detected within the FoV since the last ego CPM transmission.

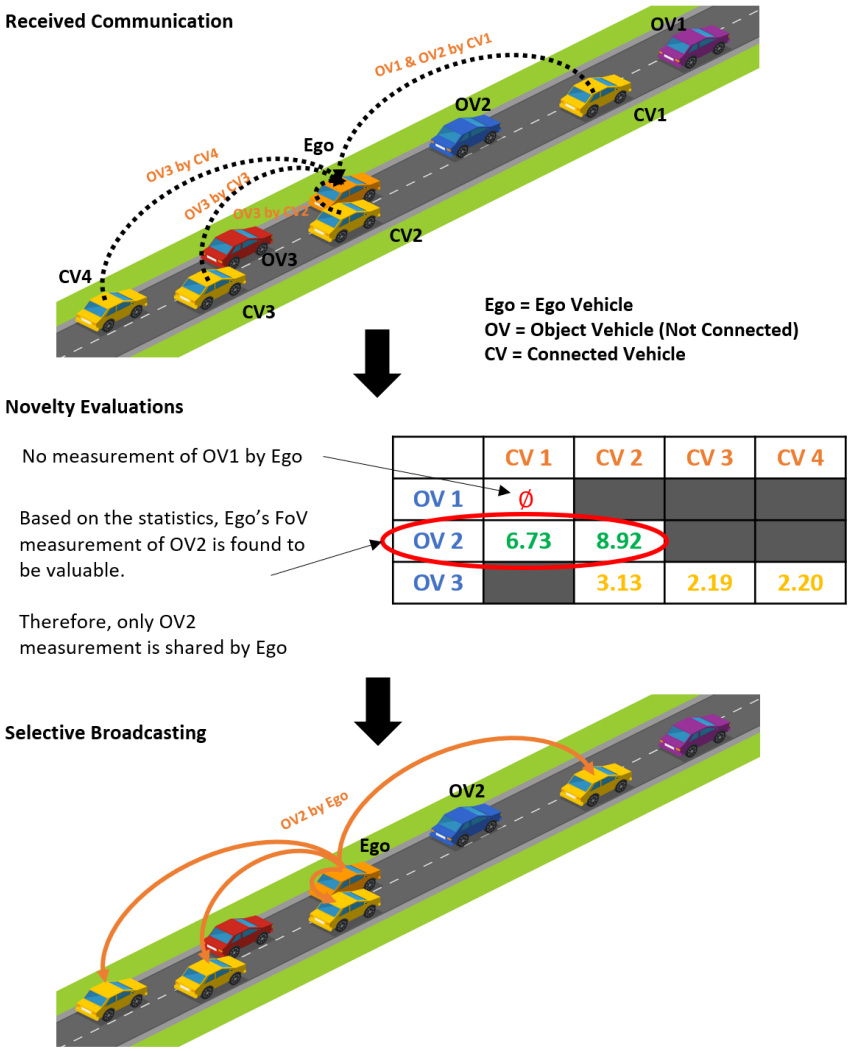

Figure 4.2: Novelty-aware Evaluation and Selective V2V Broadcasting

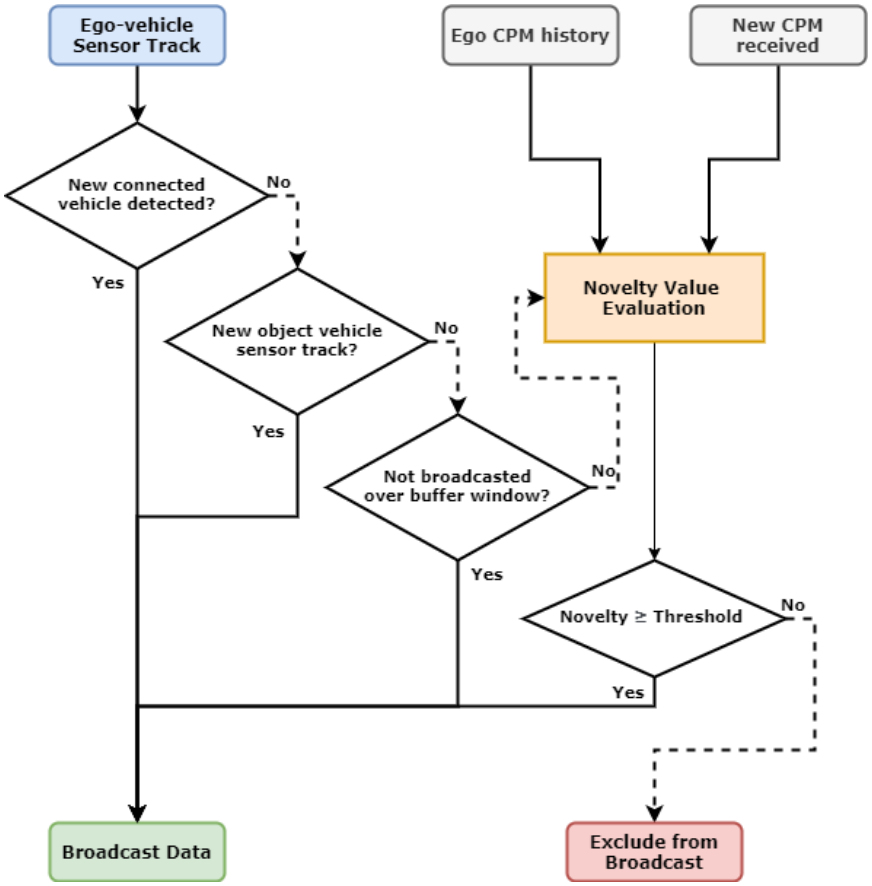

Figure 4.3: Novelty-value discriminating control flow at each ego-vehicle.

- A sensor track has not been communicated over the buffer time window.
- A sensor track has a high novelty-value than at least one of the corresponding sensor tracks (about an object vehicle, connected or not) received from other connected vehicles.

The control flow depicted in Fig. 4.3 shows the overall decision process incorporating the aforementioned conditions.

4.3.2.2 Novelty Evaluation

The novelty-aware communication constantly evaluates the perception information prior to broadcasting to assess the value of the contents and to communicate essential parts of the information selectively. To do so, we need a metric that can provide a concise and efficient statistical measure that can be computed without increasing the computational complexity of the framework. In information theory, the information gain achieved by random data distribution Q in comparison to another

random distribution P or the relative entropy of P with respect to Q is measured using the Kullback-Leibler (KL) divergence [14]:

$$D_{KL}(P,Q) = \int_{-\infty}^{\infty} p(x) \log(\frac{p(x)}{q(x)}) dx \tag{4.1}$$

where p and q denote the probability densities of P and Q. The KL divergence for two d-variate Gaussian distributions, $P_N \approx N(\mu_1, \Sigma_1)$ and $Q_N \approx N(\mu_2, \Sigma_2)$, has a closed formed expression given as [49]:

$$\begin{aligned} D_{KL}(P_N, Q_N) = \frac{1}{2}[\log \frac{|\Sigma_2|}{|\Sigma_1|} + Tr[\Sigma_2^{-1}\Sigma_1] \\ - d + (\mu_1 - \mu_2)^T \Sigma_2^{-1}(\mu_1 - \mu_2)] \end{aligned} \tag{4.2}$$

In our application, the data association step (Section. 4.3.4) must precedes the computation of the KL divergence as the association process will identify a set of communicated sensor tracks to be fused with the ego vehicle FoV sensor track. The KL divergence of the ego vehicle sensor track can then be computed with respect to each of the associated tracks. Revisiting Fig. 4.2 as an example, the evaluation of the KL divergence on the $OV2$ is computed between the ego vehicle sensor track $P_N = OV2_{Ego}$ and each of communicated and associated sensor tracks $Q_N = OV2_{CV1}$ or $OV2_{CV2}$. Only the ego vehicle sensor track that satisfies the following condition with respect to all of its associated tracks will then be broadcasted via V2V communication:

$$D_{KL}(\Psi_{ego}, \Psi_{1...N_{est}}) \geq \phi_{NVT} \tag{4.3}$$

where $\Psi_{1...N_{est}}$ is a list of communicated sensor tracks that are associated with Ψ_{ego} and ϕ_{NVT} is a novelty-value threshold (NVT) which can be set at a desired level or even adjusted dynamically to tune the desired degree of discrimination. Further discussion of the data association and definition of the sensor tracks $(\Psi_{ego}, \Psi_{1...N_{est}})$, and the novelty discrimination is given in Section 4.3.6 below.

4.3.3 Field-of-View Vehicle Tracking

An IMM filter is used for the estimation and tracking of self as well as of nearby vehicles within the ego-vehicle's FoV as described in [143]. Utilizing constant velocity (CV) and constant acceleration (CA) based Kalman filters and blending hypothesis of each mode, the IMM filter can

obtain more consistent estimates of the motion state of vehicles than what can be obtained by assuming any one of the modes alone [105]. Denoting the set of indices for the vehicles in the shared traffic T (set of vehicles) at time t by $\zeta_{T,t}$, the detected subset $\zeta_{FoV_i,t}$ in the FoV of vehicle i at time t is defined as:

$$\zeta_{FoV_i,t} = \{j \in \zeta_{T,t} | d_{(i,j),t} < R_i \wedge j \in LoS_{i,t}\} \tag{4.4}$$

where $d_{(i,j),t}$ is the Euclidean distance between vehicles i and j, at time t. Eq. (4.4) defines the FoV neighborhood such that each vehicle i has a FoV measurement Z on vehicle j, if and only if vehicle i and j are within a set on-board sensor detection range, R_i, and the line-of-sight (LoS) between the two vehicles is unobstructed ($j \in LoS_{i,t} \Leftrightarrow i \in LoS_{j,t}$). To prevent broadcasting track data comprised of estimates with premature convergence (or of large uncertainties), we set an allowable maximum threshold for the determinant of covariance matrix accompanying each track. This identifies a communicable set of FoV generated track data $\Phi_{c_i,t}$ as:

$$\Phi_{c_i,t} = \{[X_{j,t}, P_{j,t}] | det(P_{j,t}) \leq \phi_{IMM_i} \wedge j \in \zeta_{FoV_i,t}\} \tag{4.5}$$

which is about vehicles j ($j \in \zeta_{FoV_i,t}$) that are detected and estimated by vehicle i, $P_{j,t}$ is the covariance matrix accompanying IMM estimates of the states $X_{j,t}$, and t is the time index for the send time. ϕ_{IMM_i} is an allowable threshold on the convergence of the IMM filter for each track. This issue becomes more important in rapidly changing traffic where track birth and death effects are frequent [142].

4.3.4 Data Association and Fusion

The cooperative perception framework we presented in [143] lacked the retention of prior fusion computations. Therein, at every iteration of the data association and fusion process, the newly computed perception information were considered directly usable by the higher level application such as ADAS for that instant only. For the next iteration, a new set of perception information were computed without any utilization of the fusion history. Such a fusion architecture is often called a sensor-to-sensor track fusion architecture [26]. Each participating vehicle (sensor/sender) generated FoV estimates (sensor tracks) and periodically sent them to the ego-vehicle (system/receiver). The ego-vehicle then performed data association of the sensor tracks and data fusion process to form system tracks where each system track corresponds to a single hypothesized object vehicle without the

use of the previous state estimates of the system tracks. Although such an architecture could avoid correlated estimation errors, the overall process was not efficient since the prior processing history are discarded. To address this issue, we adopt the sensor-to-system track fusion architecture[26], which is depicted as follows in Fig. 4.4.

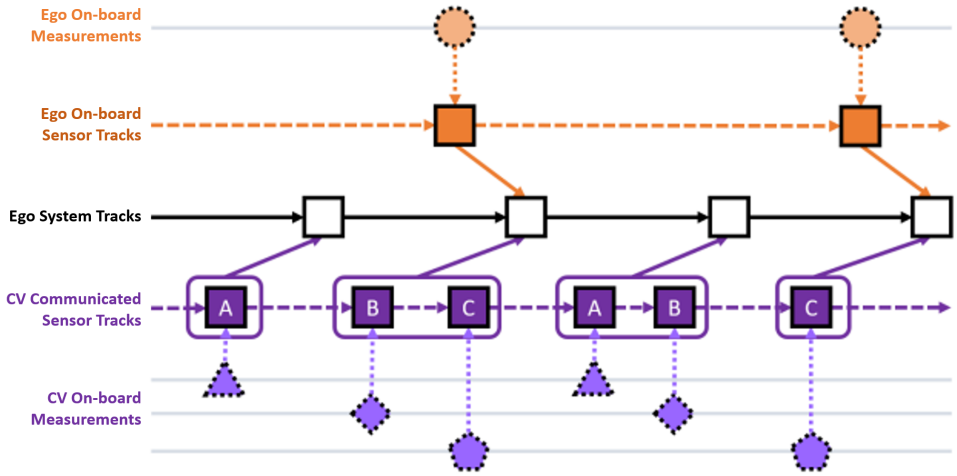

Figure 4.4: Sensor to System Track Fusion Framework

As mentioned in Section 4.3.1, all sensor tracks, generated by the ego-vehicle or received from other connected vehicles via broadcast, must go through a data association process. Dropping the time index for clarity, let $\mathbf{\Phi}_f$ be the set of FoV data (state estimates and corresponding covariances) and $\mathbf{\Phi}_c$ be the set of buffered communicated data. The combined set of estimates is:

$$\mathbf{\Psi}_{snr} = \mathbf{\Phi_f} \cup \mathbf{\Phi_c} \tag{4.6}$$

where the cardinality of the union set is $|\mathbf{\Psi}_{snr}| = N_{snr}$. Given that there is an existing set of system tracks, $\mathbf{\Psi}_{sys}$ with $|\mathbf{\Psi}_{sys}| = N_{sys}$, the Bhattacharyya distance is computed for all possible indexed pair $i = 1, \ldots, N_{snr}$ and , $j = 1, \ldots, N_{sys}$, as [11]:

$$\begin{aligned} BD_{(i,j)} = &\frac{1}{8}(X_i - X_j)^T(\frac{P_i + P_j}{2})^{-1}(X_i - X_j) \\ &+ \frac{1}{2}\ln(\frac{det(\frac{P_i + P_j}{2})}{\sqrt{det(P_i)det(P_j)}}) \end{aligned} \tag{4.7}$$

We define a set threshold, ϕ_{BD}, to identify a group of pairs of estimates that can be asso-

ciated with (directly or via neighboring estimates) one another whenever ($BD_{(i,j)} \leq \phi_{BD}$). Such a group/cluster of associated estimates are considered to potentially represent the same object or vehicle. The sensor tracks that are not associated to the pre-existing system tracks, go through a sensor-to-sensor track association process to form a new set of system tracks [143]. We denote all such groups of associated estimates by:

$$\mathbf{S}_{asso} = \{\mathbf{\Psi}_{a_1}, \mathbf{\Psi}_{a_2}, \ldots, \mathbf{\Psi}_{a_{N_v}}\} \tag{4.8}$$

where $\mathbf{\Psi}_{a_1} \cup \mathbf{\Psi}_{a_2} \cup \mathbf{\Psi}_{a_3} \cdots \cup \mathbf{\Psi}_{a_{N_v}} \subseteq (\mathbf{\Psi}_{snr} \cup \mathbf{\Psi}_{sys})$, each $\mathbf{\Psi}_{a_n} = [\mathbf{X}_{a_n}, \mathbf{P}_{a_n}]$ is a cluster set of associated estimates ($n = 1, \ldots, N_v$) that may or may not contain one of the pre-existing system tracks. The states and the covariances are $\mathbf{X}_{a_n} = \{X_{a_{n_1}}, \ldots, X_{a_{n_{N_{est,n}}}}\}$ and $\mathbf{P}_{a_n} = \{P_{a_{n_1}}, \ldots, P_{a_{n_{N_{est,n}}}}\}$ respectively, $|\mathbf{\Psi}_{a_n}| = N_{est,n}$ is the cardinality of the corresponding cluster $\mathbf{\Psi}_{a_n}$. N_v is the number of clusters.

As shown in Fig. 4.4, the proposed framework can be viewed as a centralized system with two independent sensors: the ego vehicle's on-board sensors and the vehicular communication. The sensor data (on-board measurements of ego or connected object vehicles) are processed locally to form sensor tracks (IMM) which are then sent (within the ego's system or via V2V communication) to the ego vehicle to be fused and form system tracks. While the two sensors can be considered as independent and uncorrelated, the system track has to deal with the problem of correlated estimation errors due to the presence of historical data from each of the sensor tracks.

As in our previous study [143], the Fast Covariance intersection (FCI) fusion algorithm is adopted here to manage an unknown degree of inter-estimate correlation and compute a consistent, albeit conservative, fused estimate [72, 34, 92]. Using FCI, the group of estimates in each associated cluster $\mathbf{\Psi}_{a_n}$ is fused into the single estimate $\Psi_{f_n} = [X_{f_n}, P_{f_n}]$ where:

$$\begin{aligned} P_{f_n}^{-1} &= \sum_{k=1}^{N_{est,n}} \omega_{a_{n_k}} P_{a_{n_k}}^{-1} \\ X_{f_n} &= P_{f_n} \sum_{k=1}^{N_{est,n}} \omega_{a_{n_k}} P_{a_{n_k}}^{-1} X_{a_{n_k}} \end{aligned} \tag{4.9}$$

where the non-negative fusion weights satisfy $\sum_{k=1}^{N_{est,n}} \omega_{a_{n_k}} = 1$. Fusing all associated clusters, ($\mathbf{\Psi}_{a_n} = [\mathbf{X}_{a_n}, \mathbf{P}_{a_n}] \rightarrow \Psi_{f_n} = [X_{f_n}, P_{f_n}]$ for all $n = 1, \ldots, N_v$), we arrive at the final set of fused estimates with the final fused cardinality of N_v:

$$\mathbf{\Psi}_f = \{\Psi_{f_1}, \Psi_{f_2}, \ldots, \Psi_{f_{N_v}}\} \tag{4.10}$$

4.3.5 Communication Buffer

Since sensor tracks that have been measured or transmitted at potentially different times will be compared, it is important to synchronize the tracks prior to the novelty evaluation. To this end, we use a communication buffer to not only keep all sensor tracks from CPMs synchronized to the current process time but also to compensate for intermittent communications resulting from packet drops and time synchronization issues for the data association and fusion step. The following formulation uses the latest set of stored data to estimate and fill in for recently missed information assuming a constant velocity motion model to predict the states of those object vehicles in the buffer to the current time index. Let $\mathbf{X}_{i,j} = \{X_{t_c-N_{bf}}, \ldots, X_{t_c-1}, X_{t_c}\}$, where t_c is the most current time index, be the series of estimates that have been communicated between vehicles $i \rightarrow j$, and N_{bf} is the length for the communication buffer/window. Each communication may be either successful $\xi_{i,j,t} = 1$ or unsuccessful $\xi_{i,j,t} = 0$. Then, the buffered estimate at the most current step, X_{i,j,t_c} can be computed from:

$$\begin{aligned} X_{i,j,t_c} &= \xi_{i,j,t_c} X_{i,j,t_c} + \ldots \\ &+ \sum_{l=1}^{N_{bf}} \{ (\prod_{q=1}^{l} (1 - \xi_{i,j,t_c-q+1})) \xi_{i,j,t_c-l} O(\Delta t) X_{i,j,t_c-l} \} \end{aligned} \tag{4.11}$$

where $O(\Delta t)$ is a state transition matrix of the constant velocity model with time step $\Delta t = t_{t_c} - t_{t_c-l}$. If no data is received about an object for longer than the set buffer window, no information will be retained about that object until the next successful communication.

4.3.6 Novelty Discrimination

As described in Section 4.3.2.2, each of the ego vehicle FoV sensor tracks that has one or more associated sensor tracks will be evaluated for its information novelty-value using Eq. 4.2. Then a set of FoV sensor tracks $\mathbf{\Psi}_{f_{NV}}$ can be identified based on Eq. 4.3 as:

$$\mathbf{\Psi}_{f_{NV}} = \{\Psi_{f_i} \in \mathbf{\Psi}_{a_n} | D_{KL}(\Psi_{f_i}, \Psi_{n_{1\ldots N_{est}}}) \geq \phi_{NVT}\} \tag{4.12}$$

where $\mathbf{\Psi}_{a_n}$ is an associated cluster which contains one of the ego vehicle FoV sensor track, Ψ_{f_i}, and other associated sensor tracks, $\Psi_{n_{1\ldots N_{est}}}$, that are transmitted by other connected vehicles.

4.3.7 Performance Metric

In [143], we modified the optimal subpattern assignment metric (OSPA) [112] to consider the uncertainty information associated with the corresponding estimates while weighing all possible pair-wise assignments and cardinality errors between the associated and fused outputs and the ground truth. This metric was used to evaluate the proposed scheme at scale based on various traffic scenarios and participation rates. The modified OSPA metric uses Mahalanobis distance (MD) to incorporate the covariances obtained with the state estimates. We also use the metric to compactly quantify both the localization and 2D velocity state estimation errors. Our final modified OSPA metric is given by Eq. (4.13) [143]. We shall use this metric continuing form the previous chapter to evaluate the performance of the proposed Novelty discriminating approach in the following section.

4.4 Results and Discussions

4.4.1 Simulation Settings

To evaluate the performance of the proposed framework, we will be focusing on scenarios with highly congested vehicular traffic. We created a unidirectional 4-lane traffic environment using the traffic microsimulation software PTV VISSIM [95]. A set of 30 simulation runs were taken for each case of 3 different traffic flow rates (9500, 11500, and 15500 veh/hr) with a prescribed average traffic speed of 60-70 kph, which correspond to traffic density settings of 146, 177, and 238 veh/km. Randomized driver and vehicle model parameterizations are used to represent realistic traffic. With these randomizations and multiple simulation runs we take a Monte Carlo approach for for evaluating the cooperative perception scheme in order to account for the stochastic nature of the simulated traffic as well as of the communication network.

For the communication model, a dual slope communication loss model has been adopted [1, 93] and the stochastic fading model of Nakagami-m is used to account for the path loss due to

$$d^{(c)}_{OSPA_{MD}}(\mathbf{X}_g, \mathbf{\Psi}_f) = \left(\frac{1}{N_v} \left(\min_{\pi \in \Pi_{N_v}} \sum_{i=1}^{m} MD^{(c)}(X_{g_i}, \Psi_{f_{\pi(i)}})^p + c^p(|\mathbf{\Psi}_f| - |\mathbf{X}_g|) \right) \right)^{\frac{1}{p}} \tag{4.13}$$

small scale fading of transmitted rays [89]. To consider the Medium Access Control (MAC) layer issues with the ad-hoc vehicular communication network, we adopted the Carrier-Sense Multiple Access with Collision Avoidance (CSMA/CA) protocol.

As a baseline for comparison, we considered an identical cooperative perception framework without the novelty discrimination method where all of the sensor tracks are actively communicated with other connected vehicles without any filtering process. In the following discussions and the figures, we will use the shorthand ND to refer to our proposed approach. The performance is evaluated by computing the modified OSPA metric from the perspective of each participating vehicle for a region of 150-m radius centered on that vehicle at the various geographic locations in the traffic environment under consideration (excluding the boundary entry/exit regions). In all evaluations, we vary the participation rate from 15 to 100% (fully connected and cooperative).

4.4.2 Performance of Novelty-aware Dissemination

For the comparative analysis and the evaluation for the performance of the proposed method, two different discriminating threshold settings were used ($\phi_{NVT_{High}}$ and $\phi_{NVT_{Low}}$), where the high setting utilizes a higher threshold to isolate and disseminate vehicular information of higher novelty-value. These two settings are compared with a framework without any novelty measure to show the relative benefits of the proposed dissemination method.

Fig. 4.5 and Fig. 4.6 show the average bandwidth usage and the average communication delay per vehicle for varying participation rates and at three traffic density settings. Overall, a gradual increase in the bandwidth usage (Fig. 4.5) is shown with increasing vehicular traffic density and participation rates. This trend is inevitable for the following reasons. The number of FoV sensor tracks grows with the increase in the traffic density since more and more vehicles are detected. This continues to increase until it is limited by the sensor resolution of each vehicle. In addition, the presence of increased number of vehicles in FoV also means that there will be more frequent communication LoS blockage. As a result, the increase in the participation rate has even more significant effects on both bandwidth utilization and communication delay at higher traffic density

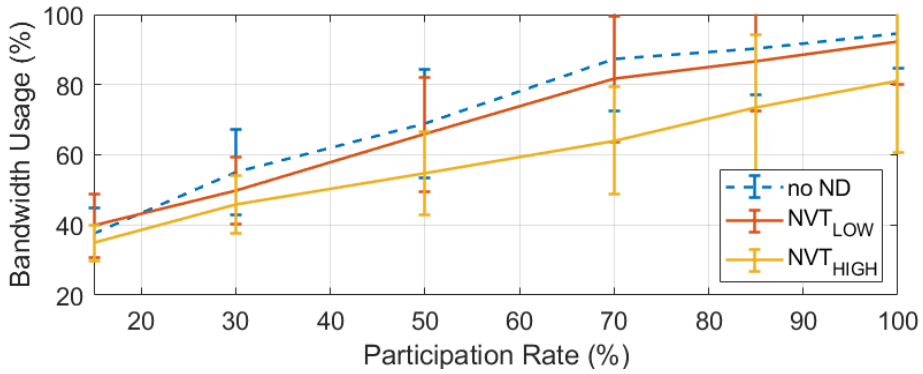

(a) 146 veh/km

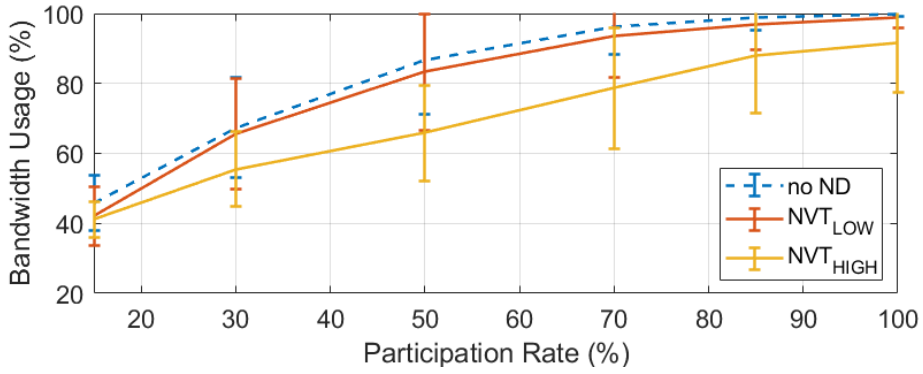

(b) 177 veh/km

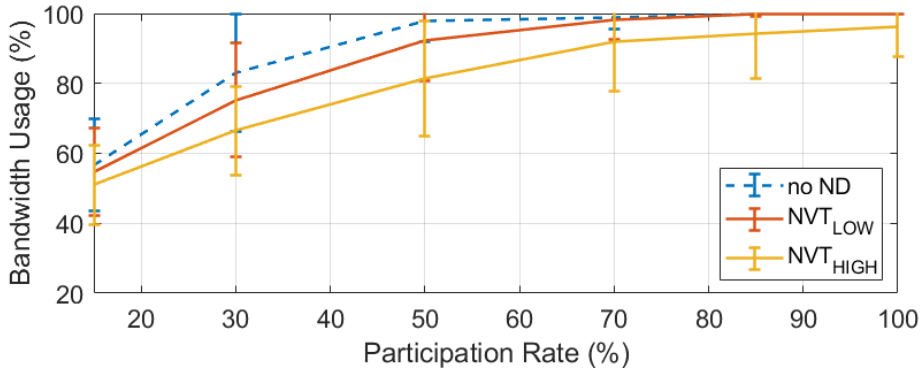

(c) 238 veh/km

Figure 4.5: Average Bandwidth Usage (%) for Each Traffic Density Setting

settings as can be seen by comparing Fig. 4.5a and Fig 4.6a with the lower density settings. Notably, without the proposed novelty discrimination scheme, we see in Fig. 4.5 that the bandwidth usage reaches the maximum utilization (100%) near 10-80% participation rate for the high traffic density of 177 and 238 veh/km. In [143], it was noted that such effects translate into computational loads that grew linearly with participation and traffic density, which motivated the use of our proposed

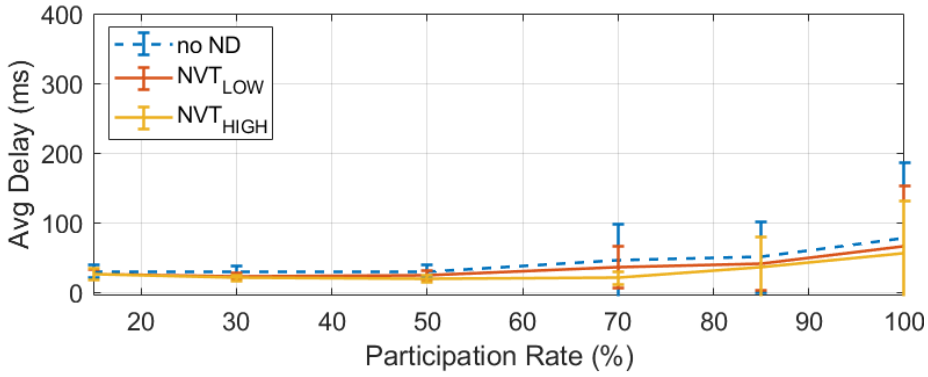

(a) 146 veh/km

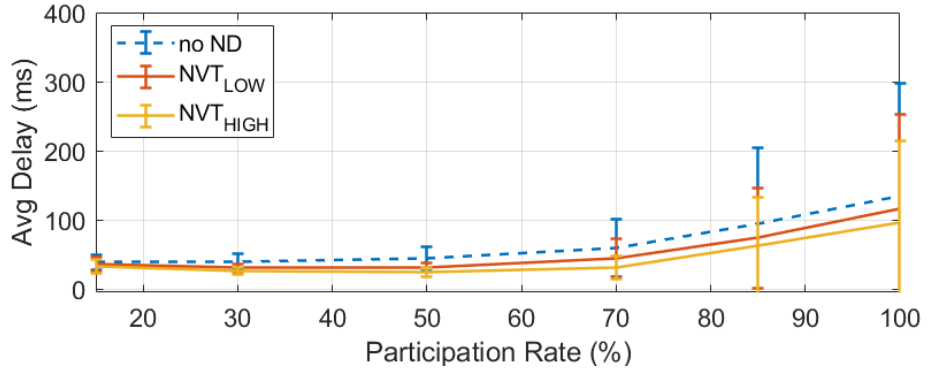

(b) 177 veh/km

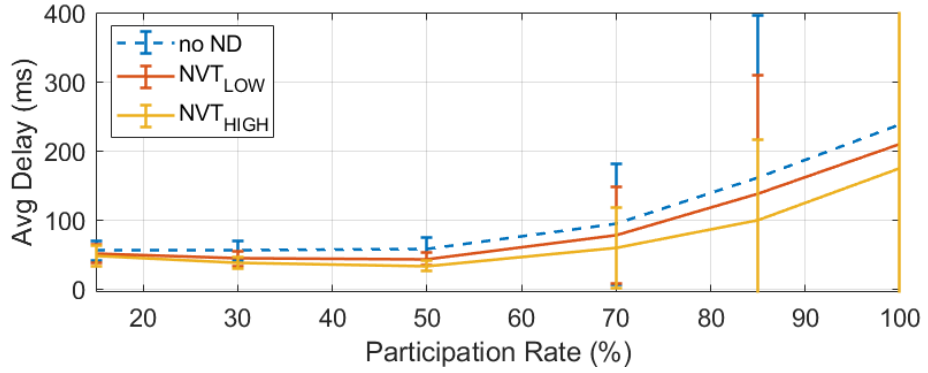

(c) 238 veh/km

Figure 4.6: Average Delay (ms) for Each Traffic Density Setting

scheme.

It can also be seen that the proposed novelty discrimination scheme does alleviate the bandwidth usage at moderate participation rates for all three traffic density settings, albeit the improvements can be small when the discrimination threshold (NVT) is low. For the highest traffic density setting (238 veh/km) with very high (90-100%) participation rates, it can be seen that the

low NVT setting could not reduce the overall bandwidth usage (Fig. 4.5c) despite of the reduction in the average delay (Fig. 4.6c). Since each participating vehicle is broadcasting only a subset of FoV perception data that are expected to have more novelty-value than others, the congestion on the V2V network is mitigated. This is backed by Fig. 4.6 which shows the substantial reduction in the average communication delay for all communicated CPMs. It is interesting to note that, at high traffic density settings, the high NVT setting had a diminishing improvement on the bandwidth usage from mid to high (60% to 100%) participation rates while it had a consistent improvement in the average delay. The latter is due to the decrease in communicated CPMs with the high filtering (high NVT setting).

While such results were expected based on the proposed framework, the important question is whether there was any sacrifice of perception accuracy due to the reduction of the communicated content in CPMs. With a high novelty-value threshold, there is a risk of filtering valuable perception data which in result can worsen the perception accuracy of the participating vehicles. In Fig. 4.7, modified OSPA values that account for 90th-percentile of the participating vehicles are shown. These values represent the average perception accuracy for the majority of participating vehicles throughout the simulation period. For the first two lower traffic density settings (146 and 177 veh/km), all three cases achieved the same modified OSPA value when the participation rate was equal to or higher than 25%. For the case of 238 veh/km, however, the proposed framework further improved the perception of the participating vehicles for 25-50% participation rate. It is important to note that the OSPA metric considers both the uncertainty of the estimates and also the cardinality errors which are heavily penalized. Therefore, the results shown in Fig. 4.7 confirms that the presented novelty value discrimination scheme does not degrade the perception accuracy starting with rather low levels of participation.

The observations in the previous two paragraphs that the bandwidth utilization as well as the average delay are improved at the high NVT setting without compromising the performance of the cooperative perception suggest that even higher NVT setting settings can be used in extremely congested environments to alleviate the congested communication medium. Dynamic adjustments of the NVT settings could also be pursued.

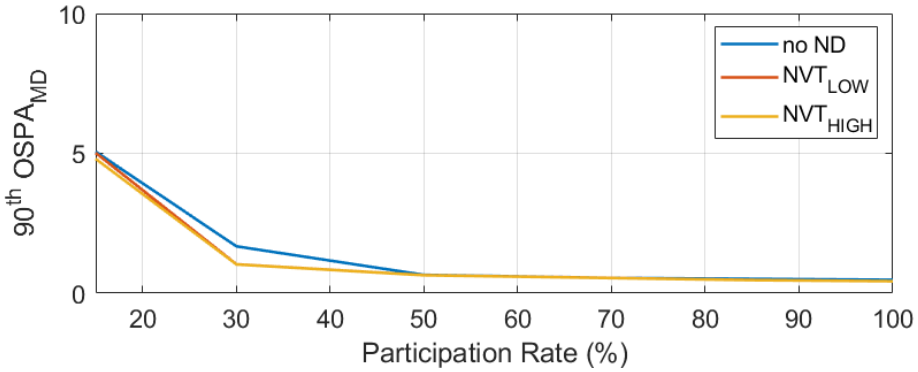

(a) 146 veh/km

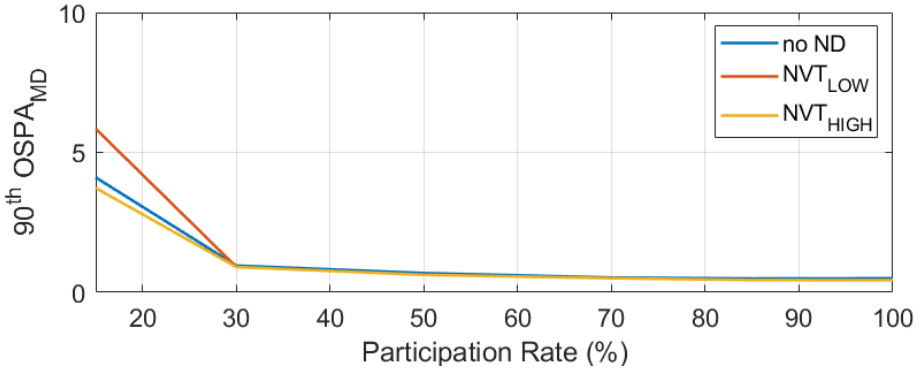

(b) 177 veh/km

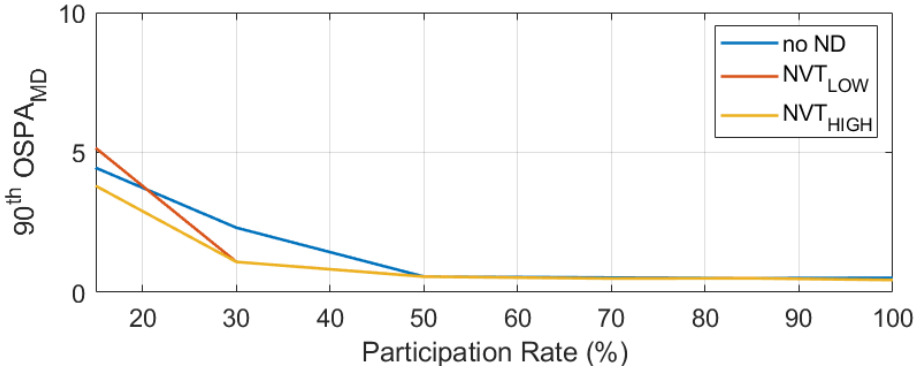

(c) 238 veh/km

Figure 4.7: 90th Percentile Modified OSPA for Each Traffic Density Setting

4.5 Conclusion

In this chapter, we have presented a novelty discrimination method for decentralized cooperative perception framework that has the potential to alleviate known shortcomings leading to bandwidth limitations and delays in V2V networks. The main idea of the method is to endow each participating ego-vehicle with a way to evaluate the novelty value of the perception data in it in-

cludes in its CPM so that only data deemed of sufficient novelty value is included. We evaluated the proposed scheme using randomized traffic simulations for a multi-lane highway environment with dense traffic settings, considering FoV sensing and communication losses.

The results showed that there is a clear benefit in the reduction of bandwidth utilization and the average communication delay with the proposed novelty discriminating approach. The average bandwidth utilization improvements appear can be up to 20% at moderate participation rates, while similar average delay improvements are achieved at high participation rates and high traffic density settings. We observed that these benefits are realized without sacrificing the perception accuracy of the main decentralize cooperative perception scheme. The effect of novelty-value threshold is also presented where the high threshold setting further reduced the bandwidth utilization and the average delay.

Chapter 5

Conclusions and Future Work

5.1 Conclusion

The dissertation focused on improving situational awareness of intelligent vehicles in connected traffic with the consideration of 1) social driver model and predictive controllers, 2) vehicular data association and fusion architecture, 3) decentralized cooperative perception strategy, and 4) effects of participation variations and other limitations on the communication network. We briefly summarize the main conclusions from each of these considerations.

First, a human-like social driver model is presented. The social aspect of human driving behavior is captured using a modified social force model (SFM) which is then implemented for predictive guidance and control via a nonlinear model predictive control (NMPC) framework. The model showed good performance in various simulated scenarios including a single-lane as well as multi-lane traffic situations and demonstrated proper behaviors such as adaptive cruise control (ACC) and lane-changes while maintaining reasonable vehicle dynamic response.

Then, a hierarchical vehicular social force control scheme is presented to utilize lane-based social force aggregation that would rely on downstream traffic information obtained via vehicular connectivity. The upper level NMPC with a long preview performs optimal lane selection computations, and the planned lanes are then passed as the reference trajectories for the lower-level NMPC which enforces lane tracking along with other social forces while maintaining proper vehicle dynamics. The presented results showed clear performance benefits in terms of more efficient guidance of the ego vehicle.

A vehicular data association and fusion architecture is presented utilizing Bhattacharyya Distance Filter (BDF) and Covariance Intersection Fusion (CIF). The performance is demonstrated for generalized cases where each communicating vehicle broadcasts ego sensor field of view (FoV) estimates along with corresponding uncertainties, and also acts as a fusing node for perception data received from other vehicles in its communication range. For the evaluation of the proposed framework, a modified Optimal Subpattern Assignment Metric (OSPA) is proposed as a compact metric that takes into account the multi-target estimation error from the perspective of any one participating vehicle.

With the proposed data processing architecture, a generalized cooperative perception framework is presented that is based on decentralized V2V vehicular communication. The framework is then evaluated on randomized traffic simulations for multi-lane highway and roundabout intersection scenarios considering both communication losses and sensor FOV resolutions. Compared to a baseline cooperative perception scheme, the presented cooperative perception framework benefits a much larger percentage of participating vehicles with lower perception errors, even at modest participation rates, in both highway and urban roundabout scenarios. It is observed that these benefits come with higher data traffic and computational costs than the baseline, specially at high participation rates, although the computational needs remain within the realm of modern on-board devices.

Finally, a novelty discrimination method for decentralized cooperative perception framework is presented to alleviate the bandwidth limitations and the communication delays in V2V networks. The method is evaluated based on randomized traffic simulations demonstrated a clear benefit in the reduction of bandwidth utilization and the average communication delay with the proposed novelty discriminating approach. The average bandwidth utilization improvement up to 20% is shown at moderate participation rates, while similar average delay improvements are achieved at high participation rates and high traffic density settings. Most importantly, these benefits are achieved without sacrificing the perception accuracy of the main decentralize cooperative perception scheme.

5.2 Future Works

There are a number of areas covered in this dissertation that require for further investigation and open avenues for future work. Some of the main ones are discussed below:

- The social force aggregation control introduced in Chapter 2 utilizes a hierarchical vehicular SFM control scheme where the upper level predictively select the most efficient lane over a long horizon covered by connectivity, and the lower level enforces the lane tracking while considering higher fidelity social force resolution and lane-changing dynamics within the shorter horizon captured by the ego vehicle's FoV. In the completed work, it was assumed that object vehicle information within the extended range are readily available for the upper level controller of the ego vehicle. In reality, the construction of the information from vehicular connectivity should explicitly consider the uncertainty associated with the medium (signal fading, losses, latencies, etc.). To consider such important dynamics, the cooperative perception framework presented in Chapter 3 will need to be integrated with the social force aggregation controller. The cooperative perception framework will work with the social force controllers simultaneously in a coordinated manner with proper update rates. In this integrated model, the fused system tracks will be sent to both the upper level for the longer horizon perception and the lower level controller for the enhanced local FoV perception. In addition, there is an uncertainty associated with the state information of object vehicles in traffic. The uncertainty information can be in fact integrated into the formulation of the object forces. The complete integrated system should then be evaluated by applying a Monte Carlo approach in order to account for the stochastic nature of the overall system. For a given simulation setting (road topology, traffic density, and speed limit), various performance metrics (number of total lane changes, average travel speed, average acceleration, etc.) should be evaluated with a careful consideration of variances such as the perception and the upper level controller update rate, the participation rate, the sensor and the communication range.
- The cooperative perception scheme discussed in Chapter 3 treated all received information as being free of malice. In practice, it is important to add algorithms that detect and isolate malicious intent in the data communicated before proceeding with the fusion computations. A reliability/confidence metric may also be shared with other connected vehicles via V2V communication to minimize repetitive evaluations. Some works already exist in this direction [65, 27].
- The evaluation of the novelty discriminating method presented in Chapter 4 suggested that further performance improvements can be possible by adopting a dynamic novelty-value threshold which can be adjusted based on the detected bandwidth utilization or even based on the statis-

tical analysis of the KL divergence across all system tracks. Ultimately, these schemes need to be incorporated and validated with connected vehicle test beds that allow high participation rates and high traffic density where the bandwidth/delay issues appear. These are capabilities that may become available in the future; in the meantime, model and simulation similar to what is proposed in this dissertation can be used to evaluate the dynamic thresholding scheme.

- The results for novelty discriminating method presented in Chapter 4 assumed that all participating vehicles adopt the same IMM model (with the same Gaussian measurement and process noise assumptions for all vehicles) to track object vehicles in their FoV and utilize the covariance matrices as uncertainty information for associated object vehicle data. The practically possible heterogeneity of the noise characteristics in traffic could have a bearing on the novelty value computations, and this aspect needs further investigations.

Appendices

Appendix A Line-of-Sight (LoS) Algorithm

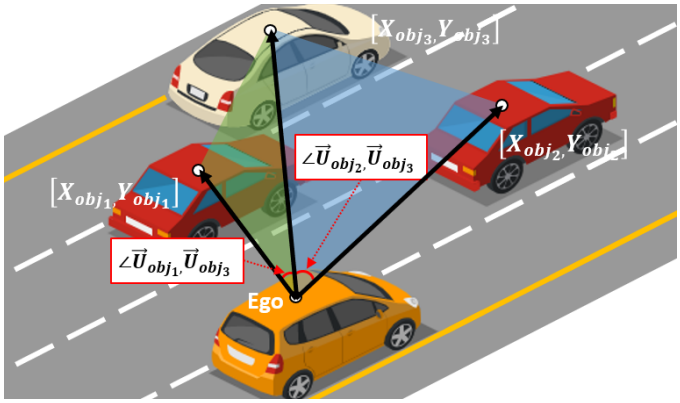

Figure 1: Illustration for the LoS Algorithm

Algorithm 1: A simple LoS evaluation algorithm for identifying objects vehicles that are detectable from an ego-vehicle.

Data: XY coordinates of ego $[X_{ego}, Y_{ego}]$, and surrounding object vehicles $[X_{obj_n}, Y_{obj_n}]$, where $n = 1, \ldots, N_{obj}$

Result: A set of LoS object vehicle indices, LoS_{ego}

LoS Proximity-based Association:

Compute $\vec{U}_{obj_n} = [X_{obj_n} - X_{ego}, Y_{obj_n} - Y_{ego}]$ for $\forall n$;

for $i = 1$ *to* N_{obj} **do**

  $k \leftarrow 0$;

  for $j = 1$ *to* N_{obj} **do**

    $\angle(\vec{U}_{obj_i}, \vec{U}_{obj_j}) \leftarrow \cos \dfrac{(\vec{U}_{obj_i}, \vec{U}_{obj_j})}{\left(||\vec{U}_{obj_i}||.||\vec{U}_{obj_j}||\right)}$;

    if $\angle(\vec{U}_{obj_i}, \vec{U}_{obj_j}) \leq \angle A_{max}$ **then**

      $T_{obj_i}(k) \leftarrow j$;

      $k \leftarrow k + 1$;

    end

  end

end

LoS Minimum Distance Object Identification:

for $i = 1$ *to* N_{obj} **do**

  $z \leftarrow T_{obj_i}(1)$;

  $M \leftarrow ||\vec{U}_{obj_z}||$;

  $k \leftarrow 1$;

  $LoS_{ego}(i) \leftarrow z$;

  $N_{T_i} \leftarrow \#|T_{obj_i}|$;

  for $k = 2$ *to* N_{T_i} **do**

    $q \leftarrow T_{obj_i}(k)$;

    if $||\vec{U}_{obj_q}|| < M$ **then**

      $LoS_{ego}(i) \leftarrow q$;

      $M \leftarrow ||\vec{U}_{obj_q}||$;

    end

  end

end

return LoS_{ego};

Bibliography

[1] Taimoor Abbas, Katrin Sjöberg, Johan Karedal, and Fredrik Tufvesson. A Measurement Based Shadow Fading Model for Vehicle-to-Vehicle Network Simulations. *International Journal of Antennas and Propagation*, 2015:1–12, jun 2015.

[2] Michael Aeberhard, Stefan Schlichtharle, Nico Kaempchen, and Torsten Bertram. Track-to-track fusion with asynchronous sensors using information matrix fusion for surround environment perception. *IEEE Transactions on Intelligent Transportation Systems*, 13(4):1717–1726, 2012.

[3] Frank J Aherne, Neil A Thacker, and Peter I Rockett. The Bhattacharyya metric as an absolute similarity measure for frequency coded data. *Kybernetika*, 34(4):363–368, 1998.

[4] G. G. Md. Nawaz Ali, Beshah Ayalew, Ardalan Vahidi, and Md. Noor-A-Rahim. Feedbackless Relaying for Enhancing Reliability of Connected Vehicles. *IEEE Transactions on Vehicular Technology*.

[5] G. G. Md. Nawaz Ali, Md. Noor-A-Rahim, Peter Han Joo Chong, and Yong Liang Guan. Analysis and Improvement of Reliability Through Coding for Safety Message Broadcasting in Urban Vehicular Networks. *IEEE Transactions on Vehicular Technology*, 67(8):6774–6787, aug 2018.

[6] Jeffery R. Anderson, Beshah Ayalew, and T. Weiskircher. Modeling a professional driver in ultra-high performance maneuvers with a hybrid cost MPC. In *Proceedings of the American Control Conference*, volume 2016-July, pages 1981–1986. Institute of Electrical and Electronics Engineers Inc., jul 2016.

[7] A. Bahr, M.R. Walter, and J.J. Leonard. Consistent cooperative localization. In *2009 IEEE International Conference on Robotics and Automation*, pages 3415–3422. IEEE, may 2009.

[8] Ramon Bauza, Javier Gozalvez, and Joaquin Sanchez-Soriano. Road traffic congestion detection through cooperative Vehicle-to-Vehicle communications. In *IEEE Local Computer Network Conference*, pages 606–612. IEEE, oct 2010.

[9] Paolo Bellavista, Luca Foschini, and Enrico Zamagni. V2X Protocols for low-penetration-rate and cooperative traffic estimations. In *IEEE Vehicular Technology Conference*. Institute of Electrical and Electronics Engineers Inc., nov 2014.

[10] A. Bemporad and C. Rocchi. Decentralized Hybrid Model Predictive Control of a Formation of Unmanned Aerial Vehicles. *IFAC Proceedings Volumes*, 44(1):11900–11906, jan 2011.

[11] Anil Bhattacharyya. On a measure of divergence between two multinomial populations. *Sankhyā: the indian journal of statistics*, pages 401–406, 1946.

[12] Giuseppe Bianchi, Luigi Fratta, and Matteo Oliveri. Performance evaluation and enhancement of the CSMA/CA MAC protocol for 802.11 wireless LANs. In *Proceedings of PIMRC'96-7th International Symposium on Personal, Indoor, and Mobile Communications*, volume 2, pages 392–396. IEEE, 1996.

[13] Chatschik Bisdikian, Lance M. Kaplan, and Mani B. Srivastava. On the quality and value of information in sensor networks. *ACM Transactions on Sensor Networks*, 9(4), jul 2013.

[14] Christopher M Bishop. *Pattern recognition and machine learning*. springer, 2006.

[15] D. Borsetti and J. Gozalvez. Infrastructure-assisted geo-routing for cooperative vehicular networks. In *2010 IEEE Vehicular Networking Conference, VNC 2010*, pages 255–262, 2010.

[16] Azzedine Boukerche, Horacio A.B.F. Oliveira, Eduardo F. Nakamura, and Antonio A.F. Loureiro. Vehicular Ad Hoc Networks: A New Challenge for Localization-Based Systems. *Computer Communications*, 31(12):2838–2849, jul 2008.

[17] Farid Bounini, Denis Gingras, Herve Pollart, and Dominique Gruyer. Real time cooperative localization for autonomous vehicles. In *2016 IEEE 19th International Conference on Intelligent Transportation Systems (ITSC)*, pages 1186–1191. IEEE, nov 2016.

[18] Mattia Brambilla, Monica Nicoli, Gloria Soatti, and Francesco Deflorio. Augmenting Vehicle Localization by Cooperative Sensing of the Driving Environment: Insight on Data Association in Urban Traffic Scenarios. *IEEE Transactions on Intelligent Transportation Systems*, 21(4):1646–1663, apr 2020.

[19] Alberto Bucchi, Cesare Sangiorgi, and Valeria Vignali. Traffic Psychology and Driver Behavior. *Procedia - Social and Behavioral Sciences*, 53:972–979, oct 2012.

[20] Franois Caron, Manuel Davy, Emmanuel Duflos, and Philippe Vanheeghe. Particle Filtering for Multisensor Data Fusion With Switching Observation Models: Application to Land Vehicle Positioning. *IEEE Transactions on Signal Processing*, 55(6):2703–2719, jun 2007.

[21] Scott E. Carpenter and Mihail L. Sichitiu. An obstacle model implementation for evaluating radio shadowing with ns-3. In *Proceedings of the 2015 Workshop on ns-3 - WNS3 '15*, 2015.

[22] Stefano Carpin. Fast and accurate map merging for multi-robot systems. *Autonomous Robots*, 25(3):305–316, oct 2008.

[23] Ricardo Omar Chavez-Garcia and Olivier Aycard. Multiple Sensor Fusion and Classification for Moving Object Detection and Tracking. *IEEE Transactions on Intelligent Transportation Systems*, 17(2):525–534, feb 2016.

[24] Lin Cheng, Benjamin Henty, Daniel Stancil, Fan Bai, and Priyantha Mudalige. Mobile Vehicle-to-Vehicle Narrow-Band Channel Measurement and Characterization of the 5.9 GHz Dedicated Short Range Communication (DSRC) Frequency Band. *IEEE Journal on Selected Areas in Communications*, 25(8):1501–1516, oct 2007.

[25] Chee-Yee Chong, Booz Allen, and Shozo Mori. Convex Combination and Covariance Intersection Algorithms in Distributed Fusion. Technical report.

[26] Chee Yee Chong, Shozo Mori, William H. Barker, and Kuo Chu Chang. Architectures and algorithms for track association and fusion. *IEEE Aerospace and Electronic Systems Magazine*, 15(1):5–13, jan 2000.

[27] Gurcan Comert, Mizanur Rahman, Mhafuzul Islam, and Mashrur Chowdhury. Change Point Models for Real-time Cyber Attack Detection in Connected Vehicle Environment. mar 2020.

[28] Stefano Di Cairano, Daniele Bernardini, Alberto Bemporad, and Ilya V Kolmanovsky. Stochastic MPC with learning for driver-predictive vehicle control and its application to HEV energy management. *IEEE Transactions on Control Systems Technology*, 22(3):1018–1031, 2013.

[29] Soenke Eilers, Jonas Martensson, Henrik Pettersson, Marcos Pillado, David Gallegos, Marta Tobar, Karl Henrik Johansson, Xiaoliang Ma, Thomas Friedrichs, Shadan Sadeghian Borojeni, and Magnus Adolfson. COMPANION – Towards Co-operative Platoon Management of Heavy-Duty Vehicles. In *2015 IEEE 18th International Conference on Intelligent Transportation Systems*, pages 1267–1273. IEEE, sep 2015.

[30] A. El Hajjaji and M. Ouladsine. Modeling human vehicle driving by fuzzy logic for standardized ISO double lane change maneuver. In *Proceedings - IEEE International Workshop on Robot and Human Interactive Communication*, pages 499–503, 2001.

[31] Abolfazl Eskandarpour and Vahid Johari Majd. Cooperative formation control of quadrotors with obstacle avoidance and self collisions based on a hierarchical MPC approach. In *2014 Second RSI/ISM International Conference on Robotics and Mechatronics (ICRoM)*, pages 351–356. IEEE, oct 2014.

[32] TCITS ETSI. Intelligent transport systems (ITS); vehicular communications; basic set of applications; definitions. *Tech. Rep. ETSI TR 102 6382009*, 2009.

[33] Paolo Falcone, Francesco Borrelli, Jahan Asgari, Hongtei Eric Tseng, and Davor Hrovat. Predictive Active Steering Control for Autonomous Vehicle Systems. *IEEE Transactions on Control Systems Technology*, 15(3):566–580, may 2007.

[34] Dietrich Fränken. Improved Fast Covariance Intersection for Distributed Data Fusion. Technical report, 2005.

[35] Sae Fujii, Atsushi Fujita, Takaaki Umedu, Shigeru Kaneda, Hirozumi Yamaguchi, Teruo Higashino, and Mineo Takai. Cooperative Vehicle Positioning via V2V Communications and Onboard Sensors. In *2011 IEEE Vehicular Technology Conference (VTC Fall)*, pages 1–5. IEEE, sep 2011.

[36] Junya Fukumoto, Naoto Sirokane, Yuta Ishikawa, Tomotaka Wada, Kazuhiro Ohtsuki, and Hiromi Okada. Analytic method for real-time traffic problems by using Contents Oriented Communications in VANET. In *2007 7th International Conference on ITS Telecommunications*, pages 1–6. IEEE, jun 2007.

[37] Jose R. Gallardo, Dimitrios Makrakis, and Hussein T. Mouftah. Performance analysis of the EDCA medium access mechanism over the control channel of an IEEE 802.11p WAVE vehicular network. In *IEEE International Conference on Communications*, 2009.

[38] Q. Gan and C.J. Harris. Comparison of two measurement fusion methods for Kalman-filter-based multisensor data fusion. *IEEE Transactions on Aerospace and Electronic Systems*, 37(1):273–279, 2001.

[39] P Gao, H.W Kaas, D Mohr, and D Wee. Automotive revolution-perspective towards 2030. *McKinsey and Company, Advanced Industries Report*, 2016.

[40] Keno Garlichs, Hendrik Jorn Gunther, and Lars C. Wolf. Generation Rules for the Collective Perception Service. In *IEEE Vehicular Networking Conference, VNC*, volume 2019-Decem. IEEE Computer Society, dec 2019.

[41] Sepideh Afkhami Goli, Behrouz H. Far, and Abraham O. Fapojuwo. Cooperative Multi-sensor Multi-vehicle Localization in Vehicular Adhoc Networks. In *2015 IEEE International Conference on Information Reuse and Integration*, pages 142–149. IEEE, aug 2015.

[42] Yanlei Gu, Yoriyoshi Hashimoto, Li Ta Hsu, Miho Iryo-Asano, and Shunsuke Kamijo. Human-like motion planning model for driving in signalized intersections. *IATSS Research*, 41(3):129–139, oct 2017.

[43] Maxime Guériau, Romain Billot, Nour-Eddin El Faouzi, Julien Monteil, Frédéric Armetta, and Salima Hassas. How to assess the benefits of connected vehicles? A simulation framework for the design of cooperative traffic management strategies. *Transportation Research Part C: Emerging Technologies*, 67:266–279, jun 2016.

[44] Hendrik-jorn Gunther, Oliver Trauer, and Lars Wolf. The potential of collective perception in vehicular ad-hoc networks. In *2015 14th International Conference on ITS Telecommunications (ITST)*, pages 1–5. IEEE, dec 2015.

[45] L Y Guo, N Li, X J Peng, and L Zhang. Modelling and simulation of vehicle behaviours based on the social force model. In *Information Science and Electronic Engineering: Proceedings of the 3rd International Conference of Electronic Engineering and Information Science (ICEEIS 2016), January 4-5, 2016, Harbin, China*, page 135. CRC Press, 2016.

[46] Hao Li and F. Nashashibi. Cooperative Multi-Vehicle Localization Using Split Covariance Intersection Filter. *IEEE Intelligent Transportation Systems Magazine*, 5(2):33–44, 2013.

[47] Dirk Helbing and Péter Molnár. Social force model for pedestrian dynamics. *Physical Review E*, 51(5):4282–4286, may 1995.

[48] Josefa Z. Hernández, Sascha Ossowski, and Ana García-Serrano. Multiagent architectures for intelligent traffic management systems. *Transportation Research Part C: Emerging Technologies*, 10(5-6):473–506, oct 2002.

[49] John R Hershey and Peder A Olsen. Approximating the Kullback Leibler divergence between Gaussian mixture models. In *2007 IEEE International Conference on Acoustics, Speech and Signal Processing-ICASSP'07*, volume 4, pages IV–317. IEEE, 2007.

[50] Takamasa Higuchi, Marco Giordani, Andrea Zanella, Michele Zorzi, and Onur Altintas. Value-Anticipating V2V Communications for Cooperative Perception. pages 1947–1952. Institute of Electrical and Electronics Engineers (IEEE), aug 2019.

[51] Tien-Shin Ho and Kwang-Cheng Chen. Performance analysis of IEEE 802.11 CSMA/CA medium access control protocol. In *Proceedings of PIMRC'96-7th International Symposium on Personal, Indoor, and Mobile Communications*, volume 2, pages 407–411. IEEE, 1996.

[52] G. M. Hoang, B. Denis, J. Harri, and D. T.M. Slock. Mitigating unbalanced GDoP effects in range-based vehicular Cooperative Localization. In *2017 IEEE International Conference on Communications Workshops, ICC Workshops 2017*, 2017.

[53] Gia Minh Hoang, Benoit Denis, Jerome Harri, and Dirk T.M. Slock. Breaking the Gridlock of Spatial Correlations in GPS-Aided IEEE 802.11p-Based Cooperative Positioning. *IEEE Transactions on Vehicular Technology*, 2016.

[54] Gia Minh Hoang, Benoit Denis, Jerome Harri, and Dirk T.M. Slock. On communication aspects of particle-based cooperative positioning in GPS-aided VANETs. In *IEEE Intelligent Vehicles Symposium, Proceedings*, 2016.

[55] Md. Anowar Hossain, Ibrahim Elshafiey, and Abdulhameed Al-Sanie. Cooperative vehicle positioning with multi-sensor data fusion and vehicular communications. *Wireless Networks*, pages 1–11, jun 2018.

[56] Andrew Howard. Multi-robot Simultaneous Localization and Mapping using Particle Filters. *The International Journal of Robotics Research*, 25(12):1243–1256, dec 2006.

[57] Hui Huang, Huiyun Li, Cuiping Shao, Tianfu Sun, Wenqi Fang, and Shaobo Dang. Data Redundancy Mitigation in V2X Based Collective Perceptions. *IEEE Access*, 8:13405–13418, 2020.

[58] S.J. Julier and J.K. Uhlmann. A non-divergent estimation algorithm in the presence of unknown correlations. In *Proceedings of the 1997 American Control Conference (Cat. No.97CH36041)*, pages 2369–2373 vol.4. IEEE, 1997.

[59] Andreas Kasprzok, Beshah Ayalew, and Chad Lau. Decentralized traffic rerouting using minimalist communications. In *IEEE International Symposium on Personal, Indoor and Mobile Radio Communications, PIMRC*, volume 2017-Octob, pages 1–7. Institute of Electrical and Electronics Engineers Inc., feb 2018.

[60] Manveen Kaur, G. G. Md. Nawaz Ali, Beshah Ayalew, and Jim Martin. Network Driven Performance Analysis in Connected Vehicular Networks. In *2019 IEEE 90th Vehicular Technology Conference: VTC2019-Fall 22–25 September 2019, Honolulu, HI, USA*.

[61] I. Khan, G. M. Hoang, and J. Harri. Rethinking cooperative awareness for future V2X safety-critical applications. In *IEEE Vehicular Networking Conference, VNC*, 2018.

[62] Been Kim, Michael Kaess, Luke Fletcher, John Leonard, Abraham Bachrach, Nicholas Roy, and Seth Teller. Multiple relative pose graphs for robust cooperative mapping. In *Proceedings - IEEE International Conference on Robotics and Automation*, pages 3185–3192, 2010.

[63] Seong-Woo Kim, Wei Liu, Marcelo H. Ang, Emilio Frazzoli, and Daniela Rus. The Impact of Cooperative Perception on Decision Making and Planning of Autonomous Vehicles. *IEEE Intelligent Transportation Systems Magazine*, 7(3):39–50, 2015.

[64] Seong-Woo Kim, Baoxing Qin, Zhuang Jie Chong, Xiaotong Shen, Wei Liu, Marcelo H. Ang, Emilio Frazzoli, and Daniela Rus. Multivehicle Cooperative Driving Using Cooperative Perception: Design and Experimental Validation. *IEEE Transactions on Intelligent Transportation Systems*, 16(2):663–680, apr 2015.

[65] Seung Hyun Kong and Sang Yun Jun. Cooperative Positioning Technique with Decentralized Malicious Vehicle Detection. *IEEE Transactions on Intelligent Transportation Systems*, 19(3):826–838, mar 2018.

[66] Yoram Koren and Johann Borenstein. Potential field methods and their inherent limitations for mobile robot navigation. In *Proceedings - IEEE International Conference on Robotics and Automation*, volume 2, pages 1398–1404. Publ by IEEE, 1991.

[67] Arda Kurt and Ümit Özgüner. Hierarchical finite state machines for autonomous mobile systems. *Control Engineering Practice*, 21(2):184–194, feb 2013.

[68] Sampo Kuutti, Saber Fallah, Konstantinos Katsaros, Mehrdad Dianati, Francis Mccullough, and Alexandros Mouzakitis. A Survey of the State-of-the-Art Localization Techniques and Their Potentials for Autonomous Vehicle Applications. *IEEE Internet of Things Journal*, 5(2):829–846, apr 2018.

[69] Yen Cheng Lai, Phone Lin, Wanjiun Liao, and Chung Min Chen. A region-based clustering mechanism for channel access in Vehicular Ad Hoc Networks. *IEEE Journal on Selected Areas in Communications*, 29(1):83–93, jan 2011.

[70] Khaoula Lassoued, Philippe Bonnifait, and Isabelle Fantoni. Cooperative Localization with Reliable Confidence Domains Between Vehicles Sharing GNSS Pseudoranges Errors with No Base Station. *IEEE Intelligent Transportation Systems Magazine*, 2017.

[71] Maosheng Li, Feng Shi, and Dafei Chen. Analyze bicycle-car mixed flow by social force model for collision risk evaluation. In *3rd International Conference on Road Safety and Simulation*, pages 1–22, 2011.

[72] Lingji Chen, P.O. Arambel, and R.K. Mehra. Estimation under unknown correlation: covariance intersection revisited. *IEEE Transactions on Automatic Control*, 47(11):1879–1882, nov 2002.

[73] Jiang Liu, Bai Gen Cai, and Jian Wang. Cooperative Localization of Connected Vehicles: Integrating GNSS With DSRC Using a Robust Cubature Kalman Filter. *IEEE Transactions on Intelligent Transportation Systems*, 18(8):2111–2125, aug 2017.

[74] Kai Liu, Hock Beng Lim, Emilio Frazzoli, Houling Ji, and Victor C. S. Lee. Improving Positioning Accuracy Using GPS Pseudorange Measurements for Cooperative Vehicular Localization. *IEEE Transactions on Vehicular Technology*, 63(6):2544–2556, jul 2014.

[75] Kai Liu, Joseph K. Y. Ng, Victor C.S. Lee, Sang H. Son, and Ivan Stojmenovic. Cooperative Data Scheduling in Hybrid Vehicular Ad Hoc Networks: VANET as a Software Defined Network. *IEEE/ACM Transactions on Networking*, 24(3):1759–1773, jun 2016.

[76] Xiaofeng Liu and Arunita Jaekel. Congestion Control in V2V Safety Communication: Problem, Analysis, Approaches. *Electronics*, 8(5):540, may 2019.

[77] R. Madhavan, K. Fregene, and L.E. Parker. Distributed heterogeneous outdoor multi-robot localization. In *Proceedings 2002 IEEE International Conference on Robotics and Automation (Cat. No.02CH37292)*, volume 1, pages 374–381. IEEE.

[78] Gustav Markkula, Ola Benderius, Krister Wolff, and Mattias Wahde. A review of near-collision driver behavior models. In *Human Factors*, volume 54, pages 1117–1143, dec 2012.

[79] Federico Mason, Marco Giordani, Federico Chiariotti, Andrea Zanella, and Michele Zorzi. An Adaptive Broadcasting Strategy for Efficient Dynamic Mapping in Vehicular Networks. *IEEE Transactions on Wireless Communications*, 19(8):5605–5620, aug 2020.

[80] Chetan Belagal Math, Ahmet Ozgur, Sonia Heemstra de Groot, and Hong Li. Data Rate based Congestion Control in V2V communication for traffic safety applications. In *2015 IEEE Symposium on Communications and Vehicular Technology in the Benelux (SCVT)*, pages 1–6. IEEE, nov 2015.

[81] Jim Misener. SAE connected vehicle standards, 2016.

[82] Sudip Misra, P. Venkata Krishna, and V. Saritha. LACAV: An energy-efficient channel assignment mechanism for vehicular ad hoc networks. *Journal of Supercomputing*, 62(3):1241–1262, feb 2012.

[83] Julien Monteil, Romain Billot, Jacques Sau, Frédéric Armetta, Salima Hassas, and Nour-Eddin El Faouzi. Cooperative Highway Traffic. *Transportation Research Record: Journal of the Transportation Research Board*, 2391(1):1–10, jan 2013.

[84] Michael Montemerlo, Sebastian Thrun, Daphne Koller, and Ben Wegbreit. FastSLAM 2.0: An Improved Particle Filtering Algorithm for Simultaneous Localization and Mapping that Provably Converges. Technical report.

[85] K.L. Moore and N.S. Flann. A Six-Wheeled Omnidirectional Autonomous Mobile Robot. *IEEE Control Systems*, 20(6):53–66, dec 2000.

[86] Y. L. Morgan. Notes on DSRC and WAVE Standards Suite: Its Architecture, Design, and Characteristics. *IEEE Communications Surveys and Tutorials*, 12(4):504–518, 2010.

[87] B. Mourllion, A. Lambert, D. Gruyer, and D. Aubert. Collaborative perception for collision avoidance. In *IEEE International Conference on Networking, Sensing and Control, 2004*, volume 2, pages 880–885. IEEE.

[88] Sharad Nagappa, Daniel E. Clark, and Ronald P. S. Mahler. Incorporating track uncertainty into the OSPA metric. *undefined*, 2011.

[89] G. G. Md. Nawaz Ali, Beshah Ayalew, and Ardalan Vahidi. Analysis of Reliabilities Under Different Path Loss Models in Urban/Sub-urban Vehicular Networks. In *2019 IEEE 90th Vehicular Technology Conference: VTC2019-Fall 22–25 September 2019, Honolulu, HI, USA*.

[90] José Neira and Juan D. Tardós. Data association in stochastic mapping using the joint compatibility test. *IEEE Transactions on Robotics and Automation*, 17(6):890–897, dec 2001.

[91] D. Ngoduy, S.P. Hoogendoorn, and R. Liu. Continuum modeling of cooperative traffic flow dynamics. *Physica A: Statistical Mechanics and its Applications*, 388(13):2705–2716, jul 2009.

[92] W. Niehsen. Information fusion based on fast covariance intersection filtering. In *Proceedings of the Fifth International Conference on Information Fusion. FUSION 2002. (IEEE Cat.No.02EX5997)*, volume 2, pages 901–904. Int. Soc. Inf. Fusion.

[93] Md. Noor-A-Rahim, G. G. Md. Nawaz Ali, Hieu Nguyen, and Yong Liang Guan. Performance Analysis of IEEE 802.11p Safety Message Broadcast With and Without Relaying at Road Intersection. *IEEE Access*, 6:23786–23799, 2018.

[94] Günther Prokop. Modeling human vehicle driving by model predictive online optimization. *Vehicle system dynamics*, 35(1):19–53, 2001.

[95] PTV GROUP. PTV Vissim Broschüre, 2014.

[96] Qi Chen, Tobias Roth, Ting Yuan, Jakob Breu, Florian Kuhnt, Marius Zollner, Miro Bogdanovic, Christian Weiss, Jorg Hillenbrand, and Axel Gern. DSRC and radar object matching for cooperative driver assistance systems. In *2015 IEEE Intelligent Vehicles Symposium (IV)*, pages 1348–1354. IEEE, jun 2015.

[97] Xiangjun Qian, Arnaud de La Fortelle, and Fabien Moutarde. A hierarchical Model Predictive Control framework for on-road formation control of autonomous vehicles. In *2016 IEEE Intelligent Vehicles Symposium (IV)*, pages 376–381. IEEE, jun 2016.

[98] Zhao-wei Qu, Ning-bo Cao, Yong-heng Chen, Li-ying Zhao, Qiao-wen Bai, and Rui-qi Luo. Modeling electric bike–car mixed flow via social force model. *Advances in Mechanical Engineering*, 9(9):168781401771964, sep 2017.

[99] Pawan Rathod, Ankit Vartak, and Neha Kunte. Optimizing the complexity of matrix multiplication algorithm. In *Proceedings of 2017 International Conference on Intelligent Computing and Control, I2C2 2017*, volume 2018-Janua, pages 1–4. Institute of Electrical and Electronics Engineers Inc., mar 2018.

[100] Andreas Rauch, Felix Klanner, and Klaus Dietmayer. Analysis of V2X communication parameters for the development of a fusion architecture for cooperative perception systems. In *2011 IEEE Intelligent Vehicles Symposium (IV)*, pages 685–690. IEEE, jun 2011.

[101] Andreas Rauch, Felix Klanner, Ralph Rasshofer, and Klaus Dietmayer. Car2X-based perception in a high-level fusion architecture for cooperative perception systems. In *2012 IEEE Intelligent Vehicles Symposium*, pages 270–275. IEEE, jun 2012.

[102] Andreas Rauch, Stefan Maier, Felix Klanner, and Klaus Dietmayer. Inter-vehicle object association for cooperative perception systems. In *16th International IEEE Conference on Intelligent Transportation Systems (ITSC 2013)*, pages 893–898. IEEE, oct 2013.

[103] Shahram Rezaei and Raja Sengupta. Kalman Filter-Based Integration of DGPS and Vehicle Sensors for Localization. *IEEE Transactions on Control Systems Technology*, 15(6):1080–1088, nov 2007.

[104] Mohsen Rohani, Denis Gingras, Vincent Vigneron, and Dominique Gruyer. A New Decentralized Bayesian Approach for Cooperative Vehicle Localization Based on Fusion of GPS and VANET Based Inter-Vehicle Distance Measurement. *IEEE Intelligent Transportation Systems Magazine*, 7(2):85–95, 2015.

[105] Guo Ronghua, Ronghua Guo, Zheng Qin, Xiangnan Li, and Junliang Chen. Interacting Multiple Model Particle-type Filtering Approaches to Ground Target Tracking. *Article in Journal of Computers*, 2008.

[106] S.I. Roumeliotis and G.A. Bekey. Distributed multirobot localization. *IEEE Transactions on Robotics and Automation*, 18(5):781–795, oct 2002.

[107] Stuart Rowell, Atanas A Popov, and Jacob P Meijaard. Predictive control to modelling motorcycle rider steering. *International journal of vehicle systems modelling and testing*, 5(2-3):124–160, 2010.

[108] M. Sahebsara, T. Chen, and S. L. Shah. Optimal filtering with random sensor delay, multiple packet dropout and uncertain observations. *International Journal of Control*, 80(2):292–301, feb 2007.

[109] Ahmed Hamdi Sakr and Gaurav Bansal. Cooperative localization via DSRC and multi-sensor multi-target track association. In *2016 IEEE 19th International Conference on Intelligent Transportation Systems (ITSC)*, pages 66–71. IEEE, nov 2016.

[110] Florian Alexander Schiegg, Nadia Brahmi, and Ignacio Llatser. Analytical Performance Evaluation of the Collective Perception Service in C-V2X Mode 4 Networks. In *2019 IEEE Intelligent Transportation Systems Conference (ITSC)*, pages 181–188. IEEE, 2019.

[111] Tom Schouwenaars, Bart De Moor, Eric Feron, and Jonathan How. Mixed integer programming for multi-vehicle path planning. In *2001 European Control Conference (ECC)*, pages 2603–2608. IEEE, sep 2001.

[112] Dominic Schuhmacher, Ba-Tuong Vo, and Ba-Ngu Vo. A Consistent Metric for Performance Evaluation of Multi-Object Filters. *IEEE Transactions on Signal Processing*, 56(8):3447–3457, aug 2008.

[113] F. Seeliger and K. Dietmayer. Inter-vehicle information-fusion with shared perception information. In *2014 17th IEEE International Conference on Intelligent Transportation Systems, ITSC 2014*, pages 2087–2093. Institute of Electrical and Electronics Engineers Inc., nov 2014.

[114] Seong-Woo Kim, Zhuang Jie Chong, Baoxing Qin, Xiaotong Shen, Zhuoqi Cheng, Wei Liu, and Marcelo H. Ang. Cooperative perception for autonomous vehicle control on the road: Motivation and experimental results. In *2013 IEEE/RSJ International Conference on Intelligent Robots and Systems*, pages 5059–5066. IEEE, nov 2013.

[115] Miguel Sepulcre and Javier Gozalvez. Coordination of Congestion and Awareness Control in Vehicular Networks. *Electronics*, 7(11):335, nov 2018.

[116] Miguel Sepulcre, Jorge Mira, Gokulnath Thandavarayan, and Javier Gozalvez. Is Packet Dropping a Suitable Congestion Control Mechanism for Vehicular Networks? In *IEEE Vehicular Technology Conference*, volume 2020-May. Institute of Electrical and Electronics Engineers Inc., may 2020.

[117] Xiaotong Shen, Zhuang Jie Chong, Scott Pendleton, Wei Liu, Baoxing Qin, Guo Ming James Fu, and Marcelo H Ang. Multi-vehicle motion coordination using v2v communication. In *Intelligent Vehicles Symposium (IV), 2015 IEEE*, pages 1334–1341. IEEE, 2015.

[118] Shingo Shimoda, Yoji Kuroda, and Karl Iagnemma. Potential field navigation of high speed unmanned ground vehicles on uneven terrain. In *Proceedings - IEEE International Conference on Robotics and Automation*, volume 2005, pages 2828–2833, 2005.

[119] Gloria Soatti, Monica Nicoli, Nil Garcia, Benoit Denis, Ronald Raulefs, and Henk Wymeersch. Implicit Cooperative Positioning in Vehicular Networks. *IEEE Transactions on Intelligent Transportation Systems*, 19(12):3964–3980, dec 2018.

[120] Christoph Sommer, David Eckhoff, Reinhard German, and Falko Dressler. A computationally inexpensive empirical model of IEEE 802.11p radio shadowing in urban environments. In *2011 8th International Conference on Wireless On-Demand Network Systems and Services, WONS 2011*, 2011.

[121] Heecheol Song and Hwang Soo Lee. A survey on how to solve a decentralized congestion control problem for periodic beacon broadcast in vehicular safety communications. In *undefined*, 2013.

[122] Yoo-Seung Song and Hyun-Kyun Choi. Analysis of V2V Broadcast Performance Limit for WAVE Communication Systems Using Two-Ray Path Loss Model. *ETRI Journal*, 39(2):213–221, apr 2017.

[123] Yu Sukdea and Cho Gihwan. A selective flooding method for propagating emergency messages in vehicle safety communications. In *Proceedings - 2006 International Conference on Hybrid Information Technology, ICHIT 2006*, volume 2, pages 556–561, 2006.

[124] Shu-Li Sun and Zi-Li Deng. Multi-sensor optimal information fusion Kalman filter. *Automatica*, 40(6):1017–1023, jun 2004.

[125] Shuli Sun, Lihua Xie, Wendong Xiao, and Yeng Chai Soh. Optimal linear estimation for systems with multiple packet dropouts. *Automatica*, 44(5):1333–1342, may 2008.

[126] Gokulnath Thandavarayan, Miguel Sepulcre, and Javier Gozalvez. Analysis of message generation rules for collective perception in connected and automated driving. In *IEEE Intelligent Vehicles Symposium, Proceedings*, volume 2019-June, pages 134–139. Institute of Electrical and Electronics Engineers Inc., jun 2019.

[127] Gokulnath Thandavarayan, Miguel Sepulcre, and Javier Gozalvez. Redundancy Mitigation in Cooperative Perception for Connected and Automated Vehicles. In *IEEE Vehicular Technology Conference*, volume 2020-May. Institute of Electrical and Electronics Engineers Inc., may 2020.

[128] Sebastian Thrun and Michael Montemerlo. The graph SLAM algorithm with applications to large-scale mapping of urban structures. In *International Journal of Robotics Research*, volume 25, pages 403–429, may 2006.

[129] K. Tischler and B. Hummel. Enhanced environmental perception by inter-vehicle data exchange. In *IEEE Proceedings. Intelligent Vehicles Symposium, 2005.*, pages 313–318. IEEE, 2005.

[130] Ming Fong Tsai, Yung Cheng Chao, Lien Wu Chen, Naveen Chilamkurti, and Seungmin Rho. Cooperative emergency braking warning system in vehicular networks. *Eurasip Journal on Wireless Communications and Networking*, 2015(1):1–14, dec 2015.

[131] Qi Wang, David W. Matolak, and Bo Ai. Shadowing Characterization for 5-GHz Vehicle-to-Vehicle Channels. *IEEE Transactions on Vehicular Technology*, 2018.

[132] Qian Wang and Beshah Ayalew. Constraint tightening for the probabilistic collision avoidance of multi-vehicle groups in uncertain traffic. In *2017 IEEE Conference on Control Technology and Applications (CCTA)*, pages 2188–2195. IEEE, aug 2017.

[133] Qian Wang, Beshah Ayalew, and Thomas Weiskircher. Optimal assigner decisions in a hybrid predictive control of an autonomous vehicle in public traffic. In *2016 American Control Conference (ACC)*, pages 3468–3473. IEEE, jul 2016.

[134] Qian Wang, Thomas Weiskircher, and Beshah Ayalew. Hierarchical hybrid predictive control of an autonomous road vehicle. In *ASME 2015 Dynamic Systems and Control Conference*, pages V003T50A006–V003T50A006. American Society of Mechanical Engineers, 2015.

[135] Yunpeng Wang, Xuting Duan, Daxin Tian, Guangquan Lu, and Haiyang Yu. Throughput and Delay Limits of 802.11 p and its Influence on Highway Capacity. *Procedia-Social and Behavioral Sciences*, 96:2096–2104, 2013.

[136] Huang Weinan and Fellendorf Martin. Social Force Based Vehicle Model for Traffic Simulation, 2012.

[137] Ming Wu, Feifei Huang, Long Wang, and Jiyin Sun. Cooperative multi-robot monocular-SLAM using salient landmarks. In *Proceedings - 2009 International Asia Conference on Informatics in Control, Automation, and Robotics, CAR 2009*, pages 151–155, 2009.

[138] Yuchen Wu, Yanmin Zhu, and Bo Li. Trajectory improves data delivery in vehicular networks. In *Proceedings - IEEE INFOCOM*, pages 2183–2191, 2011.

[139] Xuehai Xiang, Wenhu Qin, and Binfu Xiang. Research on a DSRC-based rear-end collision warning model. *IEEE Transactions on Intelligent Transportation Systems*, 15(3):1054–1065, 2014.

[140] Fei Ye, Raymond Yim, Jianlin Guo, Jinyun Zhang, and Sumit Roy. Prioritized broadcast contention control in VANET. In *IEEE International Conference on Communications*, 2010.

[141] Dohyun Daniel Yoon and Beshah Ayalew. Social Force Aggregation Control for Autonomous Driving with Connected Preview. In *American Control Conference (ACC)*, Philadelphia, PA, 2019.

[142] Dohyun Daniel Yoon, G. G. Md. Nawaz Ali, and Beshah Ayalew. Data Association and Fusion Framework for Decentralized Multi-Vehicle Cooperative Perception. In *Proceedings of the ASME 2019 International Design Engineering Technical Conferences and Computers and Information in Engineering Conference IDETC/CIE2019 August 18-21, 2019, Anaheim, CA, USA*.

[143] Dohyun Daniel Yoon, G. G. Md. Nawaz Ali, and Beshah Ayalew. Optimality of Decentralized Cooperative Perception in Heterogeneous Traffic. *IEEE Transactions on Intelligent Transportation Systems*, pages 1–13.

[144] Hongtao Yu, H. Eric Tseng, and Reza Langari. A human-like game theory-based controller for automatic lane changing. *Transportation Research Part C: Emerging Technologies*, 88:140–158, mar 2018.

[145] Ting Yuan, Tobias Roth, Qi Chen, Jakob Breu, Miro Bogdanovic, and Christian A. Weiss. Track-to-track association for object matching in an inter-vehicle communication system. volume 9596, page 959609. International Society for Optics and Photonics, sep 2015.

[146] Fusang Zhang, Beihong Jin, Zhaoyang Wang, Hai Liu, Jiafeng Hu, and Lifeng Zhang. On Geocasting over Urban Bus-Based Networks by Mining Trajectories. *IEEE Transactions on Intelligent Transportation Systems*, 17(6):1734–1747, jun 2016.

[147] Fusang Zhang, Hai Liu, Yiu Wing Leung, Xiaowen Chu, and Beihong Jin. CBS: Community-Based Bus System as Routing Backbone for Vehicular Ad Hoc Networks. *IEEE Transactions on Mobile Computing*, 16(8):2132–2146, aug 2017.

[148] Xiangmo Zhao, Kenan Mu, Fei Hui, and Christian Prehofer. A cooperative vehicle-infrastructure based urban driving environment perception method using a D-S theory-based credibility map. *Optik*, 138:407–415, jun 2017.

[149] Hao Zhu, Ka Veng Yuen, Lyudmila Mihaylova, and Henry Leung. Overview of Environment Perception for Intelligent Vehicles, oct 2017.

[150] Hongzi Zhu, Mianxiong Dong, Shan Chang, Yanmin Zhu, Minglu Li, and Xuemin Sherman Shen. ZOOM: Scaling the mobility for fast opportunistic forwarding in vehicular networks. In *Proceedings - IEEE INFOCOM*, pages 2832–2840, 2013.

[151] Ismail H. Zohdy and Hesham A. Rakha. Intersection Management via Vehicle Connectivity: The Intersection Cooperative Adaptive Cruise Control System Concept. *Journal of Intelligent Transportation Systems: Technology, Planning, and Operations*, 20(1):17–32, 2016.